ARS JOURNAL

RUSSIAN SUPPLEMENT

J. George Adashko, Editor

Published Under National Science Foundation Grant-in-Aid

Manometer Error Caused by Small Leaks in the Casing of a Satellite

S. A. KUCHAY

THE APPARATUS on the third Sputnik included manometers capable of measuring static pressures 10^{-4}–10^{-9} mm Hg under normal conditions on Earth.

In measurements in the upper atmosphere, the manometer may also encounter molecules which are brought along by the satellite itself, and which are found in the upper atmosphere either because of gas emission from the surface of the hull or as a result of leaks. Desorption from the surface stops relatively quickly, but leakage from within becomes practically constant throughout the lifetime of the whole apparatus. Thus, the possibility of the occurrence of manometer errors imposes definite demands on the tightness of the hull.

We shall call the gas molecules within the casing "proper" molecules. The manometer error resulting from the "proper" molecules getting into the manometer is evaluated herein.

Within the manometer, there is established a concentration of gas for which the streams of gas passing through a cross section of the intake tubing in the manometer are the same inward as outward. In order not to consider the influence of the walls, we assume that equality of the normal components of the streams is maintained. For low pressures and random motion of the molecules the component of the outward gas stream normal to the cross section of the tube is equal to

$$q_i = \frac{n_m v_M}{6} \pi b^2 \frac{\text{molecules}}{\text{sec}}$$

where

n_m = concentration of gas in the manometer

v_M = mean velocity of molecules at the temperature of the walls

b = radius of the cross section

The inward stream has a normal component q_s, the magnitude of which depends on the distribution of velocities in the exterior gas stream. Considering that $q_i = q_s$, we can calculate the dependence of the "manometer pressure" on this stream

$$P = \frac{6q_s}{\pi b^2 v_M} \frac{1}{N} \text{ mm Hg}$$

Here $N = 3.6 \times 10^{16}$ is the concentration of molecules at a pressure of 1 mm Hg.

Thus, to calculate the absolute manometer error it is sufficient to know the normal component of "proper" molecules at a cross section of the intake tube.

Let us consider a sphere passing through a rarefied gas, inside of which is placed a manometer. If the pressure of the gas is sufficiently small, and a direct encounter of a molecule from the surface of the sphere with the manometer is prevented by locating the latter properly, then it must be considered that the "proper" molecules can strike the manometer only as a result of single scattering from molecules of the gaseous surroundings. Among these molecules we distinguish, in addition to the unperturbed molecules of the upper atmosphere, "proper" molecules and "acquired" molecules arising from the evaporation of molecules from the surface of the sphere. The manometer error is made up of errors resulting from scattering by each of these three components.

In a system of coordinates fixed in the sphere, the molecules of the upper atmosphere, which the manometer is intended to measure, all have the same velocity V, which is significantly larger than the random velocity. We assume that the density of the upper atmosphere around the sphere is uniform.

The "proper" molecules, which are evaporated from the surface of the sphere and move away from it with a finite velocity v_p, make up a "proper" atmosphere. Its density decreases with the distance from the sphere.

The "acquired" atmosphere consists of molecules of the upper atmosphere which first hit the sphere and then evaporate from its surface. The velocity with which molecules of this type are removed from the sphere is unkown, but $v_p < v_a < V$. Since the orientation of the satellite in flight does not remain constant, we can assume that the density of the "acquired" atmosphere is symmetric with respect to the center of the sphere. It is further assumed that the evaporation of the molecules making up the "proper" and "acquired" atmosphere obeys a cosine law.

In the problems considered herein the source of the scattered molecules is either concentrated in a point or is uniformly distributed over the surface of the sphere, and the velocity distribution of scattered molecules at the surface either obeys a cosine law, or else the scattering is normal to the surface. The manometer tube is directed along a radius of the sphere (Fig. 1).

In the problems concerning concentrated leakage, we consider the worst possible position, as far as errors go, that of a manometer located "over the leak"; i.e., we calculate the reverse flow through an area coinciding with the cross section of the intake tube and located over the leak. However, the screening effect with respect to the departure of proper molecules, which would occur if the housing of an actual satellite were located in such a position, is not taken into account.

We assume that the molecules are represented by rigid spheres of equal radii and that in the system of coordinates fixed in the sphere the proper molecules are stationary, while molecules of the upper atmosphere move with a velocity V and are reflected along the line of centers at the instant of contact. The angular distribution of proper molecules scattered by molecules of the upper atmosphere is shown in Fig. 2.

For scattering in "proper" and "acquired" atmospheres we assume that after a collision a molecule can be scattered in

†Translated from "Iskusstvennyye Sputniki Zemli" (Artificial Earth Satellites), USSR Acad. Sci. Press, Moscow, 1959, no. 3, pp. 113–117. Translation provided by the U. S. Joint Publication Research Service.

any direction with equal probability. This simple model serves only to evaluate the maximum, since it clearly makes the reverse stream too large. Actually the velocities of the colliding molecules are directed away from the sphere, so that angular distribution in the same direction should predominate even after scattering.

The numerical values used in the calculation are

a = radius of sphere, 100 cm
b = radius of intake tube, 1.5 cm
h = height of the cross section above the surface, 10 cm
n_A = concentration of molecules in the upper atmosphere, 3.6×10^{10} molecules/cm^3
V = velocity of the satellite, 8×10^5 cm/sec
v_p = mean velocity of the proper molecules, 3×10^4 cm/sec
v_m = mean velocity of molecules in the manometer, 3×10^4 cm/sec
μ_0 = total leakage, 3.6×10^{16} molecules/sec
σ = scattering cross section, 5×10^{-15} cm^2

The value of n_A at room temperature corresponds to a pressure of 10^{-6} mm Hg, and the value of μ_0 corresponds to a leak of 1 liter-μ Hg/sec.

Taking into account the foregoing assumptions regarding the source of the leak, the gas ambient and the laws of scattering, several particular cases were considered. The computations are not particularly difficult and are omitted to conserve space.

1 Dispersed Leak: Scattering by "Proper" Atmosphere

The density of a dispersed source of proper molecules in this case amounts to

$$\nu_p = \mu_0/4\pi a^2$$

The normal component of the reverse stream on a unit surface of the sphere amounts to

$$\frac{Q}{4\pi a^2} = \frac{\mu_0^2\sigma}{32\pi^2 a^4 v_p} K$$

The factor K is equal to 0.27 for normally scattered molecules and 0.68 for tangentially scattered ones. In the worst case, the error does not exceed

$$P_1 = 2.7 \times 10^{-15} \text{ mm Hg}$$

2 Dispersed Leak: Scattering by "Acquired" Atmosphere

The problem reduces to the preceding one, since the "acquired" atmosphere can be considered to result from a distribution of leaks with a density $\nu_a = n_A V/4$. The error P_2 should be larger than P_1 in the ratio

$$\frac{\nu_a}{\nu_p}\frac{v_p}{v_a} = \frac{n_A V \pi a^2}{\mu_0}\frac{v_p}{v_a} = 2.5 \times 10^4 \frac{v_p}{v_a}$$

In the worst case $v_p = v_a$

$$P_2 = 6.8 \times 10^{-11} \text{ mm Hg}$$

3 Point Leak: Scattering by "Proper" Atmosphere. Molecules Scattered Normally. Manometer Over the Leak

The normal component of the stream q_s through a cross section of the manometer amounts to

$$q_s = \frac{\mu_0\sigma}{\pi v_p} - \frac{1}{b} f\left(\frac{h}{b}\right) \frac{\text{molecules}}{\text{sec}}$$

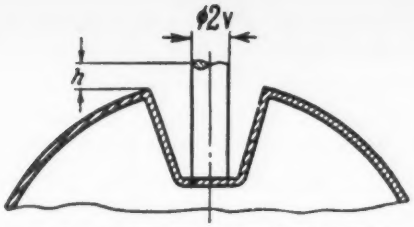

Fig. 1 Location of the manometer (h is the height of the manometer above the surface)

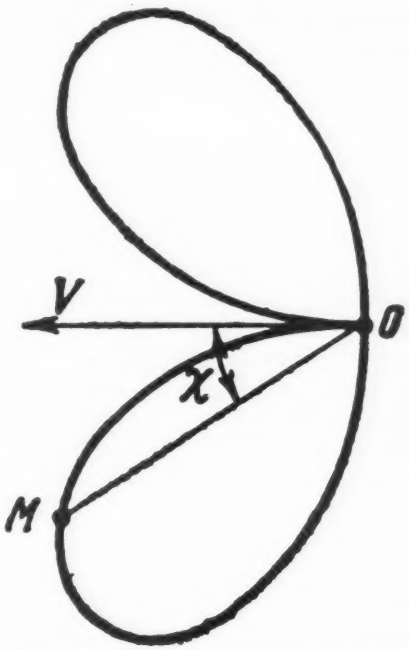

Fig. 2 Angular distribution of proper molecules scattered by molecules of the upper atmosphere. The radius vector OM is proportional to the probability of scattering through an angle χ with the direction of the velocity V

where h is the height of the cross section above the surface (see Fig. 1), and

$$f(x) = \int_0^\infty \frac{d\zeta}{(1+\zeta^2)(\zeta+x)^2}$$

For $h/b = 7$ we obtain $f(7) = 2.2 \times 10^{-2}$ and correspondingly

$$P_3 = 7.9 \times 10^{-10} \text{ mm Hg}$$

4 Point Leak: Scattering by "Acquired" Atmosphere. "Cosine-Law" Angular Distribution of Molecules Near the Leak

The magnitude

$$q_s = \frac{1}{2}\mu_0 \frac{n_A V}{4}\frac{a\sigma}{\nu_a} J\left(\frac{b}{a}\right)$$

where

$$J(x) = \int_{\xi=0}^{\infty}\int_{\eta=0}^{1} \frac{1}{1+2\eta\xi+\xi^2} \times \left[1 - \frac{\xi^2 - x^2}{\sqrt{(\xi^2-x^2)^2 + 4x^2\xi^2\eta^2}}\right] \eta d\eta d\xi$$

For the assumed values of b and a, the integral $J = 1.8 \times 10^{-2}$. In the worst case, $v_p = v_a$, one obtains

$$P_4 = 3.0 \times 10^{-6} \text{ mm Hg}$$

Under the same conditions, but with the assumption that all the molecules are normally scattered, one would obtain

$$P_4' = 3.9 \times 10^{-6} \text{ mm Hg}$$

5 Point Leak: Scattering by Molecules of the Upper Atmosphere. Molecules Scattered Normally. Manometer Located Over Point Leak at an Angle of Attack of 45 Deg

The magnitude

$$q_e = n_A \delta \mu_0 b L$$

where

$$L = \int_0^\infty d\xi \int_0^1 d\eta \frac{\eta \xi^2}{(\xi^2 + \eta^2)^{5/2}} \int_0^{2\pi} \times \frac{(\xi - \eta \cos\alpha)^2(\xi + \eta \cos\alpha)}{(\xi - \eta \cos\alpha)^2 + 4\eta^2 \sin^2\alpha} d\alpha = 4.6$$

Correspondingly

$$P_5 = 3.5 \times 10^{-6} \text{ mm Hg}$$

It is clear that leaks near the manometer are a more dangerous source of error, so that in the construction of the hull these parts should be sealed with particular care. In this connection it is best to evaluate the error under the following conditions.

In a region of radius D around the manometer the total leakage is no greater than μ_1. The remainder of the surface is characterized by a total leakage μ_2.

In an extremely unfavorable case the point source of leakage μ_1 is located above the manometer, and the leakage μ_2 is concentrated at a distance D from it. In the calculations we assume $\mu_1 \sim 10^{-2}$ liter-mm Hg/sec, $\mu_2 = 1$ liter-mm Hg/sec, $D = 20$ cm.

6 Scattering by an "Acquired" Atmosphere

The error P_6 is broken down into components P_6', caused by leakage μ_1 and P_6'' caused by leakage μ_2.

The error P_6' is calculated in the same way as P_3, but with a different value of leakage (μ_1 instead of μ_0)

$$P_6' = P_3(\mu_1/\mu_0) = 6.8 \times 10^{-12} \text{ mm Hg}$$

The value of P_6'' is calculated for a normal scattering of the molecules

$$q_e = \mu_2(n_A V/64 v_a)\sigma a J$$

where

$$J = ab^2 \int_0^\infty \frac{\zeta^2 d\zeta}{(a + h + \zeta)^2(D^2 + \zeta^2)^2}$$

For the assumed values of a, b, h, d, and for the case $v_a = v_p$

$$J = 4.3 \times 10^{-6}$$

$$P_6'' = 2.9 \times 10^{-10} \text{ mm Hg}$$

7 Scattering by Molecules of the Upper Atmosphere

The error P_7 is made of components P_7' due to leakage μ_1 and P_7'' due to leakage μ_2.

In view of the similarity with the evaluation of P_5

$$P_7'' = P_5(\mu_1/\mu_0) = 3.5 \times 10^{-10} \text{ mm Hg}$$

The value of P_7'' is calculated for normal scattering of the molecules

$$q_e = \frac{4b^2}{\pi} \mu_2 n_A \sigma \frac{1}{D} M$$

where

$$M = \int_0^1 \frac{\zeta^2 d\zeta}{(1 + \zeta^2)^{5/2}} = \frac{\sqrt{2}}{12}$$

Correspondingly

$$P_7 = 8.6 \times 10^{-11} \text{ mm Hg}$$

The results obtained permit the formulation of qualitative criteria of satellite tightness such that the manometer errors will not exceed requirements.

Reviewer's Comment

The paper contributes to the understanding of the difficult problem of vehicle leaks and outgassing in the measurement of pressure and density at very high altitudes. The approach is similar to that of Mirtov (1) who analyzed the problem at the 1958 IGY meetings in Moscow. Kuchay dismisses outgassing (desorption) as a minor problem. His view is supported by Mirtov's analysis and by data from Sputnik III given by Mikhnevich (2) which showed the desorption component decreasing at the rate of an order of magnitude per day to a negligible value after three days.

Leakage is not as easily dismissed. Sputnik III was filled with nitrogen, presumably at ground pressure, and sealed. Thus, leaks would be a source of unwanted gas for a long time. Both authors attempt to assess the magnitudes and mutual reactions of the three components of the "atmosphere" in which the satellite is immersed: 1 Ambient molecules, 2 "direct" or "proper" molecules due to leakage and 3 "acquired" or "recoiling" molecules which are ambient molecules swept up by the satellite, then evaporated.

Kuchay's numerical calculations of pressure errors due to leaks (based on an assumed leak three orders of magnitude less than that assumed by Mirtov) may be compared with the atmospheric pressure values given by Mikhnevich et al. (3). Only two cases, 4 and 5, would seem to cause trouble below 500 km where Mikhnevich shows an ambient pressure of 1.94×10^{-6} mm Hg.

A technique used in U. S. sounding rocket work (4) to handle the leakage problem is of interest. In collecting samples of the upper atmosphere the payload compartment was flooded, just prior to opening the sample intake tubes at the front of the rocket, with radioactive carbon dioxide ($C^{14}O_2$) and the samples later checked for the tracer. No significant amounts were found. In some instances the compartment was sealed and in others open to the ambient air with large ports. A similar technique might be employed on a satellite carrying a neutral molecule mass spectrometer. In this case, it would be unnecessary for the tracer gas to be radioactive.

—Leslie M. Jones

Dept. of Aeronautical and Astronautical Engineering
University of Michigan

1 Mirtov, B. A., "Disturbances of Gas Environment Caused by Satellite Flight," presented at Fifth Reunion of CSAGI, Moscow, 1958.

2 Mikhnevich, V. V., "On Pressure and Density of Atmosphere," presented at Fifth Reunion of CSAGI, Moscow, 1958.

3 Mikhnevich, V. V., et al., "Some Results of the Determination of the Structural Parameters of the Atmosphere Using the Third Soviet Artificial Earth Satellite," ARS Journal, vol. 30, no. 4, April, 1960, pp. 407–413.

4 Jones, L. M., in "Rocket Exploration of the Upper Atmosphere," Pergamon Press, New York, 1954, p. 143.

Errors of a Single-Degree-of-Freedom Integrating Gyro Due to Angular Oscillations of Its Base

S. S. ARUTYUNOV
Kazan' Aviation Institute

CERTAIN vehicles are stabilized in attitude by use of single-degree-of-freedom gyros which serve the purpose of minimizing the deviations in attitude of the vehicle from its initial orientation. In some cases, the instrument is rigidly mounted to the vehicle. In this case the gyro must have maximum sensitivity to rotations of the vehicle about its normal axis z (gyro input axis), for these rotations are indeed deviations of the vehicle from its prescribed attitude.

Assume that the y_0 axis (Fig. 1), from which the angle α of gyro motion is measured, coincides with the y (pitch) axis of the vehicle and the gyro spin axis x_0 coincides, at $\alpha = 0$, with the longitudinal (roll) axis x of the vehicle. In the functional diagram of a single-degree-of-freedom integrating gyro, shown in Fig. 1, D denotes the damper and AT the transducer of the angle α between the gyro spin axis x_0 and the longitudinal x axis of the vehicle.

It is known that under a suitable choice of parameters of the integrating gyro, rotation of the base about its normal axis z (gyro input axis) by a small angle φ causes precession of the gyro spin axis x_0 from the longitudinal axis x of the vehicle, by an angle α directly proportional to the angle φ. If the angle transducer output is linear with α, the magnitude of this signal will be directly proportional to the angle φ of rotation of the vehicle about its normal axis z. This signal is used to stabilize the attitude of the vehicle. When the case of the gyro is rigidly mounted to the vehicle, angular oscillations of the base produce an error in the integrating gyro that increases with time.

Actually, let the base execute harmonic oscillations about its normal axis z and about the longitudinal axis x in accordance with

$$\varphi = \varphi_0 \sin \omega t$$
$$\gamma = \gamma_0 \sin (\omega t + \delta) \quad \ldots\ldots\ldots\ldots\ldots\ldots\ldots\ldots\ldots\ldots [1]$$

The equation of motion of the integrating gyro will in this case have the form

$$J_{y_0}\ddot{\alpha} + h\dot{\alpha} - H\dot{\varphi}\cos\alpha + H\dot{\gamma}\sin\alpha = 0 \qquad [2]$$

where

- J_{y_0} = moment of inertia of gyro, together with all structural elements connected with it, about y_0 axis
- h = damping coefficient
- H = angular momentum of gyro
- α = angle between gyro spin axis x_0 and longitudinal axis x of vehicle

In an integrating gyro the maximum value of the angle α is limited to not more than 5 or 10 deg. In addition, the time constant of the integrating gyro

$$T_* = (J_{y_0}/h) \ll 1 \qquad [3]$$

amounts to 0.005 sec or less.

We introduce the notation

$$k = H/h \qquad [4]$$

where k is a scale coefficient, usually taken to equal unity. Taking Equations [1, 3 and 4] into account and expanding $\sin\alpha$ and $\cos\alpha$ in powers of small α, we obtain instead of Equation [2]

$$T_*\ddot{\alpha} + \dot{\alpha} = k\varphi_0\omega\left(1 - \frac{\alpha^2}{2!} + \frac{\alpha^4}{4!} - \ldots\right)\cos\omega t - k\gamma_0\omega\left(\alpha - \frac{\alpha^3}{3!} + \ldots\right)\cos(\omega t + \delta) \qquad [5]$$

The first-approximation equation is

$$T_*\ddot{\alpha} + \dot{\alpha} = k\varphi_0\omega\cos\omega t \qquad [6]$$

From this, integrating, we obtain for zero initial conditions

$$\alpha_1 = \frac{k\varphi_0}{1 + T_*^2\omega^2}[\sin\omega T_*\omega(\cos\omega t - 1)] \qquad [7]$$

To find the second approximation, we substitute for α in the right half of Equation [5] its first approximation from [7] and neglect small quantities of the order α^2 and higher, obtaining

$$T_*\ddot{\alpha} + \dot{\alpha} = k\varphi_0\omega\cos\omega t - \frac{k^2\omega\varphi_0\gamma_0}{1 + T_*^2\omega^2}[\sin\omega t - T_*\omega(\cos\omega t - 1)]\cos(\omega t + \delta) \qquad [8]$$

Integrating this equation for zero initial conditions and

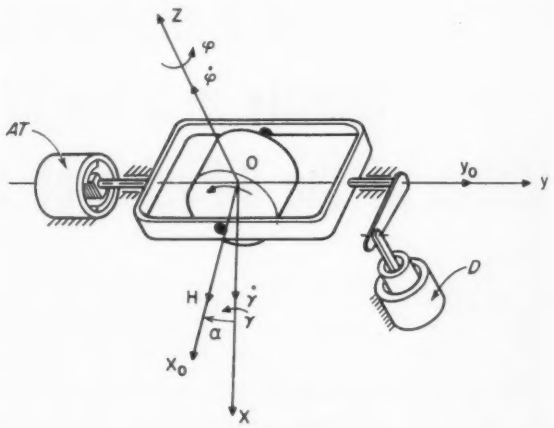

Fig. 1

Translated from *Izvestiia Vysshikh Uchebnyk Zavedenii, Priborostroenie* (News of the Higher Institutions of Learning, Instrument Building), no. 2, 1959, pp. 56–58.

neglecting small quantities of the order of $T_*^2\omega^2$, we obtain

$$\alpha_z = k\varphi_0 \sin \omega t - k\varphi_0 T_*\omega(\cos \omega t - 1) - \tfrac{1}{4}k^2\varphi_0\gamma_0[(\sin \delta - 3T_*\,\omega \cos \delta) \sin 2\omega t - (\cos \delta + 3T_*\,\omega \sin \delta) \cos 2\omega t] + \tfrac{1}{2}k^3\varphi_0\gamma_0\omega(\sin \delta - T_*\omega \cos \delta)[t - T_*(1 - e^{-t/T_*})] \quad [9]$$

Since usually the frequency ω of the angular oscillations of the base is small and the time constant T_* of the integrating gyro does not exceed 0.005 sec, the motion of the gyro can be described with sufficient accuracy by the equation

$$\alpha_z = k\varphi_0 \sin \omega t - k\varphi_0 T_*\,\omega(\cos \omega t - 1) - \tfrac{1}{4}k^2\varphi_0\gamma_0[(\sin \delta - 3T_*\omega \cos \delta) \sin 2\omega t - (\cos \delta + 3T_*\omega \sin \delta) \cos 2\omega t] + \tfrac{1}{2}k^2\varphi_0\gamma_0\omega(\sin \delta - T_*\omega \cos \delta)(t - T_*) \quad [10]$$

In Equation [10] the term $k\varphi_0 \sin \omega t$ determines the useful precession (output angle) of the gyro, which enables the instrument to develop a signal directly proportional to the angle φ of rotation of the vehicle about its normal axis z, a signal used to stabilize the vehicle in attitude. The remaining term of the right half of [10] determines the instrumental error. Here, inasmuch as the amplitudes φ_0 and γ_0 of the angular oscillations of the object are usually small, the second and third terms of the right half of [10] determine the additional small-amplitude oscillations of the gyro. The fourth term indicates that angular oscillations of the base simultaneously about the z and x axes give rise to a term of an increasing instrumental error (steady-state drift). As can be seen from Equation [10], the equation of the secular term has a maximum value when $\delta = \pi/2$.

Let, for example

$$\varphi_0 = \gamma_0 = 1 \text{ deg} \qquad k = 1$$
$$f = (\omega/2\pi) = 1 \text{ cps} \qquad \delta = (\pi/2) \quad [11]$$

From Equation [10] we obtain, allowing for [11]

$$\alpha_z = 1 \text{ deg} \sin 2\pi t - \frac{1 \text{ deg}}{4 \times 57.3} \sin 4\pi t + \frac{1 \text{ deg}\,\pi}{57.3}(t - T_*) \quad [12]$$

where t is in seconds and α_z is in degrees of angle.

As can be seen from Equation [12], the second term of this equation can be neglected compared to the first. Then, considering the smallness of the time constant T_*, we obtain for the instrumental error

$$\Delta\alpha \approx 0.005 \times t \text{ deg} \quad [13]$$

Thus, under the foregoing parameters of motion, within three minutes after the start of oscillations of the vehicle, the error in the instrument already attains a magnitude on the order of 10 deg.

If necessary it is possible to obtain the third and subsequent approximations for α. However, for practical calculations the second approximation given by Equation [10] is sufficient, and the error of the instrument can be obtained with sufficient accuracy from the expression

$$\Delta\alpha = \tfrac{1}{2}\frac{H^2}{h^2}\varphi_0\gamma_0\omega t \sin \delta \quad [14]$$

It is seen from Equation [14], incidentally, that the sign of the error is determined by the sign of δ.

—*Original received January 27, 1959*

Reviewer's Comment

The author considers the effect of sinusoidal angular motion about input and spin axes on the drift of single-degree-of-freedom integrating gyros rigidly mounted to a vehicle. The oscillations in question are of the same frequency and thus correspond to a coning motion of the vehicle. Using the equation of torque about the output axis, he obtains a result which indicates a steady-state drift rate due to this motion. The result is obtained by primarily algebraic methods, by a method of successive approximations to the basic differential equation. A solution is first obtained by neglecting all terms above first order; this solution is then applied to the equation and second-order terms are considered in obtaining a second approximation. The result is the same equation of steady-state drift derived by Cannon in "Kinematic Drift of Single-Axis Gyroscopes" (*J. Appl. Mech.* Paper no. 57-A-72). Cannon's result is somewhat more general and the treatment is geometric rather than algebraic.

Similar phenomena are discussed by Goodman and Robinson (*J. Appl. Mech.* Paper no. 57-A-30, "Effect of Finite Rotations on Gyroscopic Sensing Devices"), and in an unpublished thesis by Haff and Meltzer, MIT Aeronautics and Astronautics Dept., May 1960, where a completely general approach was used.

—Elmer J. Frey
Instrumentation Laboratory
Massachusetts Institute of Technology

Determination of Atmospheric Density at a Height of 430 km by Means of the Diffusion of Sodium Vapors

I. S. SHKLOVSKII and V. G. KURT

IN RECENT times our ideas about the basic physical characteristics of the upper layers of the atmosphere, such as the density and temperature, have undergone significant changes. Observations of the drag on Soviet and American satellites have made it possible to determine the density of the atmosphere at 220 to 750 km (1–4).[1] It was found that the density at these altitudes was many times larger than had been concluded earlier on the basis of rocket data. Together with this the scale height appeared to be significantly greater than was assumed earlier, indicating a higher temperature for

Translated from "Iskusstvennyye Sputniki Zemli" (Artificial Earth Satellites), USSR Academy of Sciences, Moscow, 1959, no. 3, pp. 66–76. Translation provided by the U. S. Joint Publication Research Service.

[1] Numbers in parentheses indicate References at end of paper.

the upper atmosphere.

In view of the extreme importance of these results, it would be very desirable to confirm them independently, since data on atmospheric density obtained from the analysis of the drag of satellites may involve systematic errors. For example, the problem of the so-called "electrical drag" (3) is not yet entirely clear. It is not easy to take into account the influence of the shape of the satellite with sufficient accuracy, and this may also have an effect on the errors. Finally, and perhaps most importantly, from observations of satellite drag one obtains only *average* values of the density. Yet we have now important indications that the density and temperature of the upper atmosphere are subject to local variations (5). As a result one must expect systematic differences of the basic characteristics of the upper atmosphere in the polar and the equatorial regions.

Thus it becomes necessary to develop a method of obtaining, at a given point and over a rather short period of time, the basic characteristics of the upper atmosphere from a single experiment.

As the most reasonable of such methods, we consider the analysis of the diffusion of sodium vapors released at a given altitude in the upper atmosphere by a rocket. The idea of investigating the upper atmosphere by introducing a small quantity of sodium vapors into it is due to Bates (6) and to several others whose papers (7–9) concern work already carried out in the United States. These articles are devoted to the study of elementary processes that cause the emission of light from sodium in the upper atmosphere. Sodium vapor is released at relatively low altitudes, 75–140 km, while the rockets are in motion, so that long, narrow, luminous bands are observed in the cloud. The problem of determining the basic characteristics of the atmosphere—the density and temperature—had not yet been solved at the time of these experiments. As will be seen later, the problem is incapable of solution, since entirely inadequate flight altitudes have been used for this purpose.

The first experiment to determine the density of the upper atmosphere by this method was made Sept. 19, 1958 with a high altitude rocket.

Descriptions of a few other experiments made with similar rockets had been published at the time (10). In our experiment, the altitude reached by the rocket was 430 km. In the rocket head were located two sodium evaporators, each containing 2 kg of metallic sodium and a corresponding quantity of thermite. The thermite was ignited at a predetermined moment when the rocket was near the top of its trajectory. The sodium vapor was ejected into the atmosphere through a nozzle in a direction perpendicular to the axis of the rocket, which was stabilized. The evaporation process lasted 10–20 sec. During all of this time the rocket was not far from the top of its trajectory.

At the time of this experiment, which was carried out before sunrise, the height of Earth's shadow at the observation point was within the limits 300–250 km. Therefore, the cloud of sodium vapor formed as a result of the evaporation process was illuminated by the sun's rays, and resonant fluorescence caused intense scattering in the D_1 and D_2 lines. A succession of photographs of this cloud was taken with a camera (f = 58 mm, d/f = 1:2) provided with an OS-14 light filter. All the photographs were calibrated. In addition, to get absolute values of the emission intensity of the cloud, a standardization was carried out by relating an out-of-focus exposure of the stars to it. The photographs obtained were developed according to standard astrophysical practice.

In Fig. 1 are shown successive photographs of different stages of growth of the cloud formed. The scale of the frames is always the same (36 × 24). The average exposure time is given for each photograph.

It can be noted that in the first instants after evaporation the shape of the cloud was rather irregular, but even at ap-

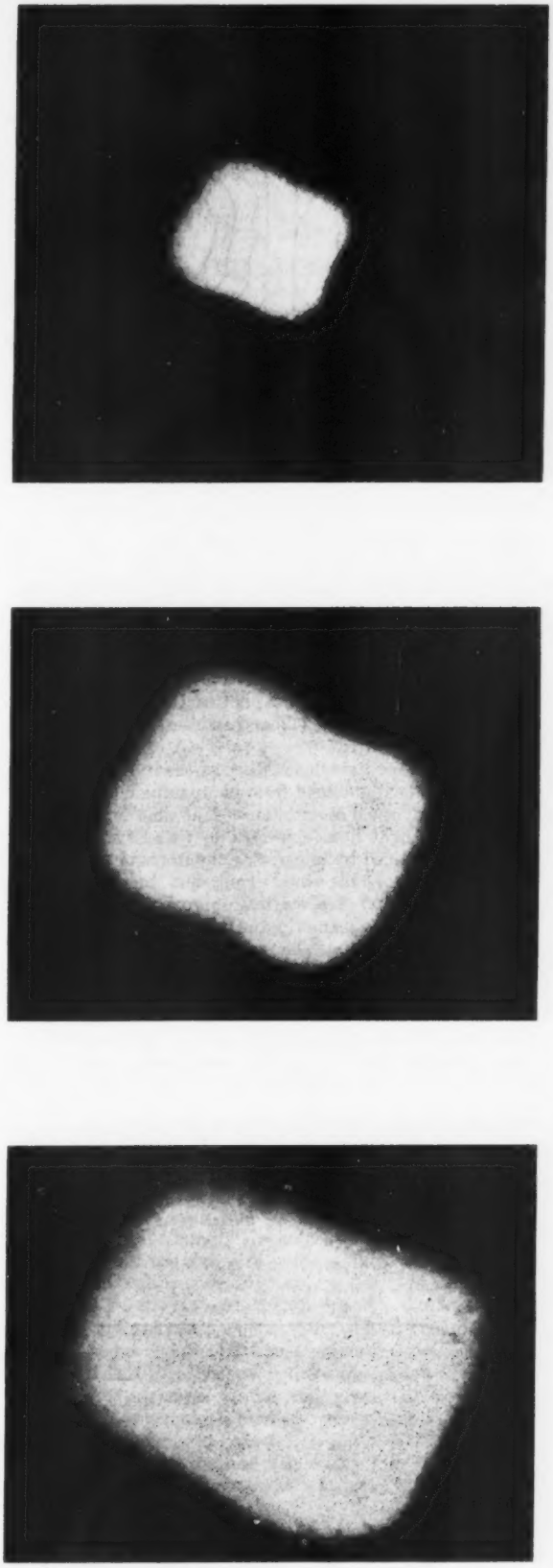

Fig. 1 Stages of development of sodium cloud. Top to bottom, at 5 sec, 20 sec and 35 sec

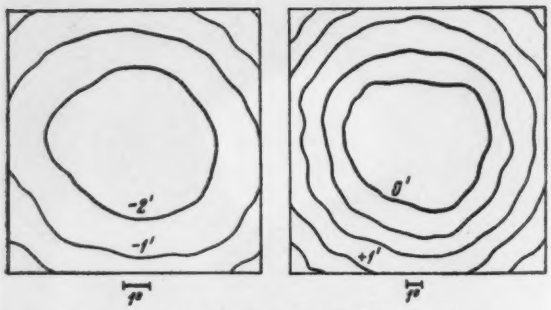

Fig. 2 Isophots of sodium cloud at 90 and 270 sec

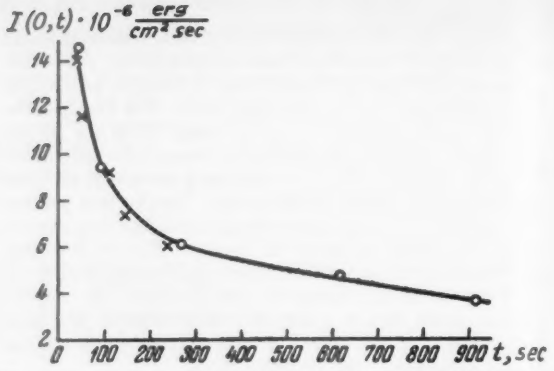

Fig. 3 Dependence of the brightness of the center of the sodium cloud on the time. ○—photographic observations, ×—photoelectric observations

proximately 100 sec the cloud assumed a circular outline and this tendency continuously increased with time. This is seen especially clearly from isophots of the cloud, which give the distribution of intensities for 90 and 270 sec (from the start of sodium evaporation) as shown in Fig. 2. Together with the photographic observations, photoelectric observations were made of the brightness of the center of the cloud. For this purpose we used a photoelectric photometer having an objective of $f = 100$ mm, $d/f = 1{:}2$, and an interference light filter with $\Delta\lambda = 30$ Å.

Fig. 3 shows the time dependence of the brightness of the center of the cloud obtained from photographic (circles) and photoelectric (crosses) observations. The time dependence of the mm total light flux (expressed in visual stellar magnitudes) was obtained by integrating the isophots. As can be seen from Fig. 4, the total light flux increases rather quickly initially, and then, starting approximately at 100 sec, remains practically constant for the next 15 min (during which observations were made). The relative smallness of the total flux in the initial stages of dispersion of the cloud are due to the considerable self-quenching. When the optical thickness of the dispersed cloud becomes significantly less than unity (which happens at approximately 100 sec) the total flux becomes constant. At this point the visual stellar magnitude of the cloud is about 8.1, in agreement with theoretical expectations.

It is important to emphasize that there are a large number of independent observations of the sodium cloud, made from different points sufficiently far away from the rocket launching point. All observers emphasize the fact that the cloud spreads out in all directions in the same way and has a circular form, at least during the first 10 min. During this time the center does not change its position with respect to the horizon of the place of observation. These independent observations showed that the spatial structure of the cloud was close to spherical and that the center of this sphere remained approximately at a constant height.

The sodium cloud formed first spread out rather quickly and then quite slowly. In Fig. 5 is given the time dependence of the square of the effective radius of the cloud S (determined from the isophot that has a surface brightness $1/e$ times the central value). As can be seen from this figure, all the points fit a straight line very well. Consequently, the relation

$$S \sim t^{1/2} \qquad [1]$$

holds, which, as is well-known, is a characteristic property of diffusion processes. From this empirical dependence it is not difficult to evaluate the concentration of atmospheric atoms in the region of sodium diffusion.

As is known, the mean displacement of a particle, resulting from diffusion, in some definite direction from the center (where the particle is located at the initial moment), will be after a time t

$$s = (n/3)^{1/2}\bar{l} \qquad [2]$$

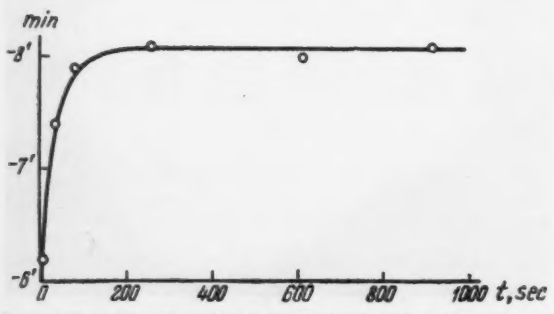

Fig. 4 Dependence of the integral visual stellar magnitude of the cloud on the time

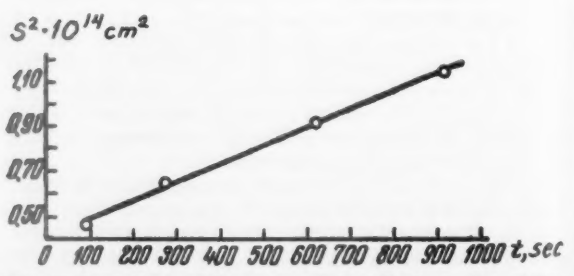

Fig. 5 Dependence of the square of the effective radius of the cloud on the time

where

l = mean free path length

n = number of collisions in a time t

Since $n = vt$ (where v is the mean velocity of the particle)

$$s = \sqrt{(1/3)v\bar{l}\,t} \qquad [3]$$

The quantity $(1/3)v\bar{l}$ (which is nearly the diffusion coefficient D) can be found directly from the graph made from the observations, given in Fig. 5. It is equal to 0.85×10^{11} cm^2 sec^{-1}. The mean velocity of the sodium atoms is

$$v = \sqrt{8kT/\pi m_{Na}} = 1.5 \times 10^5 \text{ cm/sec (for } T = 1600 \text{ deg)}$$

Hence $\bar{l} = 1.7 \times 10^6$ cm $= 1/n_1\bar{Q}_D$, where n_1 is the concentration of atoms in the atmosphere, and $\bar{Q}_D$ is the effective collision cross section, which we take equal to 3.85×10^{-15} cm^2 (see below). Hence

$$n_1 = 1.6 \times 10^9 \text{ cm}^{-3} \qquad [4]$$

If the atoms in the atmosphere at 430 km are essentially nitrogen and oxygen, then the density is

$$\delta = 4.7 \times 10^{-15} \text{ g/cm}^3 \qquad [5]$$

This value agrees well with the value for the density of the atmosphere obtained from an analysis of the drag on satellites.

We shall now solve more rigorously the problem of determining the density of the atmosphere from observations of the diffusion of a sodium cloud. In doing this we disregard, in first approximation, the influence of gravity on the process of diffusion. According to the calculations of Mitra and Rakshit (11), at 350 km (which was taken by them in accordance with the old model for the concentration of atoms in the atmosphere and which was close to the value expected for our experiment), the time of effective separation of N_2 and O_2 is about 3 hr. We note further that in our case (diffusion of sodium through atomic nitrogen and oxygen) the time of diffusion separation should be even greater, owing to the relative closeness of the atomic weights of the diffusing components. Since the time of observation (about 15 min) was less than the time of effective diffusional separation, the neglect of the effect of gravity could be considered reasonable.

We write the differential equation of diffusion for the spherically symmetric problem

$$\frac{\partial N}{\partial t} = D\left(\frac{\partial^2 N}{\partial R^2} + \frac{2}{R}\frac{\partial N}{\partial R}\right) \qquad [6]$$

where

N = concentration of sodium atoms

D = diffusion coefficient

The solution of this equation is [see, for example, (12)]

$$N = \frac{1}{2\sqrt{2\pi Dt}}\frac{1}{R}\int_0^\infty \Phi(\rho)\left\{e^{-\left(\frac{R-\rho}{2\sqrt{Dt}}\right)^2} - e^{-\left(\frac{R+\rho}{2\sqrt{Dt}}\right)^2}\right\}\rho d\rho \qquad [7]$$

where $\Phi(\rho)$ represents the distribution of diffusing sodium atoms at the time $t = 0$. We assume that the initial instant $\Phi = N_0$ within a sphere of radius R_0 and is equal to zero outside this sphere. The solution of Equation [6] is

$$N(R, t) = \frac{N_0}{2}\left\{\psi\left(\frac{R_0 - R}{2\sqrt{Dt}}\right) + \psi\left(\frac{R + R_0}{2\sqrt{Dt}}\right) + \frac{\sqrt{Dt}}{R\sqrt{\pi}}\left[e^{-\left(\frac{R_0+R}{2\sqrt{Dt}}\right)^2} - e^{-\left(\frac{R_0-R}{2\sqrt{Dt}}\right)^2}\right]\right\} \qquad [8]$$

where

$$\psi(z) = \frac{2}{\sqrt{\pi}}\int_0^z e^{-\xi^2}\,d\xi$$

Assuming $R \to 0$, we find the following law for the variation of concentration at the center of the diffusing cloud

$$\frac{N(0, t)}{N_0} = \psi\left(\frac{R_0}{2\sqrt{Dt}}\right) - \frac{R_0}{\sqrt{4\pi Dt}}\,e^{-R_0^2/4Dt} \qquad [9]$$

From Equation [9] we can determine the diffusion coefficient (and consequently also the concentration of the atoms in the atmosphere), provided it can be determined from the observations of the time variation of $N(0, t)/N_0$.

To solve the problem we must therefore first determine from observations values of $N(0,t)/N_0$ at different times, in relative units. The magnitude of $N(R,t)$ can be obtained for a given instant of time from the distribution of intensities in the sodium cloud (which is given by the isophots) through the use of the procedures usually employed in similar problems in astrophysics. $N(R, t)$ is proportional to the amount of energy $F(R, t)$ scattered by a unit volume of the sodium cloud. The surface brightness $I(\rho, t)$ is connected with the quantity $F(R, t)$ through the Abel integral equation

$$I(\rho, t) = \int_{-\infty}^{\infty} F(R, t)dy \qquad [10]$$

where the integration is carried out over the field of illumination. The solution of Equation [10], as is well-known, is

$$F(R, t) = -\frac{1}{\pi}\int_r^\infty \frac{dI(\rho, t)/d\rho}{\sqrt{\rho^2 - R^2}}\,d\rho \qquad [11]$$

The integration of Equation [11] can be carried out in closed form if the observed intensity is approximated, after correction for errors in the field of the photometer, by the function

$$I = I_0 e^{-k^2\rho^2} \qquad [12]$$

where I_0 is the value of the intensity at the center of the cloud. Then we have

$$N(R, t) - F(R, t) = \frac{I_0(t)k(t)}{\sqrt{\pi}}\,e^{-k^2R^2} \qquad [13]$$

We note that in this calculation the scattering is assumed to be spherical. Actually this is, naturally, not the case. A similar situation occurs in the determination of the electron concentration in the corona from the surface brightness of the sun; there the dispersion of scattering angles is significantly greater than in the case at hand. A calculation of anisotropic scattering in the corona, made in (13), leads to a change in the absolute values of N (relative to spherical scattering) of 20–30 per cent. In our case, these changes will be even smaller. Furthermore, we are concerned with the *relative* changes in N, which depend to an even smaller degree on the type of scattering.

The observed distribution of intensity $I(\rho, t)$ can be approximated to a sufficient degree of accuracy by Equation [12].

We obtain values of $1/k(t)$ for the following times: 92 sec–66.5 km, 270 sec–80.5 km, 620 sec–95.5 km, and 920 sec–107.5 km.

Since the light flux becomes constant at later stages of

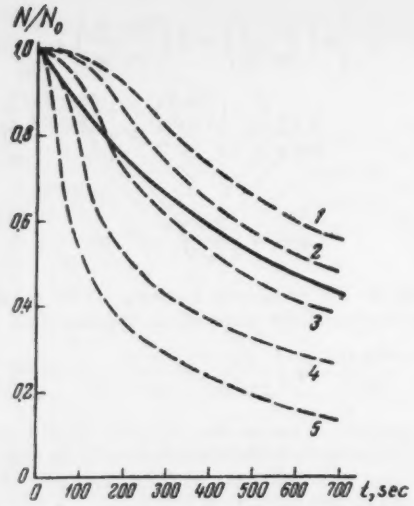

Fig. 6 Relative concentration of sodium atoms as a function of time for the center of the cloud. Solid line—experimental curve, dotted lines—family of curves for various values of the diffusion coefficient D. 1—$D = 0.37 \cdot 10^{-11}$, $n_1 = 4 \cdot 10^{-6}$; 2—$D = 0.45 \cdot 10^{-11}$, $n_1 = 3 \cdot 10^{-6}$; 3—$D = 0.74 \cdot 10^{-11}$, $n_1 = 2 \cdot 10^{-6}$; 4—$D = 1.47 \cdot 10^{-11}$, $n_1 = 10^{-6}$; 5—$D = 2.95 \cdot 10^{-11}$, $n_1 = 0.5 \cdot 10^{-6}$

growth of the cloud (see Fig. 4), the following relationship must hold

$$\pi I_0(t)/k^2(t) = L = \text{constant} \qquad [14]$$

Furthermore, from (13) for $R = 0$ we have

$$\frac{N(0, t)}{N_0} = \frac{k(t)I_0(t)}{k(0)I_0(0)} = \left\{\frac{I_0(t)}{I_0(0)}\right\}^{3/2} \qquad [15]$$

In the solution of Equation [6] we assume that $N(R, 0) = N_0$ inside a sphere of radius R_0, where R_0 is determined from the relation

$$\frac{4}{3}\pi R_0^3 N_0 = \frac{N_0 \pi^{3/2}}{[k(0)]^3} \qquad [16]$$

In other words, we approximate the initial distribution by a homogeneous sphere with a concentration of sodium atoms equal to the actual concentration at the center at the initial time. In this case

$$R_0 = \frac{\pi^{1/3}}{k(0)}\sqrt[3]{\frac{3}{4}} = \frac{1.10}{k(0)} \qquad [17]$$

The initial time is taken at $t = 270$ sec. The isophots for the cloud became practically circular at this time. We may note that almost the same result is obtained if $t = 90$ sec is taken as the initial time. This shows the slight dependence of the solution of Equation [6] on the choice of the initial time.

In Fig. 6 are shown the time dependence of $N(0, t)/N_0$ obtained directly from observations (solid curve) and a family of curves showing the dependence of $N(0, t)/N_0$ at given initial conditions for various values of the diffusion coefficient.

It can be seen from this figure that the concentration obtained from observations corresponds best to a value of the diffusion coefficient

$$D = 0.59 \times 10^{11} \text{ cm}^2 \text{ sec}^{-1}$$

It is known from (14) that the diffusion coefficient is connected with the concentration of atoms through which diffusion occurs by the expression

$$D = \frac{3\pi}{32} \times \frac{V}{n_1 \bar{Q}_D} \qquad [18]$$

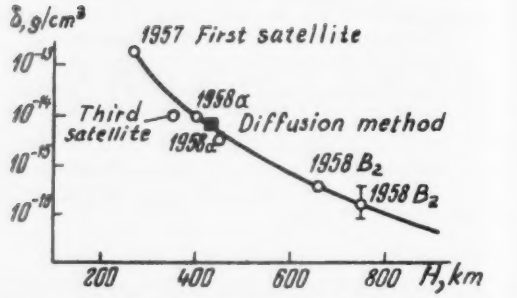

Fig. 7 Density of the atmosphere according to data from the drag on artificial Earth satellites. ■—point corresponding to our measurements

where

$V = \sqrt{\frac{8kT}{\pi}} \times \sqrt{\frac{M_1 + M_2}{M_1 M_2}}$ is the average relative velocity

M_1, M_2 = masses of atoms of the atmosphere and sodium

$\bar{Q}_D$ = effective diffusion cross section equal to πa^2

a = diameter of the atom considered as a solid sphere.

As is well-known, such a representation of collisions in diffusion processes leads to very small errors, provided the temperature is not too low. The magnitudes of a do not vary greatly for different gases (15). For our purpose it can be assumed with sufficient accuracy that $a = 3.5 \times 10^{-8}$ cm, whence $\bar{Q}_D = 3.85 \times 10^{-15}$ cm^2.

The temperature of the sodium atoms must be rather close to the temperature of the atoms of the atmosphere, since each atom of sodium will have time to collide several dozen times with atmospheric atoms and will, as a result, assume their temperature. Judging from the fact that the cloud spread out to about 100 km while maintaining its circular form, the height of the homogeneous atmosphere must be not less than 100 km.[2]

It is quite natural to assume that at such heights the basic constituent of the atmosphere is atomic oxygen. From this we conclude that the temperature of the atmosphere must be more than 1600 deg. We shall assume this value in calculating n_1 from Equation [18]. It is apparent that even relatively large changes in the assumed temperature of the atmosphere have only a slight effect on the value obtained for the concentration of the oxygen atoms, which is equal to

$$n_1 = 2.5 \times 10^8 \text{ cm}^{-3} \qquad [19]$$

from which, on the hypothesis that the atmosphere consists principally of atomic oxygen and nitrogen, we obtain the following value for the density

$$\delta = 6.7 \times 10^{-15} \text{ g/cm}^{-3} \qquad [20]$$

[2] We may remark, however, that the exact determination of the height of the homogeneous atmosphere requires specially made observation.

Our determination of the concentration of atoms in the atmosphere includes, as must any determination, a certain probable error. The diffusion coefficient D is obtained directly from the observation. To obtain n_1 from D it is necessary to know the effective diffusion cross section $\bar{Q}_D$ for sodium in oxygen and nitrogen. The experimental value of $\bar{Q}_D$ is unknown. The spread of the values of a for various vapors of interacting atoms and molecules is not large. However, an error of 20–30 per cent in the value of $\bar{Q}_D$ used by us (3.85×10^{15} cm^2) is entirely possible. Other possible errors in the determination of n_1 from observations (for example, an inexact approximation in taking the expression $I = I_0 e^{-k\rho z}$, irregular density of the atmosphere at the edges of the cloud, or wrongly neglecting the force of gravity) are obviously less essential. Thus we can estimate the probable error of our determination of n_1 as 30 per cent, i.e.

$$n_1 = (2.5 \pm 0.75) \times 10^9 \text{ cm}^{-3} \qquad [19a]$$

The value of the density of the atmosphere at 430 km obtained by us from an analysis of the diffusion of a sodium cloud can now be compared with data obtained from the analysis of the drag of artificial satellites. According to (1), at a height of 450 km the density deduced from an analysis of the drag on the satellite 1958α (Explorer I) is equal to $(9 \pm 6) \times 10^{15}$ g/cm^3. According to the data of (2), obtained from an analysis of the drag on the same satellite, at 450 km the density is 3×10^{-15} g/cm^3. Our value $(6.7 \pm 2) \times 10^{15}$ g/cm^3 is evidently in very good agreement with the data obtained from the satellites.

We note further that on the basis of data on the electron concentration in the outer regions of the ionosphere, obtained in (16) from observations of the radio signals from the first Soviet satellite, starting with the assumption that ionization is in equilibrium at 400 km, the value of the concentration of neutral atoms is found to be equal to 5×10^8 cm^{-3}. Extrapolating this value to 430 km we obtain a concentration equal to $(3.2 \text{ to } 3.5) \times 10^8$ cm^{-3}, i.e., 30–40 per cent greater than our value.

Thus we can conclude that methods based on completely different physical principles give (within the limits of observational errors) the same values for the density of the atmosphere at 400–450 km.

In Fig. 7 are shown the results presently available in the literature for the density of the upper atmosphere as determined from observations of the drag on Soviet and American satellites, as well as the result obtained from the method described in this paper. The curve is obtained from the condition that best represents the results of observations. Naturally, this curve gives only an average picture. Obviously, at such great heights there must actually be significant changes in density with time and position. Further systematic observations of the diffusion of artificial sodium vapor clouds in the upper atmosphere would enable us to discover such variations.

The method described for the determination of the density of the atmosphere can be applied over a large range of altitudes. The lower limit of this range is determined by the condition that during the time of observation (about 10 min) the atoms of sodium should not "vanish" from Earth's atmosphere as a result of chemical reactions. This height can apparently be taken at around 300 km. We may remark that if an experiment is carried out at such relatively low altitudes, the linear dimensions of the cloud will be approximately 10 times smaller at corresponding times than in our experiment. Thus only a small amount of sodium need be evaporated—20 or 30 g. Otherwise the optical density of the cloud will be significantly greater than unity, which would make photometric analysis impossible.

It can be assumed that the upper limiting region in the atmosphere where the method of determining the density is applicable lies between 500 and 600 km. On the other hand, it is not impossible that our method would be applicable at even higher altitudes if the hydrogen content there is significantly greater than has usually been assumed. This latter possibility can by no means be ruled out. We emphasize once more that the release of sodium vapors in the atmosphere must be carried out near the top of the rocket trajectory, and not during its upward motion as described in (7–9).

Simultaneously with the determination of density by the diffusion method, it is possible to determine the temperature of the atmosphere, which is of great interest. The solution of this problem requires a special technique. The question will be considered in another paper.

References

1 LaGow, H. E., Horowitz, R. H. and Ainsworth, I., IGY World Data, Center A. Rockets and Satellites, 145, 1958.

2 Siry, J. W., U.S. Naval Res. Lab., Washington, D. C., Fifth General Assembly of CSAGI 30, June 1958.

3 Harris and Jastrow, Nucl. Naval Res. Lab., Washington, D. C., Fifth General Assembly of CSAGI 30, June 1958.

4 Lidov, M. L., "Iskusstvennye Sputniki Zemli," (Artificial Earth Satellites), no. 1, 1958. Translation published by Plenum Press, N. Y.

5 Krasovskii, V. I., Report During the Fifth Assembly of the IGY, Moscow, 1958.

6 Bates, D. R., *J. of Geophys. Res.*, vol. 55, 1950, p. 347.

7 Edwards, H. D., Bedinger, J. F., Manring, E. R. and Cooper, C. D., "The Airglow and Aurorae," London 1956, p. 122.

8 Bedinger, J. F., Ghosh, S. N. and Manring, E. R., *Trudy konferentsii po kosmicheskomu prostranstvu* (works of the Conference on Cosmic Space), 1958, p. 225.

9 Bedinger, J. F., Manring, E. R. and Ghosh, S. N., *J. of Geophys. Res.* vol. 63, no. 1, 1958, p. 19.

10 Gringauz, K. I., DAN SSSR (Trans. USSR Academy of Sciences), vol. 120, no. 6, 1958, p. 1234. Translated in *Soviet Phys.-Doklady*, vol. 3, 1959, p. 620.

11 Mitra, S. K. and Rakshit, H., *Indian J. Phys.*, vol. 12, 1938, p. 47.

12 Frank and von Mises, "Differential and Integral Equations of Mathematical Physics" (Russian translation) ONTI, 1937, p. 637.

13 Bogorodskiy, A. F. and Khinkulova, N. A., *Byull. komissii po issledovaniyu Solntsa* (Bull. of the Commission on Solar Investigation), no. 5, 1950, p. 6.

14 Massey, H. S. and Burhop, E. H. S., "Electronic and Ionic Impact Phenomena" (Russian translation), Moscow, 1958, p. 318. (Oxford Univ. Press, 1952.)

15 Jeans, J., "The Dynamical Theory of Gases," Cambridge Univ. Press, 1921, p. 323.

16 Al'pert, Ya. L., Dobrokhotov, F. F., Chudesenko, E. F. and Shapiro, B. S., DAN SSSR (Trans. USSR Academy of Sciences), vol. 120, 1958, p. 743. Translated in *Soviet Phys.-Doklady*, vol. 3, 1959, p. 584.

Reviewer's Comment

The experiment described and interpreted in this paper is unique in that for the first time the injection of sodium in the high atmosphere was successfully accomplished at so great an altitude that the observation of its diffusive expansion could be used to infer atmospheric densities at levels which permit comparison with data derived from the analysis of satellite drag. Other investigators in addition to American groups, notably the French in the Sahara, and the British at Woomera in Australia, continue to pursue such work at lower altitudes. Their studies help to delineate more fully characteristics of the atmosphere in that region. However, the Soviet high altitude experiment is most useful because it is, until now, the sole direct independent means of verifying densities inferred from Satellite drag. Moreover, the future promise of the method for arriving at an estimate of the atmospheric temperature at these altitudes is especially noteworthy in view of the many efforts currently being made to assess the magnitude and variability of that elusive parameter.

—Phillip W. Mange
U. S. Naval Research Laboratory

Inertial Method of Velocity Measurement

V. N. DROZDOVICH

Leningrad Institute of Precision Mechanics and Optics

ALONG with the known methods of velocity measurement, based on the gyrodynamic and on the Doppler effects, methods based on the integration of accelerations are gaining wide use at the present time. Measurement of velocity by integrating the acceleration serves as the basis of the so-called inertial system of navigation, used to solve the complex problem of guiding a moving object along a specified trajectory (1).[1] In spite of many undisputed advantages, the integration of accelerations entails many systematic and random errors under ordinary conditions of low velocities and long time intervals (2). In this connection, it is of interest to evaluate these errors when they can be exactly accounted for, or to determine their statistical behavior if they are of random nature.

An attempt is made in this article to investigate the systematic errors due to Coriolis and centripetal accelerations, and to evaluate these errors when velocity is measured over prolonged intervals of time. The role of Coulomb friction is explained and an estimate is given of the static error due to this friction.

Equations of Motion

Imagine a gyroscope in a Cardan suspension mounted on an accelerated base (Fig. 1). The center of gravity of the gyroscope is assumed to coincide exactly with the stationary point of the suspension; the axis of this gyroscope is directed upward, making a small angle with the local vertical. Mounted on the gyroscope housing are two precision accelerometers, the sensitive axes of which are perpendicular to the axis of the gyroscope and are at right angles to each other. The accelerometers are connected in series with integrators in a torque-transducer circuit, and comprise an integral-control vertical correction network, resulting in a gyro vertical with integral correction, having the same properties as a regulator type of automatic control system. Hence, such a gyro vertical will assume plumb-line direction, accurate to ballistic deviations.

Let us associate with the gyroscope a horizontal system of coordinates $ox_0y_0z_0$, the origin of which is at the gyroscope center of mass (Fig. 2). The axes ox_0 and oy_0 are located in the plane of the horizon and form with the oz_0 axis, which is directed vertically upward, a right-handed system of coordinates. We assume from now on that the axis of rotation of the outer gimbal of the suspension coincides with the ox_0 axis. We leave the orientation of the ox_0 and oy_0 axes in the plane of the horizon undefined for the time being.

We associate with the gyroscope housing a rigidly fixed system of coordinates $oxyz$, the axes ox and oy of which are located in the equatorial plane of the gyroscope and form with the oz axis a right-hand system of coordinates, which is directed along the axis of the gyroscope in the figure. The oy axis will be aligned with the axis of rotation of the gyroscope casing.

With such a choice of coordinate systems, the position of the gyroscope casing will be defined uniquely by two angles α and β, equal respectively to the angles between y_1 and y_0 and x_1 and x_0.

We introduce the following notation

$\bar{\omega}_a$ = vector of angular rotation of system $ox_0y_0z_0$ relative to a certain inertial system of coordinates

$\bar{\omega}_r$ = vector of angular velocity of system $oxyz$ about the horizontal

$\bar{\omega}$ = vector of absolute angular velocity of system $oxyz$

$\dot{\varphi}$ = angular velocity of gyroscope rotor relative to housing

J = polar moment of inertia of gyroscope rotor

J_e = equatorial moment of inertia of gyroscope rotor plus casing

M_x, M_y, M_z = components of external torque applied to gyroscope casing on axes of system $oxyz$

v_x, v_y = horizontal components of velocity of object over Earth's surface

ω_1, ω_2 = horizontal and vertical components, respectively, of angular velocity of Earth's rotation

ψ = angle between vector $\bar{v}$ of true velocity of object and meridian, measured westward

γ = angle between ox_0 axis and vector $\bar{v}$, measured westward from ox_0 axis

R = radius of Earth

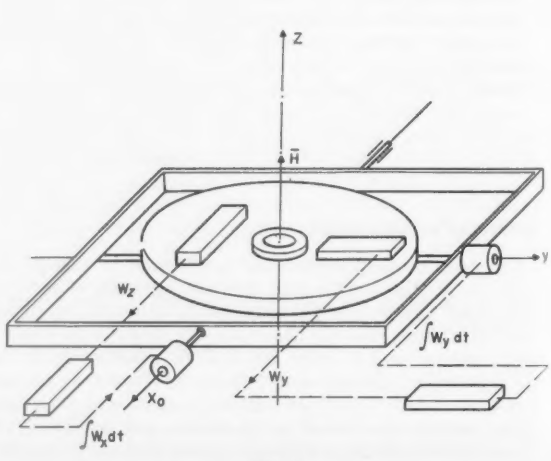

Fig. 1

Translated from *Izvestiia Vysshykh Uchebnykh Zavedenii, Priborostroenie* (Bull. Higher Institutions of Learning, Instrument Building), no. 3, 1959, pp. 29–30.

[1] Numbers in parentheses indicate References at end of paper.

We assume henceforth that the object moves along a great circle, and the ox_0 and oy_0 axes will be so related to the object that ox_0 is along the longitudinal axis of the object. We assume that γ remains constant during the entire time of motion.

Bearing in mind that

$$\bar{\omega} = \bar{\omega}_e + \bar{\omega}_r$$

and projecting this vector equation on $oxyz$ axes, we obtain

$$\begin{aligned}
\omega_x &= \dot{\alpha} + \omega_{ex}\cos\beta - \omega_{ez}\sin\beta \\
\omega_y &= \dot{\beta} + \omega_{ey}\cos\alpha + \omega_{ez}\sin\beta\sin\alpha + \omega_{ez}\cos\beta\sin\alpha \\
\omega_z &= \dot{\beta}\sin\alpha + \omega_{ex}\sin\beta\cos\alpha + \omega_{ey}\sin\alpha + \omega_{ez}\cos\alpha\cos\beta
\end{aligned} \qquad \ldots\ldots [1]$$

where

$$\begin{aligned}
\omega_{ex} &= \omega_1\cos\psi - \frac{v_y}{R} \\
\omega_{ey} &= \omega_1\sin\psi + \frac{v_x}{R} \\
\omega_{ez} &= \omega_z
\end{aligned} \qquad \ldots\ldots [2]$$

We shall assume henceforth that α, β, $\dot{\alpha}$ and $\dot{\beta}$ are infinitesimals of the same order. Confining our analysis to small oscillations of the gyroscope axis about the vertical, and neglecting the higher order terms, we obtain for the projections [2] of the absolute angular velocity of the gyroscope casing the following linearized expressions

$$\begin{aligned}
\omega_x &\doteq \dot{\alpha} + \omega_{ex} - \omega_{ez}\beta \\
\omega_y &\doteq \dot{\beta} + \omega_{ey} + \omega_{ez}\alpha \\
\omega_z &\doteq \omega_{ez} + \omega_{ex}\beta + \omega_{ey}\alpha
\end{aligned} \qquad \ldots\ldots [2']$$

Using Résal's theorem, we obtain, in terms of projections on the $oxyz$ axes, the following equation of motion for the gyroscope

$$\begin{aligned}
J_x(d\omega_x/dt) + J\omega_y(\omega_z + \dot{\varphi}) - J_z\omega_z\omega_y &= M_x \\
J_x(d\omega_y/dt) - J\omega_x(\omega_z + \dot{\varphi}) + J_z\omega_x\omega_z &= M_y \\
J[d(\omega_z + \dot{\varphi})/dt] &= 0
\end{aligned} \qquad \ldots\ldots [3]$$

Bearing in mind that $\omega_z = \omega_2 \ll \dot{\varphi}$ and assuming $M_z = 0$, we get

$$J(\omega_z + \dot{\varphi}) = J\dot{\varphi} = H = \text{const} \qquad [4]$$

We assume furthermore that $J = J_e$, and neglect the nutation terms in [3]. We then obtain from [4] the following equations of motion

$$H\omega_y = M_x \qquad -H\omega_x = M_y \qquad [5]$$

Here the moments M_x and M_y are proportional to the integrals of the accelerations as measured by the accelerometers. The coefficients must be chosen such as to minimize the ballistic deviations. The latter requirement is equivalent to the fulfillment of the Schuler condition.

Projecting all the accelerations, including the acceleration due to gravity (assumed directed along the Earth's radius) on the axes ox and oy, we obtain the following expressions for M_x and M_y

$$\begin{aligned}
M_x &= k_1\int_0^t (W_x - g\beta)dt + M_{1x} \\
M_y &= k_2\int_0^t (W_y + g\alpha)dt + M_{1y}
\end{aligned} \qquad \ldots\ldots [6]$$

where

g = acceleration due to gravity, with centripetal force neglected

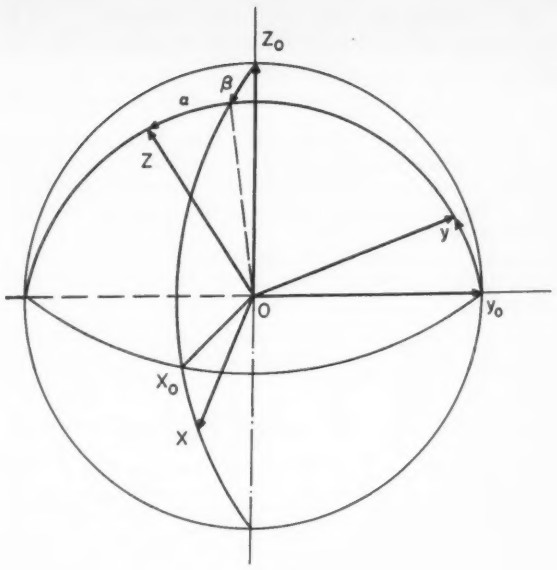

Fig. 2

W_x, W_y = components of absolute acceleration vector along ox and oy axes

M_{1x}, M_{1y} = certain additional moments, applied to gyroscope, which should compensate for horizontal component of Earth's rotation; these moments should be generated by a computer

Substituting Equation [6] in [5] and dividing both sides by H, we obtain on the basis of Equations [2′ and 2]

$$\begin{aligned}
\beta + \omega_1\sin\psi + \frac{v_x}{R} + \omega_2\alpha &= \frac{k_1}{H}\int_0^t (W_x - g\beta)dt + \frac{M_{1x}}{H} \\
\dot{\alpha} + \omega_1\cos\psi - \frac{v_y}{R} - \omega_2\beta &= -\frac{k_2}{H}\int_0^t (W_y + g\alpha)dt - \frac{M_{1y}}{H}
\end{aligned} \qquad \ldots\ldots [7]$$

It is seen from this that the additional moments must be

$$M_{1x} = H\omega_1\sin\psi \qquad M_{1y} = -H\omega_1\cos\psi \qquad [8]$$

To determine the coefficients of proportionality k_1 and k_2, we proceed as follows: We assume for the time being that the base moves along a great circle of an imaginary sphere having the same radius as the Earth, but not participating in the Earth's rotation [2]. Then the accelerations W_x and W_y will have the form

$$W_x = \dot{v}_x \qquad W_y = \dot{v}_y \qquad [9]$$

In this case the equations of motion [7] assume the very simple form

$$\begin{aligned}
\dot{\beta} + \frac{v_x}{R} &= \frac{k_1}{H}\int_0^t (\dot{v}_x - g\beta)dt \\
\dot{\alpha} - \frac{v_y}{R} &= -\frac{k_2}{H}\int_0^t (\dot{v}_y + g\alpha)dt
\end{aligned} \qquad \ldots\ldots [10]$$

Differentiating these equations with respect to the time and selecting the indeterminate coefficients k_1 and k_2 such as to eliminate the accelerations $\dot{v}_x$ and $\dot{v}_y$ from the equations, we get

$$k_1 = k_2 = (H/R) \qquad [11]$$

The equations of motion [10], with coefficients k_1 and k_2 taken from [11], assume the following form upon differentiation

$$\ddot{\beta} + (g/R)\beta = 0 \qquad \ddot{\alpha} + (g/R)\alpha = 0 \qquad [12]$$

We see now that if the condition [11] and those agreed upon in the foregoing are satisfied, the gyro vertical will not have a ballistic deviation, but will execute harmonic oscillations about the true vertical, with a period equal to Schuler's period, 84.4 min.

Let us return now to the case of great-circle motion and assume that conditions [8 and 11] are satisfied; Equation [7] then becomes

$$\dot{\beta} + \frac{v_x}{R} + \omega_2\alpha = \frac{1}{R}\int_0^t (W_x - g\beta)dt$$

$$\dot{\alpha} - \frac{v_y}{R} - \omega_2\beta = -\frac{1}{R}\int_0^t (W_y + g\alpha)dt$$

..... [13]

In these equations the accelerations W_x and W_y are somewhat more complicated than in Equation [10], for they contain not only the relative accelerations, but also the centripetal and Coriolis accelerations due to the Earth's rotation.

Acceleration in Motion Along the Earth's Great Circle

Assuming that the vector of the translational velocity $\bar{v}$ is at all times in the plane of the horizon, we neglect the vertical components of the relative acceleration.

By Coriolis' theorem, the absolute acceleration can be obtained from

$$\bar{W}_{abs} = \bar{W}_{trans} + \bar{W}_{rel} + \bar{W}_{Cor} \qquad [14]$$

The acceleration of the translational motion is due to the Earth's rotation. The vector of this acceleration lies in the plane of the meridian and is directed perpendicular to the Earth's axis of rotation, and its magnitude depends on the local latitude φ. We have the following expressions for its components along the axes of the horizontal coordinate system $ox_0y_0z_0$, oriented in the manner indicated in the foregoing

$$W_{trans\ x} = \tfrac{1}{2}R\omega_\delta^2 \sin 2\varphi \cos(\psi + \gamma)$$
$$W_{trans\ y} = \tfrac{1}{2}R\omega_\delta^2 \sin 2\varphi \sin(\psi + \gamma)$$
$$W_{trans\ z} = -\tfrac{1}{2}R\omega_\delta^2 \cos^2\varphi$$

..... [15]

The acceleration of the relative motion will have a centripetal and a rotational component. The vector of this acceleration will lie in the great-circle plane, and its components along the $ox_0y_0z_0$ axes are

$$W_{rel\ x} = \dot{v}_x \qquad W_{rel\ y} = \dot{v}_y \qquad W_{rel\ z} = -(1/R)(v_x^2 + v_y^2) \qquad [16]$$

Finally, the Coriolis acceleration will be due to the Earth's rotation and to the relative motion of the object along the great circle. The vector of this acceleration can be obtained from

$$\bar{W}_{Cor} = 2\bar{\omega}_\delta \times \bar{v} \qquad [17]$$

The projections of Equation [17] on the axes of the horizontal coordinate system are

$$W_{Cor\ x} = -2\omega_2 v_y$$
$$W_{Cor\ y} = 2\omega_2 v_x$$
$$W_{Cor\ z} = 2\omega_1\sqrt{v_x^2 + v_y^2}\cdot\sin\psi$$

..... [18]

From Equations [15, 16 and 18], we obtain the components of the vector of the absolute accelerations in the horizontal system of coordinates

$$W_x = R\omega_1\omega_2 \cos(\psi + \gamma) - 2\omega_2 v_y + \dot{v}_x$$
$$W_y = R\omega_1\omega_2 \sin(\psi + \gamma) + 2\omega_2 v_x + \dot{v}_y$$
$$W_z = -R\omega_2^2 - \frac{v^2}{R} + 2\omega_1 v \sin\psi$$

..... [19]

Here

$$\omega_1 = \omega_\delta \cos\varphi \qquad \omega_2 = \omega_\delta \sin\varphi \qquad v = \sqrt{v_x^2 + v_y^2}$$

Again we neglect the Earth's nonsphericity. It must be borne in mind, however, that for a quantitative estimate of the errors, allowance for the deviations of the real shape of the Earth's surface from spherical is of great importance.

Subtracting the centripetal and Coriolis terms from the projections of the absolute acceleration on the *oxyz* axes (which are connected with the gyroscope casing) we obtain, in first approximation, the following expression for the accelerations as sensed by the accelerometers

$$W_x \doteq W_x^* + \dot{v}_x \qquad W_y \doteq W_y^* + \dot{v}_y \qquad [20]$$

where

$$W_x^* = R\omega_1\omega_2 \cos(\psi + \gamma) - 2\omega_2 v_y$$
$$W_y^* = R\omega_1\omega_2 \sin(\psi + \gamma) + 2\omega_2 v_x$$

..... [21]

Determination of Errors Due to Centripetal and Coriolis Accelerations

In considering the simplest path along a great circle of a nonrotating sphere, we have seen that if condition [11] is satisfied the gyro vertical has no deviations. This does not necessarily mean that the output of each accelerometer will be the exact value of the velocity component. This can happen only in the case of zero initial conditions for Equation [12] of motion of the gyro vertical. If the initial conditions differ from zero, the gyro vertical will execute harmonic oscillations, and this will introduce an error, also harmonic, in the velocity measurement.

Assume, for example, that $\beta|_{t=0} = \beta_0$; $\dot{\beta}|_{t=0} = 0$; we then have from the first equation of [12] the solution

$$\beta = \beta_0 \cos\sqrt{(g/R)}t \qquad [22]$$

The magnitude of the oscillating velocity-measurement error will be

$$\Delta v_x \equiv \int_0^t g\beta dt = \beta_0\sqrt{gR}\sin\sqrt{(g/R)}t \qquad [23]$$

The error in the measurement of v_y is determined in exactly the same manner.

It is interesting to note that the period of this oscillating error is equal to that of a circular satellite in a circular orbit at the same distance from the center of the Earth, equal, as is well known, to $\sqrt{gR}$. In spite of this, the amplitude of the error can be made in principle as small as desired by reducing the initial angle of deviation β_0. Obviously the systematic character of this error makes it possible to eliminate it, provided it is not influenced during the course of motion by accidental perturbations.

Let us now return to our motion over the Earth's surface, and let us attempt to determine the influence of the centripetal and Coriolis accelerations. Substituting the expressions for W_x and W_y from [20] in [13] we get

$$\dot{\beta} + \omega_2\alpha = \frac{1}{R}\int_0^t (W_x^* - g\beta)dt$$

$$\dot{\alpha} - \omega_2\beta = -\frac{1}{R}\int_0^t (W_y^* + g\alpha)dt$$

..... [24]

Differentiating Equation [24], we obtain the following equations for the motion of the gyro vertical

$$\ddot{\beta} + \omega_2\dot{\alpha} + \dot{\omega}_2\alpha + \frac{g}{R}\beta = \frac{1}{R}W_x^*$$

$$\ddot{\alpha} - \omega_2\dot{\beta} - \dot{\omega}_2\beta + \frac{g}{R}\alpha = -\frac{1}{R}W_y^*$$

.....[25]

Assume that we know the steady-state motion of the gyro vertical and the corresponding particular solution

$$\alpha_r = \alpha_r(t) \qquad \beta_r = \beta_r(t) \qquad [26]$$

Then, putting $\xi = \alpha - \alpha_r$, $\eta = \beta - \beta_r$, we can write the following variational equation for the small oscillations of the gyro vertical about the steady-state motion [26]. The variational equations will be of the form

$$\ddot{\eta} + \omega_2\dot{\xi} + \dot{\omega}_2\xi + (g/R)\eta = 0$$

$$\ddot{\xi} - \omega_2\dot{\eta} - \dot{\omega}_2\eta + (g/R)\xi = 0$$

.....[27]

These equations are analogous to Equation [12] for the oscillating error, but unlike the latter, they are coupled. The terms containing the factor $\dot{\omega}_2$ are quite small, provided only the relative velocity v is small, and can be discarded. Without stopping to analyze Equation [27] in detail, we note only that the error will have two different periods, 24 hr and 84.4 min, which will have the nature of beats.

To calculate the errors generated by the centripetal and Coriolis accelerations, we use

$$\Delta v_x = \int_0^t (W_x^* - g\beta_r)dt$$

$$\Delta v_y = \int_0^t (W_y^* + g\alpha_r)dt$$

.....[28]

where

$$W_x^* = R\omega_1\omega_2 \cos(\psi + \gamma) - 2\omega_2 v_y$$

$$W_y^* = R\omega_1\omega_2 \sin(\psi + \gamma) + 2\omega_2 v_x$$

To valculate the errors by means of Equation [28], it is first necessary to find the particular solution [26] of Equation [25]. For this purpose we must first specify the law of motion of the object. Equation [28] can be represented, by using [25], in the form

$$\Delta v_x = R(\omega_2\alpha_r + \beta_r)$$

$$\Delta v_y = R(\omega_2\beta_r - \dot{\alpha}_r)$$

.....[29]

If the velocities v_x and v_y have small constant values, the functions $W_x^*(t)$ and $W_y^*(t)$ become slowly varying functions of time, and correspondingly α_r and β_r are also slowly varying functions of time. Under these conditions we can put approximately

$$\Delta v_x \approx R\omega_2\alpha_r \qquad \Delta v_y \approx R\omega_2\beta_r$$

where

$$\alpha_r \approx -\frac{W_y^*}{g} \qquad \beta_r \approx \frac{W_x^*}{g}$$

Setting, for example

$$v_y = 10 \text{ m/sec} \qquad v_x = 0 \qquad \varphi = 60 \text{ deg} \qquad R = 6.4 \times 10^6$$

$$\omega_\delta = 7.3 \times 10^{-5} \text{ 1/sec} \qquad \psi + \gamma = 0$$

we obtain

$$W_x^* = 6.4 \times 10^6 \times 7.3^2 \times 0.87 \times 0.5 \times 10^{-10} - 2 \times 7.3 \times 987 \times 10^{-5} \times 10 = 0.0136 \text{ m/sec}^2$$

$$W_y^* = 0$$

$$\alpha_r \approx 0$$

$$\beta_r \approx 0.0014$$

$$\Delta v_y \approx 6.4 \times 10^6 \times 7.3 \times 10^{-5} \times 987 \times 1.4 \times 10^{-3} \approx 0.67 \text{ m/sec}$$

$$\Delta v_x \approx 0$$

It is seen from this example that the errors due to the centripetal and Coriolis accelerations must be taken into account.

Effect of Coulomb Friction

As is known, Coulomb friction in the sensitive-element suspension bearings plays an important role in most precision gyroscopic instruments. The accuracy and sensitivity of the instrument depend to a considerable extent on the Coulomb friction, and this has necessitated the development of special sensitive bearings.

In view of this, it is of interest to estimate the effect of Coulomb friction forces on the accuracy of velocity measurement in an inertial system. For this purpose we consider the simplest case of platform motion, when there are no Coriolis and centripetal accelerations. Turning to the corresponding equations of motion [10], subject to condition [11], and taking into account the bearing friction moments of the Cardan suspension we obtain the following equations of motion

$$\dot{\beta} + \frac{g}{R}\int_0^t \beta dt = -\rho_1 \operatorname{sign}\dot{\alpha}$$

$$\dot{\alpha} + \frac{g}{R}\int_0^t \alpha dt = \rho_2 \operatorname{sign}\dot{\beta}$$

.....[30]

Here ρ_1 and ρ_2 are the moments of the Coulomb friction forces, referred to the kinetic moment of the gyroscope, i.e.

$$\rho_1 = \frac{M_{fx}}{H} \qquad \rho_2 = \frac{M_{fy}}{H} \qquad [31]$$

It is easy to see that the Coulomb friction does not change the position of the dynamic equilibrium of the gyro vertical. The situation is different in the case of the integrators, the outputs of which will contain, in addition to the useful components of the measured velocity, supplementary components that compensate for the friction moments. These additional components will indeed be the static errors generated by the friction moments M_{fx} and M_{fy}. The limiting values of the static errors in the measurement of the velocity components will be

$$|\Delta v_x| \equiv g\left|\int_0^\infty \beta dt\right| = \frac{M_{fx}R}{H}$$

$$|\Delta v_y| \equiv g\left|\int_0^\infty \alpha dt\right| = \frac{M_{fy}R}{H}$$

.....[32]

Let us assume, for example, that $|\Delta v_x| \approx 0.01$ m/sec; then the corresponding drift due to Coulomb friction will be

$$\frac{M_{fx}}{H} \equiv \frac{|\Delta v_x|}{R} = \frac{0.01}{6.4 \cdot 10^6} \approx 1.6 \times 10^{-9} \text{ radians/sec}$$

We see thus that a gyroscope in an inertial system must satisfy more stringent drift requirements than presently specified for bearings of modern precision gyro compasses.

Conclusions

For an exact measurement of velocity by the inertial method, over a great-circle route, it is not enough to introduce an integral correction that satisfies the Schuler condition. To compensate for the systematic errors due to Coriolis and centripetal accelerations, the correction system must include additional devices that take into account the parameters of the course and the position of the object on the course. The presence of integral correction insures the absence of velocity errors that increase without limit with time.

References

1 Slomyanskii, G. A. and Pryadilov, Yu. N., "Poplavkovye giroskopy i ikh primenenie" (Floated Gyroscopes and Their Application), Oborongiz, 1958.

2 Ishlinskii, A. Yu., "On the Equations of the Problem of Determining the Location of a Moving Object by Means of Gyroscopes and Acceleration Meters," *Prikladnaya matematika i mekhanika* (Applied Mathematics and Mechanics), vol. XXI, no. 6, 1957.

—*Original received May 30, 1959*

Reviewer's Comment

This Russian study of errors in inertial navigators is of interest primarily because it involves some insight as to what is being accomplished in this field by the Russians. It is interesting to note that this particular work was done in the classified literature in this country more than five years ago by the reviewer, also by Donald Duncan, and more recently by Myron Kayton.

There are several items of interest to point out:

1 The Russians have an interest in errors that lie within six miles of their inertial navigators.

2 The author did not point out a relatively simple mechanism of heading-saving where it can be utilized to compensate for these Coriolis errors.

It is of further interest to note the nature of the gyro errors which are studied:

1 From the point of view that it was considered, a 0.0003-deg-per-hour level of gyro performance was somewhat better than was concurrently being achieved by their best gyro compasses.

2 Nothing was said about such errors in the gyro as unbalance or iso-elasticity.

—Charles J. Mundo Jr.
Raytheon Manufacturing Co.

Dependence of Secular Variations of Orbit Elements on Air Resistance

P. E. EL'YASBERG

THE PROBLEM of the influence of air resistance on the secular variations of the elements of satellite orbits has been the subject of several papers (1, 2 and 3).[1] The present paper is a further extension of the idea, proposed in (1), of expanding the secular variations of the orbit elements in Bessel functions of imaginary argument. This results in simple and illustrative formulas, which can be used to solve many problems, e.g., determination of the dependence of the secular variations of the orbit elements on the values of the elements themselves, estimate of the accuracy of determination of the air density from the measured secular variations of the orbit elements, etc.

If the atmosphere is considered stationary with respect to Earth (in an inertial system of coordinates), then the equations of the osculating elements (the Lagrange equation) for the case of motion in a resisting medium and in the absence of other perturbations, can be written

$$\frac{dp}{d\vartheta} = -bpp^2 \frac{\sqrt{1 + 2e\cos\vartheta + e^2}}{(1 + e\cos\vartheta)^2}$$

$$\frac{de}{d\vartheta} = -bpp \frac{(e + \cos\vartheta)\sqrt{1 + 2e\cos\vartheta + e^2}}{(1 + e\cos\vartheta)^2} \qquad [1]$$

where

$$b = C_D F_M / m \qquad [2]$$

Translated from "Iskusstvennye Sputniki Zemli" (Artificial Earth Satellites), USSR Acad. Sci. Press, Moscow, 1959, pp. 54–60.

[1] Numbers in parentheses indicate References at end of paper.

and

C_D = coefficient of air resistance
F_M = area of the midsection of the satellite
m = satellite mass
ρ = air density
p = orbit parameter
e = eccentricity
ϑ = true anomaly

Let us change over now in Equation [1] from the true anomaly ϑ to the eccentric anomaly E. Along with the variations in p and e, we consider here the variation of the semimajor axis a, the period of rotation T and the distance from the perigee to Earth's center r_p. Then, using the known relations between these quantities we obtain after elementary transformations

$$\Delta p = -b\int_0^{2\pi} \rho p^2 \frac{\sqrt{1-e^2\cos^2 E}}{1-e^2}\,dE$$

$$\Delta e = -b\int_0^{2\pi} \rho p \frac{\cos E\sqrt{1-e^2\cos^2 E}}{1-e\cos E}\,dE$$

$$\Delta a = -b\int_0^{2\pi} \rho a^2 \frac{1+e\cos E}{1-e\cos E}\sqrt{1-e^2\cos^2 E}\,dE$$

$$\Delta T = -\frac{3\pi}{\sqrt{\mu}}\,b\int_0^{2\pi} \rho a^{3/2} \frac{1+e\cos E}{1-e\cos E}\sqrt{1-e^2\cos^2 E}\,dE$$

$$\Delta r_p = -b\int_0^{2\pi} \rho a^2(1-e) \frac{1-\cos E}{1-e\cos E}\sqrt{1-e^2\cos^2 E}\,dE$$

.....[3]

where

Δp, Δe, ΔT, Δa, Δr_p = changes in the corresponding quantities during one loop of the orbit
μ = coefficient in the expression for the acceleration due to gravity $g = \mu/r^2$
r = distance to the center of Earth

We now expand the integrands in the right-hand sides of these equations in powers of e. We note here that when $e > 0.1$ it is possible to discard in these series all the terms higher than the third degree. As a result we obtain

$$\Delta p = -b\int_0^{2\pi} \frac{\rho p^2}{1-e^2}\left(1-\frac{1}{2}e^2\cos^2 E-\ldots\right)dE$$

$$\Delta e = -b\int_0^{2\pi} \rho p\left(\cos E+e\cos^2 E+\frac{e^2}{2}\cos^3 E+\frac{e^3}{2}\cos^4 E+\ldots\right)dE$$

$$\Delta a = -b\int_0^{2\pi} \rho a^2\left(1+2e\cos E+\frac{3}{2}e^2\cos^2 E+e^3\cos^3 E+\ldots\right)dE$$

$$\Delta T = -\frac{3\pi}{\sqrt{\mu}}\,b\int_0^{2\pi} \rho a^{3/2}\left(1+2e\cos E+\frac{3}{2}e^2\cos^2 E+e^3\cos^3 E+\ldots\right)dE$$

$$\Delta r_p = -b\int_0^{2\pi} \rho a^2(1-e)\left[(1-\cos E)+e(\cos E-\cos^2 E)+\frac{e^2}{2}(\cos^2 E-\cos^3 E)+\frac{e^3}{2}(\cos^3 E-\cos^4 E)+\ldots\right]dE$$

.....[4]

The air density ρ contained in the right-hand sides of these equations depends in general not only on the flying altitude h but also on many other factors. We neglect here, however, the influence of these factors and assume $\rho = \rho(h)$. Since the changes in the orbit elements are affected most by the air resistance in the perigee region, the function $\rho(h)$ must be chosen so as to insure the maximum accuracy of calculation at the perigee altitude h_p. Starting with these considerations, we assume

$$\rho(h) = \rho_p \exp\{-k(h-h_p)\} \qquad [5]$$

where

ρ_p = $\rho(h_p)$ is the air density in the perigee region
k = coefficient that characterizes the rate at which ρ decreases with altitude (inverse of the scale height)

Using the well known relations, we can transform Equation [5] as follows

$$\rho(h) = \rho_p \exp(-\nu+\nu\cos E) \qquad [6]$$

where

$$\nu = aek \qquad [7]$$

We insert Equation [6] in the right-hand sides of Equations [4]. Next, in view of the smallness of the variation of the orbit elements during one loop, we neglect the variation in e, p and a when integrating the right sides of these equations. As a result we obtain

$$\Delta p = -\frac{b\rho_p p^2}{1-e^2}\exp(-\nu)\left(F_0-\frac{1}{2}e^2F_2+\ldots\right)$$

$$\Delta e = -b\rho_p p\exp(-\nu)\left(F_1+eF_2+\frac{e^2}{2}F_3+\frac{e^3}{2}F_4+\ldots\right)$$

$$\Delta a = -b\rho_p a^2\exp(-\nu)\left(F_0+2eF_1+\frac{3}{2}e^2F_2+e^3F_3+\ldots\right)$$

$$\Delta T = -\frac{3\pi}{\sqrt{\mu}}\,b\rho_p a^{3/2}\exp(-\nu)\times\left(F_0+2eF_1+\frac{3}{2}e^2F_2+e^3F_3+\ldots\right)$$

$$\Delta r_p = -b\rho_p a^2(1-e)\exp(-\nu)\left[(F_0-F_1)+e(F_1-F_2)+\frac{e^2}{2}(F_2-F_3)+\frac{e^3}{2}(F_3-F_4)+\ldots\right]$$

.....[8]

where

$$F_n = \int_0^{2\pi} \exp(\nu\cos E)\cos^n E\,dE \qquad n = 0, 1, 2\ldots \qquad [9]$$

It is obvious that the F_n are functions of ν and can be readily expressed in terms of Bessel functions of imaginary argument $I_n(\nu)$. We use for this purpose the well known relations (4)

$$I_n(\nu) = \frac{1}{2\pi}\int_0^{2\pi} \exp(\nu\cos E)\cdot\cos nE\,dE$$

$$I_{n-1}(\nu) - I_{n+1}(\nu) = 2nI_n(\nu)/\nu$$

.....[10]

As a result we obtain

$$F_0(\nu) = 2\pi I_0(\nu)$$
$$F_1(\nu) = 2\pi I_1(\nu)$$
$$F_2(\nu) = 2\pi[I_0(\nu) - I_1(\nu)/\nu]$$
$$F_3(\nu) = 2\pi\left[I_1(\nu)\left(1 + \frac{2}{\nu^2}\right) - \frac{1}{\nu} I_0(\nu)\right]$$
$$F_4(\nu) = 2\pi\left(1 + \frac{3}{\nu^2}\right)\left[I_0(\nu) - \frac{2}{\nu} I_1(\nu)\right]$$

.....[11]

Using [7, 8 and 11] we can calculate, with the aid of tables of Bessel functions, the increments in the orbit elements We are more interested, however, not in the development o approximate computation methods (since more exact calcu lations can always be made with electronic computers), but in the derivation of simple expressions that determine the character of the dependence of the increase in the orbit elements on the magnitudes of the elements themselves and on the principal atmospheric parameters. To derive such relations we make use of the fact that on the principal portions of the orbits under consideration, the quantity ν is relatively large, so that available asymptotic expansions can be used (4)

$$I_0 = \frac{\exp(\nu)}{\sqrt{2\pi\nu}}\left(1 + \frac{1}{8}\cdot\frac{1}{\nu} + \frac{9}{128}\cdot\frac{1}{\nu^2} + \frac{75}{1024}\cdot\frac{1}{\nu^3} + \ldots\right)$$
$$I_1 = \frac{\exp(\nu)}{\sqrt{2\pi\nu}}\left(1 - \frac{3}{8}\cdot\frac{1}{\nu} - \frac{15}{128}\cdot\frac{1}{\nu^2} - \frac{105}{1024}\cdot\frac{1}{\nu^3} + \ldots\right)$$

.....[12]

As is known, these expansions can be used when $\nu \gg 1$. In practice, even when

$$\nu > 4 \qquad [13]$$

these expansions (in computations making use of the foregoing number of terms) yield values of the functions $I_0(\nu)$ and $I_1(\nu)$ accurate to 0.1 per cent, which can be considered quite satisfactory.

Assuming that $k = 0.02$ km^{-1} at an altitude $h = 220$–230 km, and also that $a \approx 7000$ km, condition [13] can be replaced by the inequality

$$e > 0.028 \qquad [14]$$

As is well known, considerably greater eccentricities were observed in the principal portions of the orbits of the existing satellites (on the order of 0.05–0.15).

It follows directly from [11 and 12] that

$$F_n = \sqrt{2\pi/\nu}\exp(\nu) f_n \qquad [15]$$

where

$$f_0 = 1 + \frac{1}{8}\cdot\frac{1}{\nu} + \frac{9}{128}\cdot\frac{1}{\nu^2} + \frac{75}{1024}\cdot\frac{1}{\nu^3} + \ldots$$
$$f_1 = 1 - \frac{3}{8}\cdot\frac{1}{\nu} - \frac{15}{128}\cdot\frac{1}{\nu^2} - \frac{105}{1024}\cdot\frac{1}{\nu^3} + \ldots$$
$$f_2 = 1 - \frac{7}{8}\cdot\frac{1}{\nu} + \frac{57}{128}\cdot\frac{1}{\nu^2} + \frac{195}{1024}\cdot\frac{1}{\nu^3} + \ldots$$
$$f_3 = 1 - \frac{11}{8}\cdot\frac{1}{\nu} + \frac{225}{128}\cdot\frac{1}{\nu^2} - \frac{954}{1024}\cdot\frac{1}{\nu^3} + \ldots$$
$$f_4 = 1 - \frac{15}{8}\cdot\frac{1}{\nu} + \frac{489}{128}\cdot\frac{1}{\nu^2} - \frac{5445}{1024}\cdot\frac{1}{\nu^3} + \ldots$$

.....[16]

After substituting Equation [15] in [8] we obtain

$$\Delta p = -\frac{b\rho_p p^2}{1-e^2}\sqrt{\frac{2\pi}{\nu}}\left(f_0 - \frac{1}{2}e^2 f_2 + \ldots\right)$$
$$\Delta e = -b\rho_p p^2\sqrt{\frac{2\pi}{\nu}}\left(f_1 + e f_2 + \frac{e^2}{2}f_3 + \frac{e^3}{2}f_4 + \ldots\right)$$
$$\Delta a = -b\rho_p a^2\sqrt{\frac{2\pi}{\nu}}\left(f_0 + 2e f_1 + \frac{3}{2}e^2 f_2 + e^3 f_3 + \ldots\right)$$
$$\Delta T = -\frac{3\pi}{\sqrt{\mu}} b\rho_p a^{3/2}\sqrt{\frac{2\pi}{\nu}}\left(f_0 + 2e f_1 + \frac{3}{2}e^2 f_2 + e^3 f_3 + \ldots\right)$$
$$\Delta r_p = -b\rho_p a^2(1-e)\sqrt{\frac{2\pi}{\nu}}\left[(f_0 - f_1) + e(f_1 - f_2) + \frac{e^2}{2}(f_2 - f_3) + \frac{e^3}{2}(f_3 - f_4) + \ldots\right]$$

.....[17]

It is advisable to simplify these expressions further. By way of an example let us consider the first of Equations [17]. Using Equations [16], we can write

$$f_0 - \frac{1}{2}e^2 f_2 + \ldots = f_0\left(1 - \frac{1}{2}e^2 + \ldots\right) + \frac{1}{2}e^2(f_0 - f_2) + \ldots$$
$$= f_0\left(1 - \frac{1}{2}e^2 + \ldots\right) + \frac{1}{2}e^2 \times \left(\frac{1}{\nu} - \frac{3}{8}\cdot\frac{1}{\nu^2} - \frac{15}{128}\cdot\frac{1}{\nu^3} + \ldots\right) + \ldots \qquad [18]$$

We note now that the series in the parentheses following f_0 corresponds to the series used in the first formula of Equations [4] in the case when $\cos E = 1$. Therefore, comparing with the first formula of Equation [3], we get

$$1 - \tfrac{1}{2}e^2 + \ldots = \sqrt{1-e^2}$$

We can next show that if Equation [13] is satisfied, the remaining terms of the series [18] amount to much less than 1 per cent of the determined quantity. We can thus write

$$f_0 - \tfrac{1}{2}e^2 f_2 + \ldots \approx f_0\sqrt{1-e^2}$$

Analogous simplifications can be made also in the right sides of the remaining equations of [17]. As a result we obtain the following expressions

$$\Delta p \approx -\frac{b\rho_p p^2}{\sqrt{1-e^2}} f_0\sqrt{\frac{2\pi}{\nu}}$$
$$\Delta e \approx -b\rho_p p\sqrt{\frac{1+e}{1-e}} f_1\sqrt{\frac{2\pi}{\nu}}$$
$$\Delta a \approx -b\rho_p a^2\frac{1+e}{1-e}\sqrt{1-e^2} f_0\sqrt{\frac{2\pi}{\nu}}$$
$$\Delta T \approx -\frac{3\pi}{\sqrt{\mu}} b\rho a^{3/2}\frac{1+e}{1-e}\sqrt{1-e^2} f_0\sqrt{\frac{2\pi}{\nu}}$$
$$\Delta r_p \approx -b\rho_p a^2\sqrt{1-e^2}\frac{1}{2\nu} f'\sqrt{\frac{2\pi}{\nu}}$$

.....[19]

In these equations

$$f' = 2\nu(f_0 - f_1) = 1 + \frac{3}{8}\cdot\frac{1}{\nu} + \frac{45}{128}\cdot\frac{1}{\nu^2} + \ldots \qquad [20]$$

As a further simplification, we can assume in these formulas

$$f_0 \approx f_1 \approx f' \approx 1 \qquad [21]$$

We note that Equations [17 and 19] are suitable only at eccentricities that are not too small, when condition [13] is satisfied. If this condition is not satisfied, relations [8] must be used. In particular, when $e = 0$ (circular orbit) we obtain directly from Equation [9]

$$F_i(0) = \begin{cases} 2\pi \text{ when } i = 0 \\ 0 \text{ when } i > 0 \end{cases}$$

hence

$$\Delta p = \Delta a = \Delta r_p = -2\pi b \rho_p a^2$$
$$\Delta e = 0$$
$$\Delta T = -(6\pi^2/\sqrt{\mu}) b \rho_p a^{3/2} \quad \ldots\ldots [22]$$

Obviously [22] cannot be derived from [19] by simply going to the limit as $e \to 0$.

In conclusion we note that formulas [19], unlike expressions [17], remain in force even at large eccentricities (the condition $e > 1$ is sufficient)

When deriving these relations we neglect the influence of nonsphericity of Earth and the fact that the gravitational field is noncentral. However, this influence can be partially taken into account by finding the quantity ρ_p, which enters into expressions [8, 17 and 19], as the density of the air at the point of the real orbit, located at the minimum altitude above Earth's surface, h_{min} (and not in the perigee of the osculating orbit).

To verify the accuracy of the obtained approximate relations [17 and 19], we compared them with the results of numerical integration of the exact equations of motion. The calculations were made for the orbits of the first and second Soviet Earth satellites. The result was that at $e < 0.04$ the error in calculating the increments Δa, Δe, Δp and ΔT by the approximate formulas did not exceed 1 or 2 per cent of the determined quantity. As the eccentricity is decreased, these errors increase, reaching 6 per cent at $e = 0.023$ and 15 to 20 per cent at $e = 0.012$. The error in the calculation in the increment of Δr_p (which in itself is relatively small) is somewhat greater and reaches 10 to 40 per cent.

Thus, the proposed approximate formulas are quite suitable for a qualitative analysis of the relations under consideration. In particular, it is seen from them that the secular variations of Δa, Δe, Δp and ΔT are proportional to the quantity $b\rho_p \nu^{-1/2}$, and the variation of Δr_p is proportional to $b\rho_p \nu^{-3/2}$. Consequently, in using Equations [7] we find that by determining the air density from measurements of the secular variations of ΔT or Δa we actually obtain not the quantity ρ_p but the ratio $\rho_p/\sqrt{k}$. To determine the value of the coefficient k it is necessary to determine with sufficient accuracy, along with the changes in the period of rotation ΔT, the drop in the perigee Δr_p. Actually, using Equations [19], we can write

$$\frac{\Delta r_p}{\Delta T} \approx \frac{1}{\nu} \cdot \frac{\sqrt{\mu}}{6\pi\sqrt{a}} \cdot \frac{1-e}{1+e} \frac{f'}{f_0} \qquad [23]$$

Thus, the ratio $\Delta r_p/\Delta T$ is proportional to $1/k$ and is independent of b or of ρ_p. Hence it follows that by measuring this ratio we can calculate the coefficient k.

References

1 Yatsunskii, I. M., *Uspekhi Fiz. Nauk* (Advances in Physical Sciences), vol. 63, no. 1a, 1957. English translation by International Physical Index, N. Y.

2 Okhotsimskii, D. E., Eneev, T. M. and Taratynova, G. P., *ibid.*

3 Taratynova, G. P., *ibid.*

4 Watson, G. N., "A Treatise on the Theory of Bessel Functions, Part I," 2nd ed., Cambridge University Press, N. Y., 1944 (Russian translation, Foreign Literature Press, 1949).

Reviewer's Comment

The paper "Dependence of Secular Variations of Orbit Elements on Air Resistance" represents an extension of some earlier Russian work. As noted by the author, his general perturbations method utilizes an expansion of the series representing the perturbative variation of the orbital elements in terms of Bessell functions having imaginary coefficients. More specifically, the perturbative variations of the elements per pass (Eqs. [3 and 4]) are combined with an exponential density variation (Eq. [6]), both expressions given in terms of the eccentric anomaly. Instead of further expanding these relationships in terms of the mean anomaly, the author introduces Bessel functions (Eq. [10]) and recognizes their integrals as series expressions interims of $\nu = aek$ (Eq. [12]).

The use of Bessel functions is not new in celestial mechanics; in fact Sterne (1) has a very similar formulation (in Sterne's notation $\nu = c$). Perhaps the most interesting aspect of this paper is the author's qualitative discussions found after Equation [18]; in particular his recognition of the problem of near zero eccentricities is appreciated. The literature in the field of general perturbations as applied to satellite drag is extensive—in fact so extensive that many of the papers duplicate one another and are not cumulative to the state of the art. The interested reader's attention should however, be directed to some of the initial and original efforts of Roberson (2), King-Hele (3), Blitzer (4), Sterne (1), and Nonweiler (5) in order to provide a background for a better understanding of the present Russian paper.

—Robert M. L. Baker Jr.
Department of Astronomy
University of California, Los Angeles

1 Sterne, T. E., "Formula for Inferring Atmospheric Density from the Motion of Artificial Earth Satellites," *Science*, vol. 127, no. 3308, 1958, p. 1245.

2 Roberson, R. E., "Effect of Air Drag on Elliptic Satellite Orbits," Jet Propulsion, vol. 28, 1958, pp. 90–96.

3 King-Hele, D. G., "The Effect of the Earth's Oblateness on the Orbit of a Near Satellite," Proc. Roy. Soc., vol. 247, 1958, pp. 49–72.

4 Blitzer, L., "Apsidal Motion of an IGY Satellite Orbit," *J. Appl. Phys.*, Nov. 1957.

5 Nonweiler, T. R. F., "Perturbation of Elliptic Orbits by Atmospheric Contact," *J. Brit. Interplanet. Soc.*, vol. 16, 1958, pp. 368–379.

Radio-Frequency Mass Spectrometer for the Investigation of the Ionic Composition of the Upper Atmosphere

V. G. ISTOMIN

THE DETERMINATION of the composition of the upper atmosphere, and particularly the composition of its ionized regions, is one of the most important problems in the investigation of the physical parameters of the Earth's atmosphere. Without knowledge of the composition it is impossible to formulate a general theory of the atmosphere, and a study of the atmosphere and ionosphere becomes inconceivable. Data on the chemical composition of the ionosphere at various altitudes and in various regions of the Earth and data on the variation of the composition from day to night and from day to day are very important for investigations of the interaction between the ultraviolet and corpuscular radiation from the sun with the Earth's atmosphere, and for an approach to a solution of such an important geophysical and astrophysical problem as the sun-Earth problem. The same data on the composition of ionized layers are essential for a correct interpretation of the results of other ionospheric experiments,[1] and also for a solution of certain problems of purely applied character.

The only presently known method of direct determination of ionic composition of the upper atmosphere is through mass-spectroscopic analysis. By mounting an ion mass analyzer on a rocket or satellite traveling through the ionosphere and by telemetering its readings to the Earth we can obtain information on the ion mass spectrum and draw conclusions on this basis concerning the chemical composition of the ionosphere.

A mass spectrometer intended for an investigation of the composition of the upper layers of the atmosphere should differ substantially from the well-known laboratory and plant instruments of this type. Like all equipment mounted on rockets or satellites, it must be exceedingly reliable, simple in operation and must operate automatically for a long time without requiring any additional maintenance or adjustments. It is necessary that the instrument withstand considerable temperature fluctuations and be resistant to strong vibration and static overloads, retaining its operating ability after being subjected to them. The instrument must also satisfy, if possible, the somewhat contradictory requirements of small weight and compactness. In addition, it is necessary that the mass spectrometer consume little power, have a short time lag and satisfy other specific requirements.

A radio-frequency mass spectrometer (3),[2] particularly the Bennett version (4), is such an instrument. This mass spectrometer was first used for rocket research by John Townsend Jr. (United States) in 1952 (5). In spite of the fact that investigations of the composition of the atmosphere and ionosphere have been carried out in the United States for seven years (6–9), reliable data were obtained only very recently. Thus, three rocket flights launched from Fort Churchill (Canada) as part of the IGY program, yielded data on the ionic composition of the arctic winter ionosphere up to altitudes of 251 km (10 and 11).

In the Soviet Union, investigations of the ion composition of the upper layers of the atmosphere began in 1957. As a result of work performed as part of the IGY program with high altitude geophysical rockets and the third artificial Earth satellite, data were obtained on the mass spectrum of positive ions of the ionosphere at altitudes up to 885 km (12). The radio-frequency mass spectrometer described in the present article was used in these investigations.

The theory of mass spectrometers of various types operating on the principle of velocity separation of the ions in a high frequency electric field, was treated in the literature many times (3,4,13–15). It is therefore assumed that the operating principle of the instrument is known, and it will not be considered here.

Construction of the Instrument

The RMS-1 mass spectrometer consists of three principal elements and is built in three units: The mass-spectrometer tube (radio-frequency mass analyzer) with preamplifier, the electronic block and the power supply block (Fig. 1).

1 The mass-spectrometer tube is a three-step seven-five cycle analyzer. The available literature data (5,15,16) suggest that the seven-five cycle variant is one of the optimal ones as regards the harmonic level and sensitivity; this explains its choice for our instrument.[3]

A tube of high mechanical strength was developed to our geometrical and electrical specifications by one of the enterprises of the USSR State Committee on Radio Electronics of the Council of Ministers (chief designer—Z. G. Petrenko). All the tubes for the mass spectrometer were also made at the same enterprise. The technical specifications for the tube construction were drafted, together with the electrical and geometrical parameters, after preliminary laboratory experi-

Translated from "Iskusstvennye Sputniki Zemli" (Artificial Earth Satellites), no. 3, USSR Acad. Sci. Press, Moscow, 1959, pp. 98–112.

[1] Such experiments include, for example, the measurement of the concentration of positive ions (1)[2] and the measurement of electrostatic fields in the ionosphere (2).

[2] Numbers in parentheses indicate References at end of paper.

[3] A laboratory model of the Bennett-type seven-five cycle mass spectrometer, but intended for entirely different purposes, was first built in the USSR at the West-Siberia branch of the USSR Academy of Sciences, by a group headed by A. N. Borsin (17). The author expresses his deep gratitude to M. Ya. Shcherbakova, E. F. Doil'nitsyn and A. U. Trubetskoy of this branch for their help in this investigation.

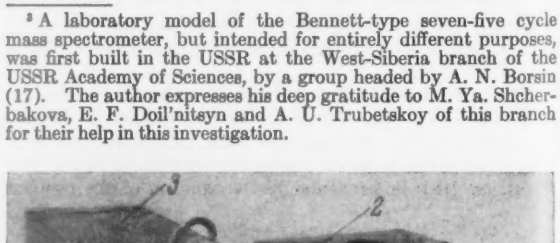

Fig. 1 Radio-frequency mass spectrometer RMS-1: 1—mass-spectrometer tube with preamplifier; 2—electronic block; 3—power supply block (satellite model)

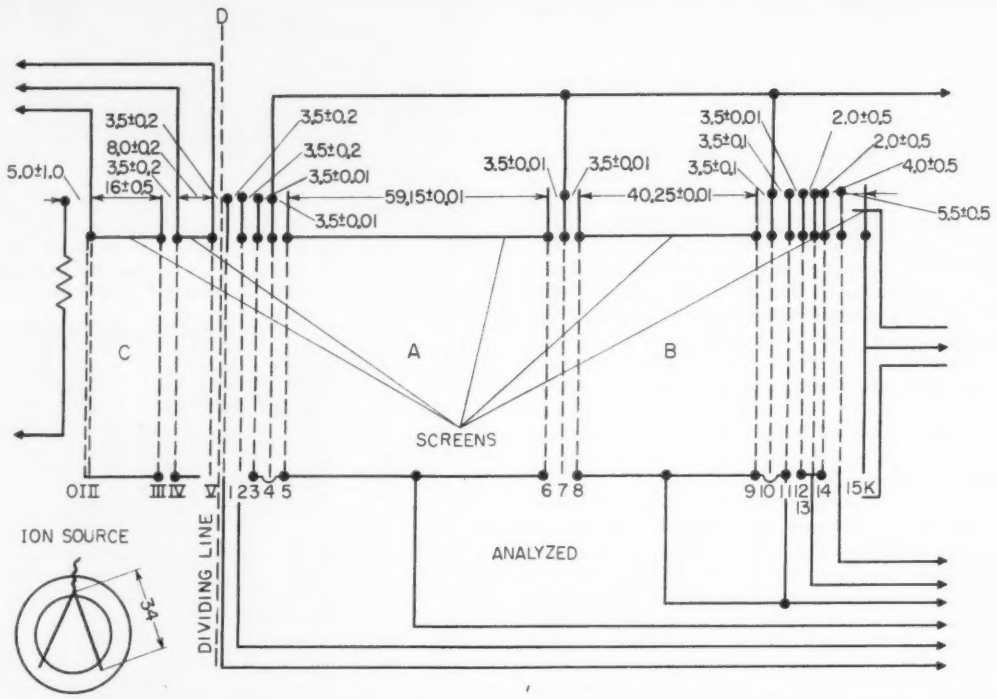

Fig. 2 Diagram showing arrangement of grids of the analyzer and ion source of the radio-frequency mass spectrometer: 0—V-shaped cathode (VT-10 tungsten, 100 μ); I to V—grids of ion source; C—ionization region; D—line of separation between analyzer and ion source; 1, 2—drawing grids of the analyzer; 3, 4, 5—first stage; A—ion drift space (7 cycles); 6, 7, 8—second stage; B—ion drift space (5 cycles); 9, 10, 11—third stage; 12, 13, 14—retarding grids; 15—shielding grid; K—ion collector

ments. The arrangement of the analyzer grids and of the ion source, along with the distances between grids and the specified tolerances, is shown in Fig. 2. Fig. 3 is an over-all view of the analyzer.

One of the features of our instrument is that unlike the previously described radio-frequency mass-spectrometer designs (3,4,16), the grids used in the analyzer and in the ion source (17) are of the single-row type, prepared by winding a tungsten wire over a kovar ring. To fasten the grid windings to the principal ring, a second thin kovar washer (only 0.1 mm thick) is placed over the wound wire and is spot welded. Fig. 4 shows a photograph of such a grid. The working diameter of the grid is 30 mm, the winding thickness is 20 μ and and winding pitch is 0.5 mm. The transmission factor of a grid prepared in this manner is 96 per cent. A high grid transmission is very important, since the analyzer consists of 15 such grids, and the ion currents obtained from the tube collector, other conditions being equal, increases with the over-all transmission of all the grids. The use of single-row grids makes the construction of the instrument simple and economical without adversely affecting its operating properties.

The grids are so mounted in the instrument that the windings of each successive grid make an angle of 120 deg with the windings of the preceding grid. The grids are placed plane-parallel relative to each other accurate to ± 0.01 mm, and electric insulation is provided between neighboring grids, by means of polished metal-glass ring liners. The large distances between grids, limited by the ion drift space (A and B, Fig. 2) are set by turned copper cylinders, which serve simul-

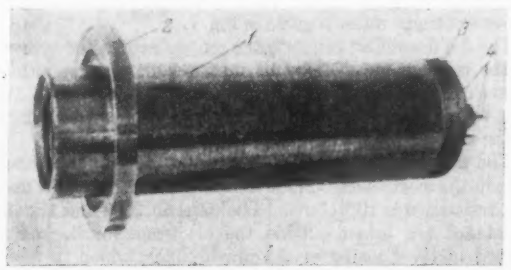

Fig. 3 Mass-spectrometer analyzer: 1—analyzer bulb; 2—flange for securing analyzer to rocket or satellite; 3—thread fastening the preamplifier; 4—analyzer electrode leads

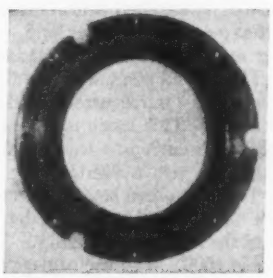

Fig. 4 Grid of mass-spectrometer analyzer

taneously as the screens for the drift spaces. The grids and metal-glass ring liners are stacked as a unit with the screens and with the collector block and are mounted between three polished ceramic rods (4 mm in diam) and placed in the bulb of the analyzer, which is then crimped on the side of the first grid. The leads from the collector and the analyzer grids pass through kovar metal-glass bushings in the base of the tube. The kovar bottom of the base is fused to the bulb.

The bulb of the mass-spectrometer analyzer is made of stainless steel. The bulb has a flange that serves both to mount the analyzer on a rocket or satellite and to join it to the ion-source analyzer. The mass-spectrometer tube as a whole is of dismountable metal-glass construction (Fig. 5). The all-metal analyzer is joined to the ion source through a vacuum seal with a copper liner. The ion source has a V-shaped cathode (thoriated tungsten VT-10, 0.1 mm in diam) and five grids of the same type as used in the analyzer. The ion source is used to adjust the instrument in the laboratory, to verify the operating ability of the instrument all further tests, and to obtain calibration records. Naturally, there is no need for an ion source if the instrument is used for analysis of the ion composition of the atmosphere, since the ions are provided by the atmosphere itself.

The tube of the mass spectrometer, with the ion source connected, is thoroughly degassed by heating to 400 deg for several hours, and is then filled with a mixture of argon and neon at a pressure of approximately 3×10^{-5} mm mercury and sealed off the vacuum pump. Two or three hours after sealing, the operating ability of the tube is checked to see that it is free of excessive leakage. This is followed by introduction of a getter to absorb the gas that is liberated from the ion-source cathode during operation and enters the tube through the seal. Experience has shown that the tube can be stored in this form for months and operate for a long time without requiring the use of a vacuum pump.

2 The electronic circuitry of the mass spectrometer is placed in a separate block (Fig. 6). It contains the following; a—d-c amplifier; b—high frequency generator; c—rectifiers for the bias and stopping voltages; d—sawtooth voltage generator; e—600-v d-c inverter; f—commutation system for telemetering; g—relay system to turn the instrument on and off and for control tests.

A block diagram of the mass spectrometer, showing the above electronic units, is given in Fig. 7.

The d-c amplifier[4] converts the ion current in the collector of the mass-spectrometer tube into a signal in the form of pulses (mass "peaks") ranging from 0 to +6 v, which is then sent to the radio telemetering channel. A complete diagram of the amplifier is shown in Fig. 8.

The first stage—electrometer—uses a 6Zh1Zh tube operating in the electrometer mode normal for this tube. The input resistance is 10^{10} ohms. The 6Zh1Zh tube and the high resistance are taken outside the electronic block and are placed in the housing of the preamplifier, which in turn is placed directly on the tail portion of the mass-spectrometer tube. The principal diagrams of the analyzer and preamplifier are shown in Fig. 9. The preamplifier is connected to the electronic block by a multiconductor shielded cable and a RK-19 coaxial cable terminated with suitable plugs. The cables are somewhat more than a meter long.

The remaining amplifier tubes are subminiatures of the "Drob" series. The second stage with the 6Zh1B tube (T_{11}) operates in the so-called "microcurrent mode," with a plate resistance of 10^6 ohms. This mode is characterized by high gain at negligible plate current. In the third stage of the amplifier (T_{12}) there is also a 6Zh1B tube connected as a normal triode. The first three stages are included in a 100 per cent negative voltage feedback loop, by virtue of which the voltage gain of the first stages is unity. The voltage gain without feedback is 1000. The use of negative feedback reduces the time constant of the amplifier and increases its

[4] The amplifier is based on a circuit recommended in (18).

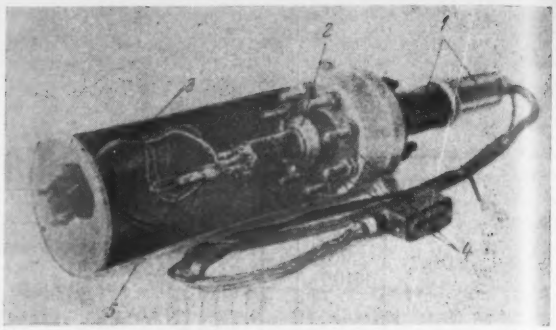

Fig. 5 Mass-spectrometer tube: 1—analyzer preamplifier; 2—ion source—3—protective cover (one half removed); 4—tightening bolts; 5—stub with evaporized getter

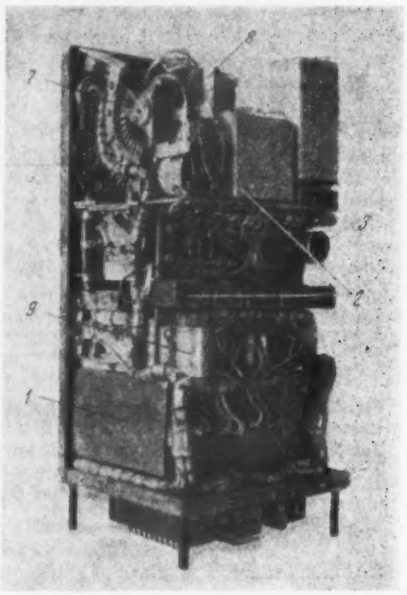

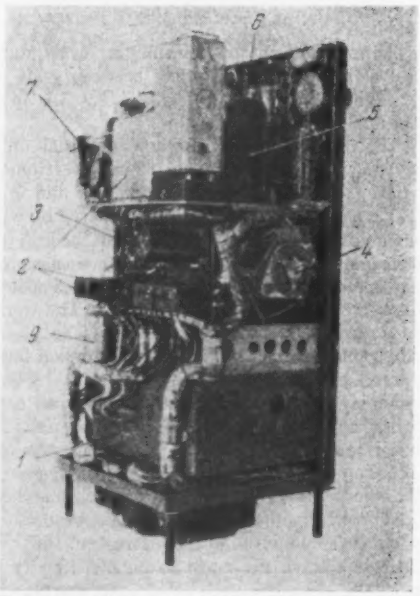

Fig. 6 Electronic block of radio-frequency mass spectrometer (protective cover removed): 1—screen of ion current amplifier; 2—relay system; 3—crystal; 4—generator tuned circuit; 5—high frequency generator tube; 6—bias and stop rectifiers; 7—stepping selector; 8—sawtooth voltage generator tube; 9—condensation battery (B_5)

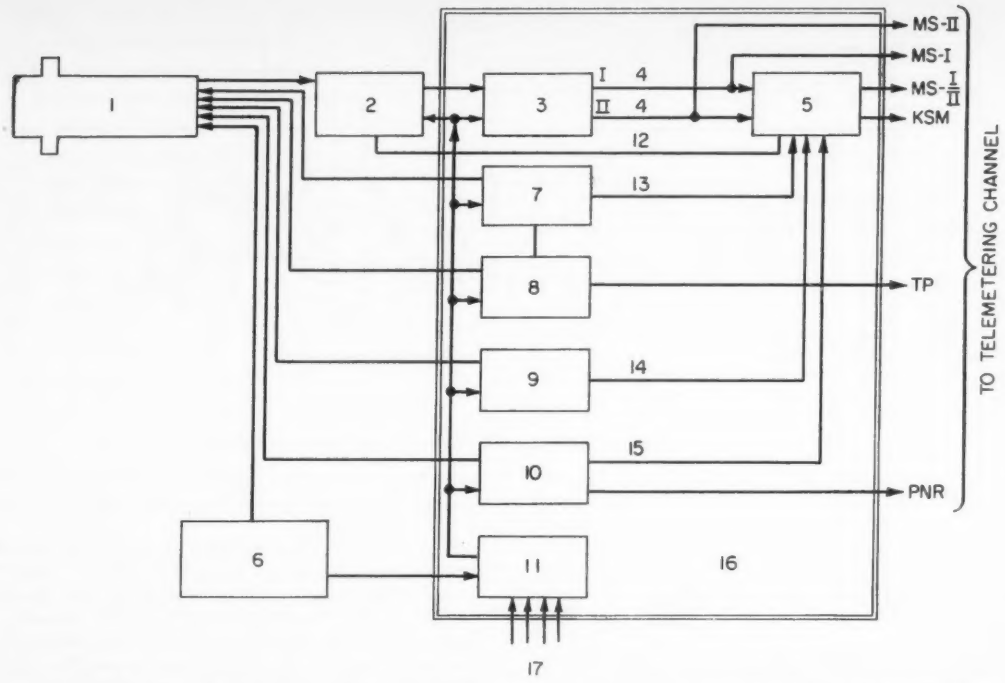

Fig. 7 Block diagram of radio-frequency mass spectrometer: 1—analyzer; 2—preamplifier; 3—d-c amplifier; 4—output; 5—output switch ShI-11; 6—power supply; 7—high frequency generator; 8—bias and stop rectifier; 9—600-v inverter; 10—sawtooth generator; 11—relay system; 12—filament control for electrometer tube; 13—high frequency control; 14—control of 600-v source; 15—control pulses for ShI-11; 16—electronic block; 17—from program device

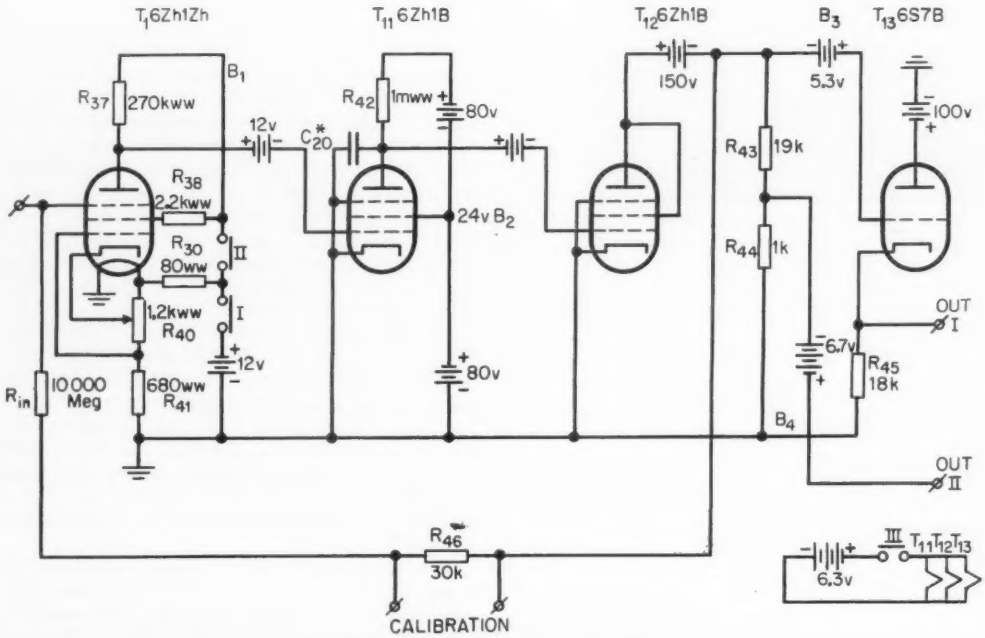

Fig. 8 Principal diagram of d-c amplifier

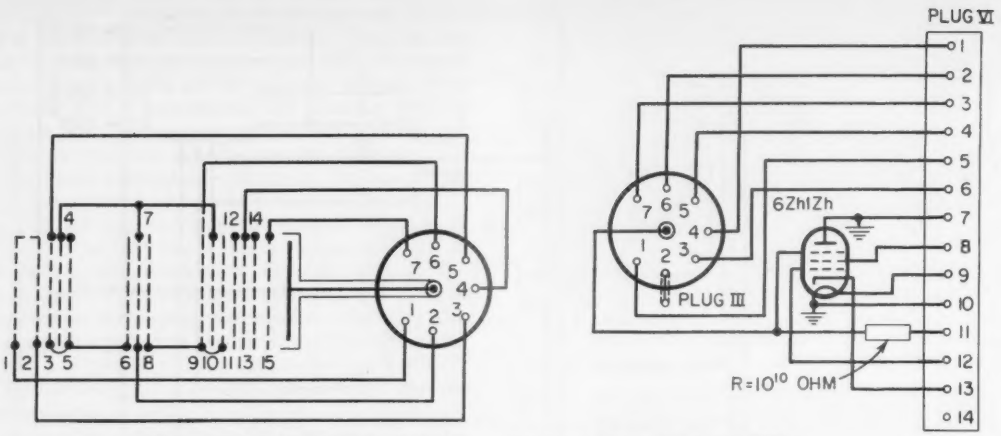

Fig. 9 Principal diagrams of analyzer and mass-spectrometer preamplifier

stability. The time constant of the amplifier is such as to ensure undistorted amplification of the ion-current pulses (mass "peaks") from the mass-spectrometer collector. An idea of the value of the time constant can be gained from the oscillogram (Fig. 10) showing the variation of the amplifier output voltage in response to a unit step input voltage. As can be seen, the time constant does not exceed 5×10^{-3} sec.[5] This is an acceptable value, since the durations of the ion-current pulses in the operating mode of the mass spectrometer are 3 to 5×10^{-2} sec.

[5] The amplifier time constant is greatly affected by the value of the capacitance C_{23}. This capacitance is necessary to prevent self-excitation of the amplifier and can vary with the quality of the wiring and the placement of the components. In this instrument this capacitor had to be increased to 3300 $\mu\mu$f because of the exceeding compactness of the wiring, which, apparently, gave rise to many possibilities for positive feedback leading to self-excitation of the amplifier. In the laboratory models, the value of C_{23} could be made two or three times smaller, thereby considerably reducing the time constant.

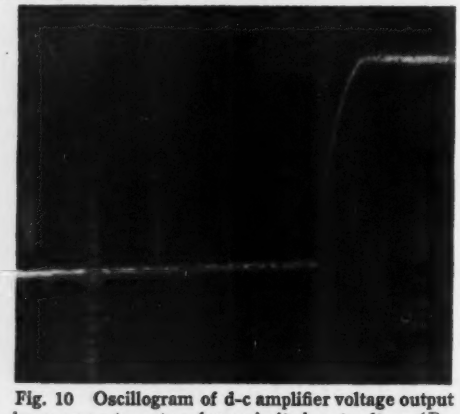

Fig. 10 Oscillogram of d-c amplifier voltage output in response to a step change in its input voltage (R_{in} = 10^{10} ohms). The short markers are spaced 2×10^{-3} sec apart

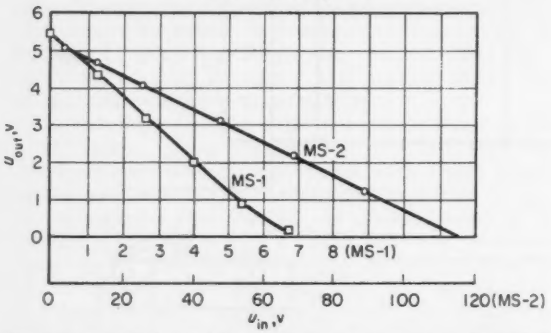

Fig. 11 Amplitude characteristics of the mass-spectrometer amplifier

The last stage of the amplifier (T_{13}—cathode follower with a 6S7B tube) is needed to match the sensitive output with the input of the radio-telemetering system. All the stages are coupled through batteries (B_1, B_2, B_3) built into the amplifier. Batterty B_4, also mounted inside the amplifier, produces the positive voltage at the low sensitivity output. Batteries B_1 to B_4 are made up of OR-1K miniature mercury-oxide elements.

The sensitive output of the amplifier (cathode follower) is linear up to approximately 5.5-v input voltage, and the voltage gain corresponding to this output is approximately 0.8. The low sensitivity output (voltage divider R_{43}-R_{44}) is linear up to 110 v input at a voltage gain of approximately 0.05. The amplitude characteristics of the amplifier are shown in Fig. 11.

The filaments of the amplifier tubes are fed from silver-zinc storage batteries, while the plate circuits are fed from oxide-mercury cells located in the power pack of the mass spectrometer. To increase the amplifier stability, the filament, plate and screen-grid of the electrometer stage (first tube) are fed from a separate set of storage batteries.

A diagram of the electronic block of the instrument is shown in Fig. 12. In the development of the supply circuit for the mass-spectrometer tube, we leaned on the circuit published by Townsend (5). The crystal-stabilized high frequency generator is based on the Pierce circuit and uses a 6P9 tube (T_5). Unlike the Townsend circuit, the mass-spectrometer tube is fed with high frequency through a capacitive divider, made up by capacitor C_{10} and the capacitances of grids 4, 7 and 10 of the analyzer. Such a high frequency supply circuit reduces the power drain of the generator. The amplitude of the high frequency voltage is regulated by varying the voltage on the screen grid of the 6P9 tube with resistor R_{17}. The bias and stop (retarding potential) voltages are obtained by rectification with voltage doubling through tubes 6D6A (T_6-T_9). Such a supply circuit insures constancy of the tube conditions under small fluctuations in the high frequency voltage, because the bias and stop voltages do not vary proportionally in this case. A small part of the high frequency voltage, rectified by a 6D6A tube (T_{20}), serves to control the generator operation. The bias and stop voltages are regulated by potentiometers R_{24} and R_{22}. The plate voltage of the high frequency generator is stabilized by two voltage stabilizer tubes SG-1P (T_3 and T_4).

The sawtooth mass-sweep voltage is generated by a circuit using a TG-1B thyratron (T_1) with linearizing pentode 6Zh1B (T_2). The thyratron is somewhat overdriven because the plate battery voltage is 450 ± 23 v. The amplitude of the sawtooth voltage is approximately 400 v in this case and is

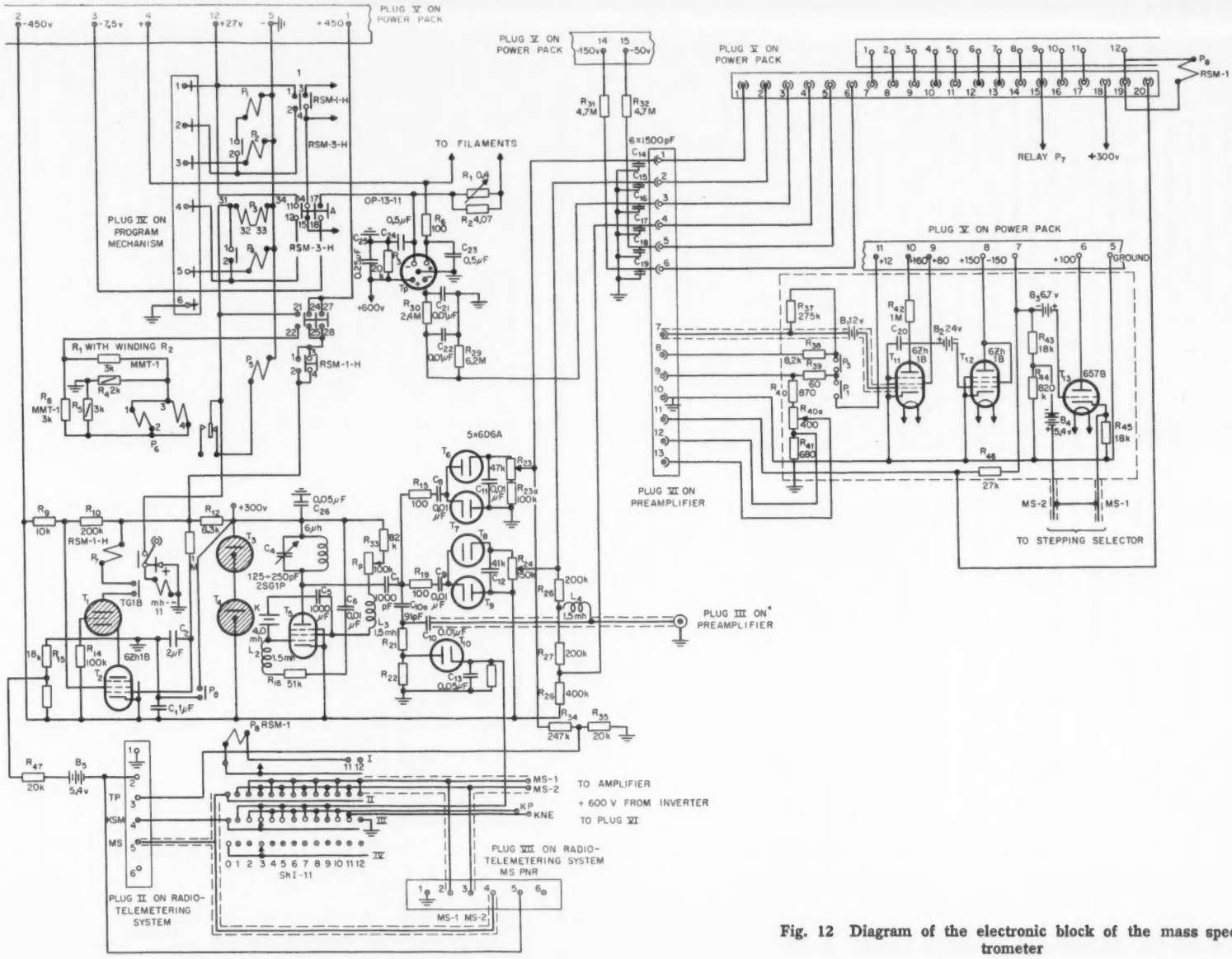

Fig. 12 Diagram of the electronic block of the mass spectrometer

remarkably linear. For operation of the mass spectrometer it is necessary that the sawtooth be negative with respect to the housing of the tube. Consequently, the terminals of the 450-v battery should be insulated from "ground," i.e., from the housing of the instrument. The sweep generator is fed with unstabilized voltage and this leads to a systematic variation of the maximum value of the circuit voltage, and consequently to a corresponding variation in the maximum mass registered. This, however, does not give rise to any difficulties, since the sawtooth sweep voltage is controlled by the radio telemetering system. A relay (P_7) is connected in the thyratron-plate circuit. The discharge-current pulses flowing through the thyratron during the return trace of the sweep (charging of capacitance C_1) cause this relay to operate, and this relay in turn controls the operation of the stepping selector ShI-11. The normally closed contacts of the stepping selector, connected so as to disconnect the plate circuit of the thyratron, open during the time of operation of the stepping selector and prevent a possible uncontrolled discharge of the thyratron.

The electronic block of the mass spectrometer contains a semiconductor inverter (Pr), which feeds high voltage to grid 15 of the analyzer. The inverter delivers approximately 600 v d-c at a load current of approximately 50 μa, and consumes approximately 8 milliamp at 6.3 v from the filament battery. A portion of the converter voltage, picked off the divider R_{20}-R_{23}, is used to control its operation. This voltage (about 1 v) is applied to the even blades of sec. III of the stepping selector. Connected to the odd blades of the same section are the high frequency generator control voltage and the filament voltage for the first amplifier tube. Thus, three control parameters are switched by the stepping selector at the mass-sweep frequency and are applied to a single telemetering channel (the KSM parameter—control of the mass-spectrometer circuit). This is done to reduce the number of telemetering channels needed to operate the instrument. In addition to the foregoing parameters, part of the "stop" voltage, picked off from divider R_{24}-R_{25} (the TP-parameter, the stopping potential) and a portion of the sawtooth mass sweep voltage (parameter PNR) are also telemetered. The PNR parameter voltages are picked off divider R_{13}-R_{15}, but since the polarity of the sawtooth is negative with respect to "ground," a condensation battery is included in its circuit. Like the batteries B_1-B_4, it is made up of OR-1K miniature mercury-oxide cells.

In addition to control parameters, the stepping selector switches also the outputs of the d-c amplifier (sec. II). This is done to make possible operation of the mass spectrometer with only one high interrogation telemetering channel. As can be seen from the diagram of the electronic block (see Fig. 12), however, both outputs of the amplifier are also led out without being switched, so that in normal operation they can be telemetered independently both as the sensitive output (parameter MS-1—mass spectrum, first range) and the low sensitive output (parameter MS-2—mass spectrum, second range). Sec. IV of the stepping selector can be used in various manners, depending on the particular problems solved in each individual experiment. In particular, with the aid of sec. IV it is possible to vary periodically the retarding potential used in the analyzer[6] and to obtain up to 12 different values for this potential.

The relay system P_1-P_4 serves to turn two instrument circuits on and off in response to signals from the program control. These signals are produced by closing momentarily the contacts of disconnect switch IV. The closing of contacts 1-2 of disconnect switch IV causes operation of relay P_1, contacts 3-4 of the relay are used to connect the filament circuit of the electrometer tube 6Zh1Zh in the amplifier, while contacts 1-2 block contacts 1-2 of disconnect IV, so that relay P_1 remains connected until a disconnect command is received. The filament circuit of the electrometer tube is turned on 15 min before the start of operation, to stabilize the null of the amplifier. The remaining circuits of the instruments are connected by a closing momentarily of contacts 1-4 of disconnect switch IV. In this case the contacts 11-12 of relay P_3 also block contacts 1-4 of disconnect switch IV, and relay P_3 remains connected until a disconnect command is received. The disconnect command is produced also by momentary closing of contacts 1-5 of disconnect switch IV. This causes relay P_4 to operate and its normally closed contacts 1-2 interrupt the supply to the winding of relay P_3. The filament supply to the electrometer tube is opened in a similar manner, by momentarily closing contacts 1-3 of disconnect switch IV.

In view of the use of a thyratron for the sawtooth voltage generator, the plate voltage cannot be turned on simultaneously with the tube filaments. Therefore the plate voltage is applied 20-40 sec after the filament circuit is closed. The delay is produced by a thermal relay. A polarized relay OR-64 (P_6) is connected in the diagonal of a bridge comprising two MMT-1 thermistors (R_7 and R_8) and two MLT resistances (R_4 and R_5). One of the thermistors is heated by the filament current of the tubes, through a winding (R_2) placed over one of the thermistors; this winding carries part of the filament current. This unbalances the bridge, causes operation of the polarized relay and turns on relay P_5, which closes the plate-voltage circuit to the mass-sweep generator and to the high frequency generator.

3 The power supply block of the mass spectrometer feeds the electronic circuitry of the instrument and drawing grids 1 and 2 of the analyzer. The power supply comprises silver-zinc storage batteries of high rating and small weight and volume, and mercury-oxide batteries, which are also the most compact and most suitable weightwise from among all the electrochemical systems now existing.

Mass-Spectrometer Operating Procedure

In preparing for the experiments on the determination of the ion composition of the ionosphere, it became clear that for a qualitative interpretation of the obtained data it would be necessary to determine the voltage of the parameter PNR (mass-sweep sawtooth voltage[7]) with great accuracy. An error of approximately 2 per cent in the determination of the PNR voltage would lead to an error of 1 amu in the determination of the mass unit, which would be quite unacceptable. The required accuracy can be obtained by thorough calibration of all the instruments, apart from the telemetering system (with registration of the spectrum and measurements of the PNR level corresponding to definite mass numbers) and again together with the telemetering system but now without registration of the spectrum. However, any intermediate calibrations would unavoidably increase the total error in the determination of the levels of the telemetered parameters, since it is difficult to use high precision instruments for the calibration, for many reasons. It was therefore very important to find a way of performing a so-called true calibration of the entire system of the mass spectrometer plus the telemetering channel, by recording of the mass spectrum of a gas mixture of known composition. At first such a calibration seemed difficult, since a vacuum system was necessary for the analyzer in order to operate the instrument and to produce the mass spectrum. The situation improved after laboratory experi-

[6] Thus, in an experiment made on Sept. 9, 1957 (12) the retarding potential was periodically increased to exclude false ("harmonic") peaks, which could appear in the mass spectra under the influence of the intrinsic charge (19).

[7] It follows from the theory of the instrument that the mass number corresponding to a given collector ion-current peak is related to the sawtooth sweep voltage by $M = V/k$, where V is the value of the sawtooth sweep voltage (volts) at the instant of appearance of the peak, M is the mass number corresponding to a given peak (amu), and k a constant that depends on the parameters of the analyzer and the operating mode of the instrument. For the instrument described here, $k = 7.2$ v/amu.

ments showed that the analyzer could operate for a long time sealed off from the vacuum system. It was for this purpose that the degassing and gettering operations described above were carried out with the mass spectrometer tube.

Operation with a sealed tube filled with a mixture of known inert gases offered great convenience and advantages. Above all, it became possible to record the spectrum with the radiotelemetering system at any stage of preparation for the experiment, and thus obtain a record from which to prepare a mass calibration curve for the instrument. This allowed us to bypass all the intermediate stages of calibration and thus increase considerably the accuracy in the determination of the mass numbers. The calibration characteristic was plotted against five reference points on the mass scale: A^{40}, A^{36}, N_2^{28}, Ne^{22} and Ne^{20}. The presence of a stable filler in the mass-spectrometer tube permitted rapid adjustment of the instrument, setting the required operating mode (resolution) with the aid of the peaks of Ne^{20} and Ne^{22}, and also made it possible always to verify the operation of the instrument and to see to it that its adjustment and operating mode did not change.

To obtain reproducible and comparable results, all the instruments were filled with mixtures of more or less uniform composition, at a fixed pressure where possible. Simple batching devices, which ensured in first approximation the required homogeneity of the filling, were used to prepare the mixture and to admit it into the tube. The pressure of the mixture in the tube during filling was estimated with a VI-3 ionizing vacuum meter. After sealing the tube, the pressure inside it could also be estimated from the ion current of the second grid of the analyzer at a fixed emission current, with the first two grids in the normal mode and the mass-spectrometer electronic block disconnected. The calibration for the purpose of estimating the pressure was made with one tube; a calibration curve is shown in Fig. 13.

All the instruments were adjusted in an identical manner. The high frequency level was set at maximum, 12-14 v (effective). This was followed by a setting of the bias voltage for the maximum of the Ne^{20} or Ne^{22} peak. This in turn was followed by adjustment of the retarding potential. To obtain comparable results all the instruments were adjusted to the same setting, namely, to obtain a resolution on the order of 20 at the base of the peak in the region of mass 20. The resolution was estimated visually by means of peaks Ne^{20} and Ne^{22}, which were viewed on the screen of a control oscilloscope.

For laboratory operation of the instrument, and also for all subsequent stages of preparation for the experiment, special control panels were developed (Fig. 14). The control panel permits performance of the following operations: a—Connecting and disconnecting the mass spectrometer; b—control of all the power supply voltages; c—control of the operating mode of the mass spectrometer; d—control of voltages at the telemeter outputs; e—calibration of the mass-spectrometer amplifier and control of the calibrator voltages (ten voltage steps from 1.3 to 90 v); f—supplying ion source of the mass-spectrometer tube, control and regulation of the emission current, and also control of the ionization voltage; g—calibration of the sawtooth sweep voltage; h—observation of the mass spectrum on the screen of the cathode ray oscilloscope[8]; i—recording of the mass spectrum and all other telemetered parameters on a loop oscillograph.[9]

A typical mass spectrum of the gas mixture filling the tube is shown in Fig. 15.

The normal operating condition of the instrument is as follows[10] (all voltages are relative to the tube housing):

Grid no. 1—50 v.

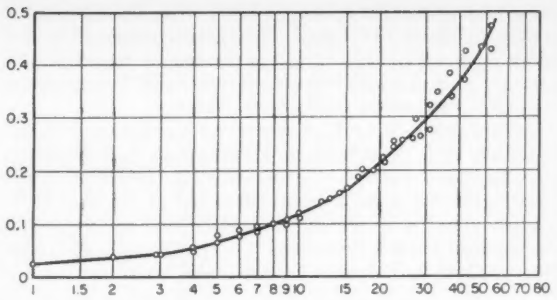

Fig. 13 Calibration curve for estimating the pressure in the sealed-off tube of the mass spectrometer: Abscissa—pressure 10^{-6} mm Hg; ordinates—ma

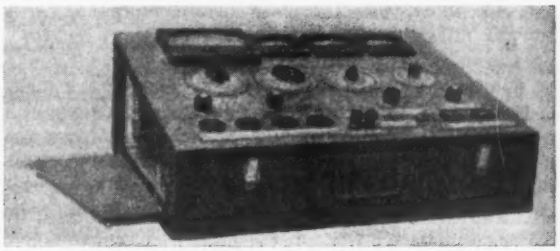

Fig. 14 Control panel of mass spectrometer

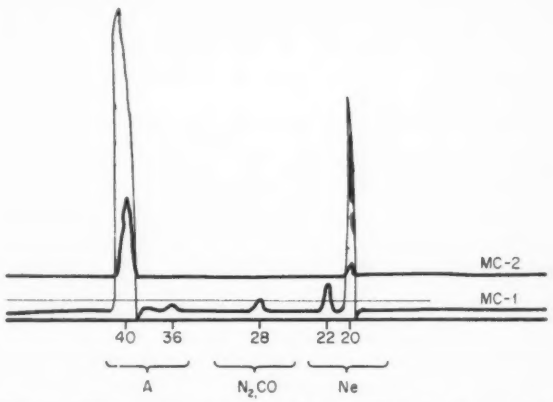

Fig. 15 Mass spectrum of gas mixture filling the mass-spectrometer tube

Grid no. 2—130 v.

Grids nos. 3-11—10-400 v (sawtooth mass-sweep voltage).

Grids nos. 4, 7 and 10—11.7 v (effective) (4.0 megacycles high frequency).

Grids nos. 12, 13 and 14—+63 v (retarding or stop potential).

Thus, the instrument operates in a mode of $U_{stop}/U_{hf} = 5.4$.

Grid no. 15—450-480 v.

In addition, −23-v bias voltage is applied to grids nos. 3, 5 and 6 relative to grids nos. 8, 9 and 11.

In this mode the mass spectrometer has a resolution of 20 in the region of mass 20 (at the base of the peak). The mass range of the instrument is from 6 to 48 atomic mass units. The time required to cover the entire range of masses (mass-

[8] The control oscilloscope used was a type EO-7 standard model, for which additional d-c imputs were provided in the vertical and horizontal circuits.

[9] A type POB-12 loop oscillograph was used.

[10] The conditions given here are for the mass spectrometer as installed in the third artificial Earth satellite.

sweep period) is approximately 1.7 sec. The input resistance of the amplifier is 10^{10} ohms. The dynamic range of the amplifier is approximately 500; it is insured by means of two outputs: A high sensitivity output, 0-5 $\times$ 10^{-10} amp and a low sensitivity output, 0-100 $\times$ 10^{-10} amp.

In conclusion, the author expresses his gratitude to Z. G. Petrenko, O. F. Lantsman, A. I. Sedov and R. P. Shirshov, who did much work on the construction, preparation and testing of the mass-spectrometer tube; to L. P. Chulkin, O. V. Radionov and A. A. Perno, who constructed and tested the electronic blocks and the control panel for the mass spectrometer, and to S. V. Vasyukov for help in this work.

References

1 Gringauz, K. I. and Zelikman, M. Kh., *Uspekhi Fiz. Nauk* (Advances in Physical Sciences), vol. 63, no. 1, 1957, p. 239; translation published by Internatl. Phys. Index, New York.
2 Imyanitov, I. M., *ibid.*, p. 267.
3 Redhead, P. A., *Canad. J. of Phys.*, vol. 30, no. 2, 1952, p. 1.
4 Bennett, W. H., *J. Appl. Phys.*, vol. 21, no. 2, 1950, p. 143.
5 Townsend, J. W., *Rev. Sci. Instr.*, vol. 23, no. 10, 1952, p. 538.
6 Townsend, J. W., Meadows, E. B. and Pressley, E. S., "Rocket Investigations of the Upper Atmosphere" (Russian translation), Foreign Literature Press, Moscow, 1957, p. 192.
7 Johnson, C. Y. and Meadows, E. B., *J. Geophys. Research*, vol. 60, no. 2, 1955, p. 193.
8 Johnson, C. Y. and Heppner, J. P., *J. Geophys. Research*, vol. 60, no. 4, 1955, p. 533.
9 Johnson, C. Y. and Heppner, J. P., *J. Geophys. Research*, vol. 61, no. 3, 1956, p. 575.
10 Meadows, E. B. and Townsend, J. W., "Diffusive Separation in the Winter Nighttime Arctic Upper Atmosphere, 112 to 150 km," paper presented during the Fifth Assembly of SK MGG (IGY), Moscow, 1958.
11 Istomin, V. G., "Investigations of the Ionic Composition of the Earth's Atmosphere on Rockets and on the Satellite," *ibid.*
12 Istomin, V. G., "Study of the Ionic Composition of the Earth's Atmosphere from Rocket and Sputnik Data," *ibid.*
13 Redhead, P. A. and Crowell, C. R., *J. Appl. Phys.*, vol. 24, no. 3, 1953, p. 331.
14 Wherry, T. C. and Karasek, F. W., *J. Appl. Phys.*, vol. 26, 1955, p. 582.
15 Shcherbakova, M. Ya., *J. Tech. Phys.* (*USSR*), vol. 27, no. 3, 1957 p. 599; translation in *Soviet Phys.—Tech. Phys.*, vol. 2.
16 Doil'nitsyn, E. F., Trubetskoy, A. U. and Shcherbakova, M. Ya., *J. Tech. Phys.* (*USSR*), vol. 27, no. 2, 1957, p. 404; translation in *Soviet Phys.—Tech. Phys.*, vol. 2.
17 Istomin, V. G., *Pribory i tekhnika eksperimenta* (Instruments and Measurement Engineering), no. 2, 1958, p. 111.
18 Tsvang, L. R., "Pulse Measurement of the Spectrum of Light Ions in the Atmosphere," Dissertation, Inst. of Applied Geophysics Acad. Sci. USSR, 1956.
19 Mirtov, B. A. and Istomin, V. G., *Uspekhi Fiz. Nauk* (Advances in Physical Sciences), vol. 63, no. 1, 1957, p. 227; translation published by Internatl. Phys. Index, New York.

Reviewer's Comment

This article describes the basic instrumentation used by Soviet scientists to investigate the positive ion composition of the Earth's ionosphere. Although Istomin is primarily concerned with the spectrometer as installed in Sputnik III, the instrumentation was first used in the Soviet vertical rocket sounding program and probably with minor modifications in the Soviet space probes to detect hydrogen and helium ions.

The article is well written and easily understood; inferring from published results (1) I believe it gives an accurate description of the instrumentation and state of ion mass spectrometry in the USSR in 1958.

As stated in the article the Soviet instrumentation follows work performed at the U. S. Naval Research Laboratory as reported in 1952 (2) and 1955 (3). It is interesting to note the following points: The Soviet ion composition program began in 1957 after the United States program had made the initial investigation (3) and after the basic problems of mass identification and relative ion abundances in the *E* and *F* regions in 1956 (4) had been solved. Soviet scientists would have benefitted by employing the technique of varying the stopping potential to distinguish "harmonics" from fundamental peaks (5). If this had been done in Sputnik III it would have permitted them to identify absolutely the mass of ions detected. Moreover, it would have established the operating conditions of the spectrometer for each ion peak when that peak was influenced by the apparent potential due to the satellite's velocity through the ionosphere. Provisions were incorporated in the instrumentation to change the stopping potential but appear not to have been used for the purpose described in Sputnik III.

Because this instrumentation for the determination of ion composition was the first to be successfully flown in a satellite, the English translation of this article is of interest. The Western World can now critically examine this scientific achievement of Soviet science.

In this reviewer's opinion the major contribution of the Sputnik III instrumentation and results (1) was the extension of the ion composition measurements above the 250-km level obtained by the United States in 1956.

1 Istomin, V. G., "Some Results of the Measurement of the Spectrum Mass of Positive Ions by the Third Artificial Earth Satellite," Translation F-7, April 1960.
2 Townsend, J. W., Jr., *Rev. Sci. Instr.*, vol. 23, 1952, pp. 538–541.
3 Johnson, C. Y. and Meadows, E. B., *J. Geophys. Research*, vol. 60, 1955, pp. 193–203.
4 Johnson, C. Y. Meadows, E. B., and Holmes, J. C., *J. Geophys. Research*, vol. 63, 1958, p. 443.
5 Holmes, J. C. and Johnson, C. Y., Astronautics, vol. 4, no. 7, 1959, p. 30.

—Charles Y. Johnson
U. S. Naval Research Laboratory
Washington, D. C.

System for Determination of the Parameters of the Motion of a Body in Space

G. O. FRIDLENDER

1 Basic Premises

AN AUTONOMOUS determination of the velocity and acceleration coordinates of a body moving in space is a very complicated problem.

It is known that when any vehicle moves in space and is not acted upon by non-field-like (i.e., nongravitational) forces, the objects contained inside the vehicle are in a "weightless" state, and consequently systems which have unperturbability periods (such as the Schuler period) lose their major advantage, namely the corrections (proportional either to the first or second integral of the accelerations) that they provide for the platform (vertical) position.

A solution therefore suggests itself—that of determining the coordinates, velocities and accelerations of the missile by expressing, for example, the coordinates in terms of three angles between the lines of sight from the vehicle to three planets (the coordinates of which are, naturally, known) or to the sun and two planets. The first derivative of the coordinate readings obtained in this manner yields the velocity, and the second derivative yields the acceleration of the vehicle.

One can conceive, however, of a system that employs a correction signal proportional to the second integral of the measured accelerations. Such a system operates essentially as follows. Assume we have a three-gyroscope system stationary relative to stellar space. If the gyroscopes are of sufficiently high quality, "stationarity" of the gyro system can be insured in the usual manner, by using two optical systems aimed on any two stars. Let this gyro system be connected to two platforms, each with two degrees of freedom with respect to this system. The two angles that the first platform makes with the gyro system will be proportional to the double integral of the accelerations, measured in two mutually perpendicular directions by accelerometers located on the first platform. The double integral of the acceleration measured by the third accelerometer, which is located on the second platform and which is perpendicular to the first two accelerometers, will determine the position of the second platform. In this case the double integrals will yield the path covered in the interplanetary space, and the first integrals will yield the velocities, provided we neglect the acceleration due to the gravitational fields of the sun and of the planets, as well as the instrument errors of the system. Naturally, the errors due to gravitation and imperfect system components (accelerometers and integrators) may reach considerable values. But the "correction" which is used in analogous geosystems[1] cannot be used here because of the "weightlessness" of the sensitive elements of the accelerometers.

To eliminate these errors, we can employ the following scheme. Assume we have two optical systems aimed at two planets or at the sun and one planet. The angles of rotation of the first platform should be proportional to the sum of the double integrals of the accelerations and to the inclinations (measured respectively in two mutually perpendicular planes) of the platform of the first optical system. Thus, these inclinations become equivalent to the accelerometer signals obtained in a geosystem when the direction of acceleration measurement deviates from a position perpendicular to the local vertical (more accurately, from a direction perpendicular to the local direction of the force lines of the gravitational field).

The position of the second platform will be determined by the double integrals of the accelerations and of the inclinations of the platform of the second optical system (which is placed at an angle close to $\pi/2$ with the first system).

In such a scheme the period of platform oscillations will depend only on the coefficients of proportionality between the platform angles and the double integrals of their inclinations to the optical systems.

Naturally, a more refined system would also depend on the frame of reference relative to which the missile position is determined within the solar system.

We shall consider later, as an example, a spherical coordinate system with origin at the center of the sun, with an initial plane coinciding with the plane of the ecliptic, and with an initial meridian passing through the point of the vernal equinox.

Other systems, naturally, can also be chosen, for example, one with the origin at Earth's center and an initial plane coinciding with the plane of the celestial equator, or else an "orthodromic" system, a rectangular system, etc. Apparently, for automatic guidance it is best to use a coordinate system with origin at the target point.

It must be noted that, since all planets are located close to the plane of the ecliptic, the coordinate system adopted here is in practice close to "orthodromic."

In the first of the aforementioned coordinate systems, the position coordinates of the vehicle are the angles between the radius vector of the missile and the initial plane φ (Fig. 1) and between the initial meridian and the meridian of missile position α. The third coordinate is the modulus r of the radius vector of the missile. In this case the simplest way to locate the first platform is to mount its "plane" perpendicular to the radius vector (this, however, is not the only possible position). The angles of rotation of this platform with respect to the gyro system will be φ and α. The position of the platform relative to the radius vector should obviously be such that the measurement axes of the two accelerometers connected with the platform coincide with the "meridian" and "parallel" of the chosen coordinate system. Accordingly,

Translated from *Izvestiia Akademii Nauk SSSR, Otdelenie Tekhnicheskikh Nauk, Energetika i Avtomatika* (Bull. USSR Acad. Sci., Div. Tech. Sci., Power and Automation), no. 6, 1959, pp. 108–117.

[1] By "geosystems" we mean systems intended for missiles moving with relatively small velocities along Earth's surface.

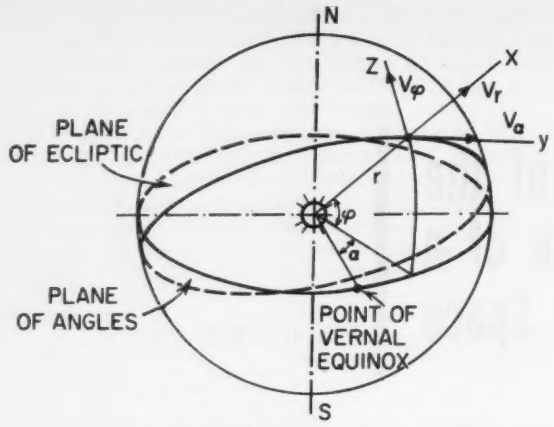

Fig. 1

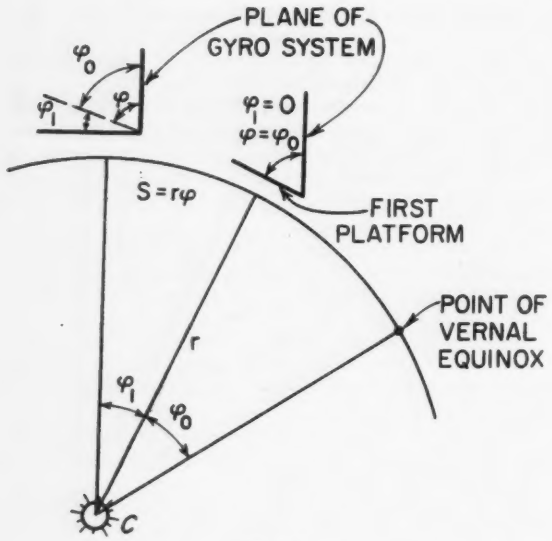

Fig. 2

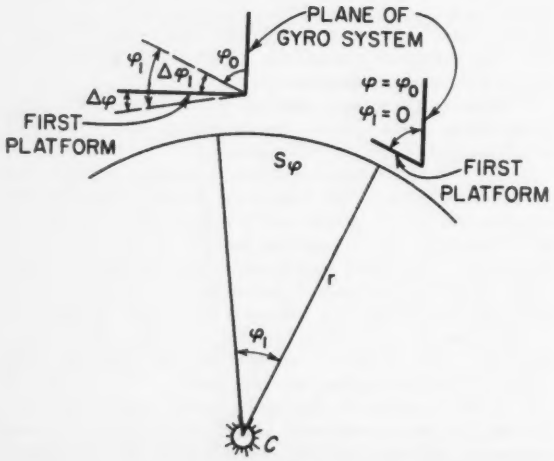

Fig. 3

the deviations from the radius vector $\Delta\varphi$ and β, as determined by the first optical system, should lie in the plane of the "meridian" and in a plane perpendicular to it and passing through the origin, i.e., in the plane of the angles β.

The simplest (but not unique) orientation of the second platform will be one in which the measurement axis of the third accelerometer coincides with the direction of the radius vector, i.e., with the axis of the first optical system, aimed at the sun (or planet). The position relative to the radius vector depends in turn on the direction of the second optical system. The angle between the second optical system and the "plane" of the second platform is obviously equal to the angle between the directions to the sun and to the planet (or to the angle between the directions to the planets). In moving along the radius vector and in the course of time, this angle will change and the angle between the optical system aimed at the planet and the "plane" of the second platform will change accordingly. The deviations of the second platform from the specified (calculated) position relative to the second optical system must also be integrated twice, and the second platform should be corrected by means of the signal obtained after the double integration.

Let us determine now the advantages and shortcomings of this system, compared with the system first indicated. The shortcoming is that instead of the three optical systems needed in the first system we now need four. Its advantage is as follows. In the first scheme the velocities of the vehicle are determined, as already indicated, by differentiating the coordinate readings. It is easy to see that after differentiation changes in the coordinate errors cause, generally speaking, greater errors in the vehicle velocity readings. The more rapid the variation in the coordinate error, the greater the velocity errors. If the second system is used, the optical system sighting errors (corresponding to the coordinate errors in the first scheme) can produce only platform oscillations with amplitudes equal to the magnitude of the error and with periods that depend on the coefficient of proportionality between the double integral of the platform deviation (from the direction to the celestial body) and the angle of rotation of the platform. This period can be chosen sufficiently large, so that the velocity error of the moving missile can be made considerably less than the velocity error obtained in the first scheme. This is indeed natural, for it is known that differentiation increases the errors, whereas integration smoothes them. Obviously, the foregoing applies even more to acceleration measurements. Whereas in the first scheme the acceleration is the result of double differentiation, in the second it is the result of direct measurement (we disregard here the acceleration due to gravitational forces of the sun and of the planets).

It must be noted in addition, that in this system damping will not produce the same errors that are produced by damping in a geosystem. Damping can be obtained by making the platform rotation also proportional to the single integral of the platform inclinations relative to the optical system.

2 Equations of Motion of the Platforms

Although the position of the first platform relative to a "stationary" gyro system is defined by the angles φ and α, nevertheless, since the correction of the platform takes place in the plane of the angles φ and β, we shall first derive the equations of motion of the platform in terms of the angles φ and β.

The angle φ will be determined from

$$\varphi = \varphi_1 + \varphi_0$$

where φ_0 is the initial angle between the first platform and the gyro system, and depends on the initial coordinates of the vehicle. If the radius vector of the vehicle lies at the initial instant of time in the plane of the ecliptic, then φ_0 is 0.

The angles φ, φ_0 and φ_1 are defined in Fig. 2.

It is obvious that changes in the angle φ_1, which can be effected by special devices, should be proportional to the double integrals of the accelerations measured by the accelerometers, i.e.

$$\Delta\varphi_1 = \nu_\varphi \int_0^t \int \sum j_z dt\, dt$$

where

ν_φ = proportionality coefficient
$\sum j_z$ = sum of all the accelerations measured by the accelerometer along the z axis (Fig. 1)

On the other hand, it is seen from Fig. 3 that $\Delta\varphi_1 = \varphi_1 - \Delta\varphi$, where $\Delta\varphi$ is the inclination of the first platform from the calculated position, specifically from the position perpendicular to the radius vector.

Since

$$\varphi_1 = S_\varphi / r$$

then

$$\Delta\varphi_1 = S_\varphi / r - \Delta\varphi$$

or

$$\Delta\varphi = \frac{S_\varphi}{r} - \nu_\varphi \int_0^t \int \sum j_z dt\, dt$$

Let us evaluate the quantities under the double integral sign. For this purpose we determine the accelerations measured by the accelerometers j_x, j_y and j_z. It is known that

$$\sum j_x = V_x' + \omega_y V_z - \omega_z V_y$$
$$\sum j_y = V_y' + \omega_z V_x - \omega_x V_z$$
$$\sum j_z = V_z' + \omega_x V_y - \omega_y V_x$$

where

V_x', V_y', V_z' = projections of the accelerations due to non-field-like forces on the moving axis
V_x, V_y, V_z = integrals of these projections
ω_x, ω_y, ω_z = projections of the total angular velocity of the moving coordinate system on the moving axes

Bearing in mind that in our case

$$V_x = V_r \qquad V_y = V_\alpha \qquad V_z = V_\varphi$$
$$\omega_x = (V_\alpha / r)\tan\varphi \qquad \omega_y = -V_\varphi / r \qquad \omega_z = V_\alpha / r$$

we obtain

$$\sum j_x = V_r' - \frac{V_\varphi^2 + V_\alpha^2}{r}$$

$$\sum j_y = V_\alpha' + \frac{V_\alpha V_r}{r} - \frac{V_\varphi V_\alpha}{r}\tan\varphi$$

$$\sum j_z = V_\varphi' + \frac{V_\varphi V_r}{r} + \frac{V_\alpha^2}{r}\tan\varphi$$

Let us substitute the resultant values in the equations of motion of the platforms. We have

$$\Delta\varphi = \frac{S_\varphi}{r} - \nu_\varphi \int_0^t \int \left(V_\varphi' + \frac{V_\varphi V_r}{r} + \frac{V_\alpha^2}{r}\tan\varphi \right) dt\, dt$$

We impose certain conditions on the coefficient ν_φ. Let

$$\nu_\varphi = 1/r$$

It is then easy to see that

$$\frac{S_\varphi}{r} = \nu_\varphi \int_0^t \int V_\varphi' dt\, dt$$

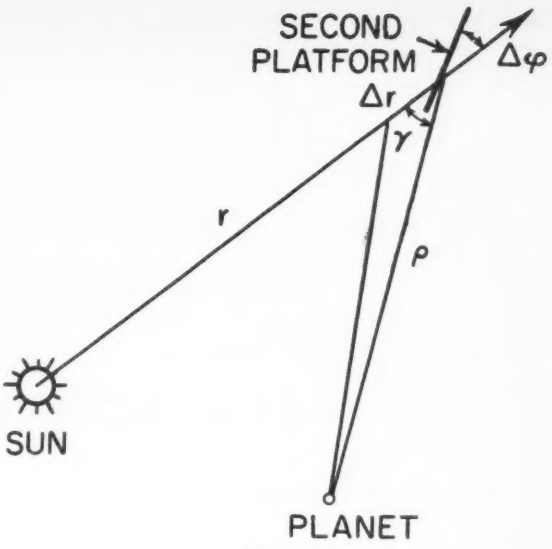

Fig. 4

The equation will then become

$$\Delta\varphi = -\nu_\varphi \int_0^t \int \left(\frac{V_\varphi V_r}{r} + \frac{V_\alpha^2}{r}\tan\varphi \right) dt\, dt \qquad [2.1]$$

Proceeding in an analogous manner for the plane of the angles β, we obtain

$$\beta = -\nu_\beta \int_0^t \int \left(\frac{V_\alpha V_r}{r} - \frac{V_\varphi V_\alpha}{r}\tan\varphi \right) dt\, dt \qquad [2.2]$$

It must be noted that V_α and V_α' can also be designated V_β and V_β' (but $\alpha \neq \beta$, these angles lie in different planes).

For the second platform, the equation will be set up somewhat differently. Actually, for the second platform we can obtain

$$\Delta\psi = \frac{\Delta r \sin\gamma}{\rho} - \nu_\psi \sin\gamma \int_0^t \int \sum j_z dt\, dt$$

where

$\Delta\psi$ = angle of rotation of the second platform relative to the radius vector of the missile
γ = angle between the directions to the sun and to the planet (Fig. 4) (or between the directions to two planets)
ρ = distance from the vehicle to the planet

Inserting the value of $\sum j_z$ into this equation and noting that

$$\frac{\Delta r \sin\gamma}{\rho} = \nu_\psi \sin\gamma \int_0^t \int V_r' dt\, dt$$

where ν_ψ is the proportionality coefficient, which should be equal to $1/\rho$, we find

$$\Delta\psi = \nu_\psi \sin\gamma \int_0^t \int \frac{V_\varphi^2 + V_\alpha^2}{r} dt\, dt \qquad [2.3]$$

Let now the angles $\Delta\varphi$, β and $\Delta\psi$ vary not only in proportion to the double integrals of the accelerations, but also in proportion to the sums of the double and single integrals of

the angles themselves, i.e., assume we have

$$\Delta\varphi = -\nu_\varphi \int_0^t \int \left(\frac{V_\varphi V_r}{r} + \frac{V_\alpha^2}{r} \tan \varphi \right) dt\, dt - k_2 \int_0^t \int \Delta\varphi\, dt\, dt - k_1 \int_0^t \Delta\varphi\, dt \quad [2.4]$$

Analogously

$$\beta = -\nu_\beta \int_0^t \int \left(\frac{V_\alpha V_r}{r} - \frac{V_\varphi V_\alpha}{r} \tan \varphi \right) dt\, dt - k_4 \int_0^t \int \beta dt\, dt - k_3 \int_0^t \beta\, dt \quad [2.5]$$

$$\Delta\psi = \nu_\psi \sin\gamma \int_0^t \int \frac{V_\varphi^2 + V_\alpha^2}{r} dt\, dt - k_6 \int_0^t \int \Delta\psi dt\, dt - k_5 \int_0^t \Delta\psi\, dt \quad [2.6]$$

where

ν_β, k_1 to k_6 = coefficients of proportionality
ν_β = $1/r$
k_1 to k_6 = constants

Differentiating the equations twice, we obtain for the first equation

$$\Delta\varphi'' + k_1\Delta\varphi' + k_2\Delta\varphi = -\nu_\varphi \left(\frac{V_\varphi V_r}{r} + \frac{V_\alpha^2}{r} \tan\varphi \right) - 2\frac{\partial \nu_\varphi}{dt} \int_0^t \left(\frac{V_\varphi V_r}{r} + \frac{V_\alpha^2}{r} \tan\varphi \right) dt - \frac{d^2\nu_\varphi}{dt^2} \int_0^t \int \left(\frac{V_\varphi V_r}{r} + \frac{V_\alpha^2}{r} \tan\varphi \right) dt\, dt$$

At a velocity equal to the second cosmic velocity (escape velocity) and at a value of r equal to the distance from Earth to the sun, the first term in the right-hand side is on the order of 3.2×10^{-4} sec^{-2} (corresponding to a linear acceleration of 4.8×10^{-4} m per sec^2). The second and third terms (which, generally speaking, increase with time), however, will reach values of this order only after 150 and 200 days, respectively. At the beginning of the motion, the second and third terms will be vanishingly small.

Analogously we obtain for the angles β and $\Delta\psi$

$$\beta'' + k_3\beta' + k_4\beta = -\nu_\beta \left(\frac{V_\alpha V_r}{r} - \frac{V_\varphi V_\alpha}{r} \tan\varphi \right) - 2\frac{d\nu_\beta}{dt} \int_0^t \left(\frac{V_\alpha V_r}{r} - \frac{V_\varphi V_\alpha}{r} \tan\varphi \right) dt - \frac{d^2\nu_\beta}{dt^2} \int_0^t \int \left(\frac{V_\alpha V_r}{r} - \frac{V_\varphi V_r}{r} \tan\varphi \right) dt\, dt$$

$$\Delta\psi'' + k_5\Delta\psi' + k_6\Delta\psi = \nu_\psi \sin\gamma \frac{V_\varphi^2 + V_\alpha^2}{r} + 2\frac{d(\nu_\psi \sin\gamma)}{dt} \int_0^t \frac{V_\varphi^2 + V_\alpha^2}{r} dt + \frac{d^2(\nu_\psi \sin\gamma)}{dt^2} \int_0^t \int \frac{V_\varphi^2 + V_\alpha^2}{r} dt\, dt$$

3 Determination of the Coefficients of the Equations of Motion of the Platforms

Let us determine the period of the platform oscillations and the values of the coefficients of the equations, starting out by specifying the required accuracy of the velocity readings. If the accuracy required is 0.5 per cent of the vehicle velocity, the period of platform oscillations can be readily determined, and consequently also the coefficients, by assuming that the damping is semi-aperiodic, the amplitude of the platform oscillations does not exceed 10 to 12″, and the velocity of motion is equal to seven times escape velocity. This is the average velocity needed to get to Mars during the time of the great opposition in approximately 1 month.

It is obvious that

$$T = 2\pi A r/\Delta V$$

where

T = period of platform oscillations
A = amplitude of oscillations
r = distance from the missile to the celestial body
ΔV = permissible velocity errors

Since

$A = 10/3438 \times 60 \approx 4.85 \times 10^{-6}$, average value $r \approx 1.85 \times 10^{11}$ m

$$\Delta V = \frac{7 \times 11.2 \times 10^3 \times 0.5}{100} \approx 3.92 \times 10^2 \frac{\text{m}}{\text{sec}}$$

then

$T = (6.28 \times 4.85 \times 10^{-6} \times 1.85 \times 10^{11})/(3.92 \times 10^2) \approx 1.44 \times 10^4$ sec $= 40$ hr

Hence, knowing that the damping must be semi-aperiodic, i.e.

$$k_1^2 = k_3^2 = k_5^2 = k_{odd}^2 = 2k_2 = 2k_4 = 2k_6 = 2k_{even}$$

we find that the frequency of the oscillations should be $k_{odd}/2$ or $\sqrt{k_{even}/2}$.

Thus

$$\sqrt{k_{odd}} = \sqrt{2}\,\frac{2\pi}{T} = \frac{2 \times \sqrt{2}\pi}{1.44 \times 10^4} \approx 6.16 \times 10^{-4} \frac{1}{\text{sec}}$$

$$k_{odd} = 3.8 \times 10^{-11}\ 1/\text{sec}^2 \qquad k_{even} = 8.7 \times 10^{-6}\ 1/\text{sec}$$

From this we readily determine the error due to the right half of the equations of motion of the platforms.

We can put approximately $\alpha' r = \varphi' r = r'$, and $\varphi = 0$. Then, setting the velocity equal to $7V_{2k}$, where V_{2k} is the second cosmic velocity, we obtain

$$\alpha' r = \varphi' r = r' = V = \frac{7}{\sqrt{3}} V_{2k} = 45.3 \frac{\text{km}}{\text{sec}}$$

Furthermore

$$\frac{\nu V^2}{r} = \frac{V^2}{r^2} = 6 \times 10^{-14} \frac{1}{\text{sec}^2}$$

and the error is

$$\delta = 6 \times 10^{-14}/3.8 \times 10^{-11} \approx 1.58 \times 10^{-3} \approx 5.4'$$

It follows therefore that the value of this error is intolerably large and must be eliminated.

4 Elimination of Methodological Errors of the System

To eliminate the errors due to the right sides of the equations it is enough to cancel out the integrands in Equations [2.1–2.3]. This will cause all terms of the right sides of Equations [2.4–2.6] (not only the first) to vanish. To eliminate these errors we employ a method based essentially on the following. Knowing $V_{\varphi p}$, $V_{\alpha p}$ and V_{rp} (the readings of the first integrators), and also φ_p and r_p (the readings of the second integrators of the corresponding accelerations), we synthesize with the aid of these quantities the functions under the double integrals in Equations [2.1–2.3]. We then

apply signals proportional to these functions to the integrators, with signs opposite to those of the accelerations under the integrals. If the values of the readings are correct, the compensation is complete. If the readings are subject to errors, the results of the compensation require further analysis. We shall carry out below an error analysis of such a compensated system.

Since both the second and third terms of the right sides of the equations are vanishingly small at the beginning of the flight, it is enough, for an analysis of the system stability, to determine exactly only whether the first term is compensated for. Here we can naturally assume that ν_φ, ν_β, ν_ψ and also γ are constant quantities.

Let us move the coefficients ν_φ, ν_β and $\nu_\psi \sin\gamma$ outside the parentheses in the right sides of Equations [2.4–2.6] and introduce the correction terms. We then obtain

$$\Delta\varphi = -\nu_\varphi\left[\int_0^t\int\left(\frac{V_\varphi V_r}{r}+\frac{V_\alpha^2}{r}\tan\varphi+\frac{k_2}{\nu_\varphi}\Delta\varphi+\frac{k_1}{\nu_\varphi}\frac{d\Delta\varphi}{dt}-\Phi\right)dt\,dt\right]$$

$$\beta = -\nu_\beta\left[\int_0^t\int\left(\frac{V_\alpha V_r}{r}-\frac{V_\varphi V_\alpha}{r}\tan\varphi+\frac{k_4}{\nu_\beta}\beta+\frac{k_3}{\nu_\beta}\frac{d\beta}{dt}-B\right)dt\,dt\right]$$

$$\Delta\psi = \nu_\psi\sin\gamma\left[\int_0^t\int\left(\frac{V_\varphi^2+V_\alpha^2}{r}-\frac{k_6}{\nu_\psi\sin\gamma}\Delta\psi-\frac{k_5}{\nu_\psi\sin\gamma}\frac{d\Delta\psi}{dt}-\Psi\right)dt\,dt\right] \quad \ldots\ldots [4.1]$$

where

$$\Phi = \frac{V_{\varphi p}V_{rp}}{r_p}+\frac{V_{\alpha p}^2}{r_p}\tan\varphi_p$$

$$B = \frac{V_{\alpha p}V_{rp}}{r_p}-\frac{V_{\varphi p}V_{\alpha p}}{r_p}\tan\varphi_p$$

$$\Psi = (V_{\varphi p}^2+V_{\alpha p}^2)/r$$

$V_{\varphi p}$, $V_{\alpha p}$, V_{rp}, φ_p and r_p, as already indicated, are the readings of the system.

We denote the quantities in brackets in the right sides of [4.1] by ΔS_φ, ΔS_β and ΔS_ψ, respectively. We can then write instead of [4.1]

$$\Delta\varphi = -\nu_\varphi\Delta S_\varphi$$
$$\beta = -\nu_\beta\Delta S_\beta$$
$$\Delta\psi = \nu_\psi\sin\gamma\Delta S_\psi \quad \ldots\ldots [4.2]$$

Furthermore

$$\Delta S_\varphi'' = a\delta V_\varphi + b\delta V_r - c\delta r + d\delta V_\alpha + e\delta\varphi + \frac{k_2}{\nu_\varphi}\Delta\varphi + \frac{k_1}{\nu_\varphi}\Delta\varphi'$$

$$\Delta S_\beta'' = -f\delta V_\varphi + g\delta V_r - h\delta r + j\delta V_\alpha - k\delta\varphi + \frac{k_4}{\nu_\beta}\beta + \frac{k_3}{\nu_\beta}\beta'$$

$$\Delta S_\psi'' = l\delta V_\varphi - m\delta r + n\delta V_\alpha - \frac{k_6}{\nu_\psi\sin\gamma}\Delta\psi - \frac{k_5}{\nu_\psi\sin\gamma}\Delta\psi'$$

At the same time it is easily seen that

$$\nu_\varphi\delta V_\varphi = \delta\varphi' \qquad \delta V_\alpha = \Delta S_\beta' \qquad \Delta S_\psi = \delta r$$
$$\Delta S_\varphi' = \delta V_\varphi \qquad \delta V_r = \delta r'$$

The coefficients a to n are the partial derivatives of the integrands of the first terms in Equations [2.4–2.6]

$$a = \frac{V_r}{r} \qquad b = \frac{V_\varphi}{r} \qquad c = \frac{V_\varphi V_r + V_\alpha^2\tan\varphi}{r^2}$$

$$d = \frac{2V_\alpha}{r}\tan\varphi$$

$$e = \frac{V_\alpha^2}{r\cos^2\varphi} \qquad f = \frac{V_\alpha}{r}\tan\varphi \qquad g = \frac{V_\alpha}{r}$$

$$h = \frac{V_\alpha(V_r - V_\varphi\tan\varphi)}{r^2}$$

$$j = \frac{V_r}{r}-\frac{V_\varphi}{r}\tan\varphi \qquad k = \frac{V_\varphi V_\alpha}{r\cos^2\varphi} \qquad l = \frac{2V_\varphi}{r}$$

$$m = \frac{V_\varphi^2+V_\alpha^2}{r^2} \qquad n = \frac{2V_\alpha}{r}$$

These coefficients can be considered constant over a limited time interval. It must be noted that this will hold even for a time interval greater than the period of oscillation of this system. As can be seen from the foregoing, the latter depend on the values of the coefficients k_1 to k_6.

Thus, we finally have a system consisting of 11 equations and 11 unknowns.

By reducing the order of the characteristic determinant to six, i.e., by eliminating the five unknowns δV_φ, δV_α, δV_r, $\delta\varphi$ and δr, we obtain

$$\begin{vmatrix} \nu_\varphi & 0 & 0 & 1 & 1 & 0 \\ 0 & \nu_\beta & 0 & 0 & 0 & 1 \\ 0 & 0 & -\nu_\psi\sin\gamma & 0 & 0 & 0 \\ p^2-ap-e\nu_\varphi & -dp & c-bp & -\frac{1}{\nu_\varphi}(k_1p+k_2) & -\frac{1}{\nu_\beta}(k_3p+k_4) & 0 \\ fp+k\nu_\varphi & p^2-jp & h-gp & 0 & 0 & \frac{1}{\nu_\psi\sin\gamma}(k_5p+k_6) \\ -lp & -np & p^2+m & 0 & & \end{vmatrix} = 0$$

Here p is the differentiation operator. Expanding this determinant, inserting the numerical values in the coefficients of the characteristic polynomials, and applying the Routh-Hurwitz criterion to this polynomial, we readily find that the system is stable, since all the inequalities of the criterion are satisfied.

We see thus that the system is stable (the errors tend to zero).

5 System Readings

It is easily seen that direct readings are obtainable only from the indicating devices of the first platform. If $\Delta\varphi$ and β

are equal to zero, then the angles of the platform relative to the gyro system yield φ and α directly.

As to the third coordinate r, it is obtained by integrating twice the accelerations and the angle $\Delta\psi$, multiplying by the running value of $(1/v_\varphi)$ sin γ.

Naturally, the velocities α', φ' and r' are obtained after the first integration of the accelerations and of the angles β, $\Delta\varphi$ and $\Delta\psi$ sin γ. To obtain α' and φ' it is necessary to divide the first integrals by r. The accelerations due to non-field-like forces are obtained directly from the accelerometers.

The accelerations produced by gravitational fields can be determined indirectly from the values of the angles $\Delta\varphi$, β and $\Delta\psi$. It should be noted, furthermore that a scheme is possible in which only the inclinations $\Delta\varphi$, β and $\Delta\psi$ are integrated, but the accelerometer readings are not. In such a scheme the angles $\Delta\varphi$, β and $\Delta\psi$ will characterize the over-all acceleration produced by both field-like and non-field-like forces. To separate from the over-all reading the accelerations due to the non-field-like forces, it is necessary, in analogy with the foregoing, to use the accelerometer readings.

As already indicated, another system of coordinates can be employed for the system. In the case when coordinates other than those considered are used, apparently a more complicated computer system is necessary, the structure of which depends on the method of mounting the accelerometers in the apparatus. A considerable variety is possible here too. For example, the accelerometers may be rigidly mounted on the gyro platform or directly on the vehicle. Naturally, to obtain the necessary coordinates one must solve the corresponding functions prior to integration or after the first integration. The determination of the optimum version of the coordinate system and of the method of mounting the accelerometers, from the point of view of simplicity of instrumentation, is a problem that should be solved in the nearest future.

Conclusions

1 The use of systems designed for Earth-bound flying objects on objects that move in interplanetary space entails difficulties due to the weightlessness of the sensitive elements of the accelerometers and the absence of suitable corrections.

2 The method of double integration of the deviation between the reading of the system, referred to the position of an optical system aimed at the sun or some planet, from the actual position of the optical system, circumvents the foregoing difficulty and makes it possible to determine the parameters of motion in space.

3 The method indicated makes it possible to obtain a system with a considerably smaller period from the "imperturbability period" of the system, and to introduce damping into the system without disturbing the system by acceleration, as in the case of Earth-bound navigational systems.

References

1 Wrigley, W., Woodbury, R. B. and Hovorka, J., "Inertial Guidance," SMF Fund Paper no. FF-16, IAS, N. Y., 1957.

2 Carroll, J., "Interplanetary Navigation by Optical Resection and Inertial Systems," *Aero/Space Engng.*, March 1959.

—*Original received October 15, 1959*

Reviewer's Comment

The system for interplanetary navigation proposed by Fridlender was inspired, as he indicates, from consideration of "geosystems" by which he means pure inertial navigation systems having platforms that are slaved to the local veritical. Such slaved or torqued systems operating in vehicles in the atmosphere utilize the sensing of aerodynamic accelerations to determine the local vertical. For example, in the simple case of an aircraft flying at constant altitude, accelerometers mounted on the inertial platform sense various accelerations including those due to the aerodynamic forces that maintain the vehicle at fixed altitude. These altitude maintaining forces are equal in magnitude to the local gravity forces but are oppositely directed, and thus some writers say that the accelerometers sense the gravity accelerations.

Mr. Fridlender says that the accelerometers sense only nongravitational accelerations. This apparent contradiction is semantic rather than real and should be borne in mind if we are to understand his system for navigation in interplanetary space where aerodynamic forces are essentially nonexistent. His contention, quite properly, is that an accelerometer on a freely falling interplanetary vehicle is in a "weightless" state and does not sense the gravity acceleration, since the sensitive mass and the frame of the accelerometer undergo (practically) equal accelerations (1, 2).[2]

Recognizing this fundamental inability to sense the local vertical in free fall with conventional accelerometers, Fridlender suggests the use of "star" trackers to sight distant planets, a technique that has been mentioned by other writers (3).

If angles are measured between two pairs of celestial bodies, the vehicle position may be determined with relatively high precision. At least three nearby celestial objects must be sighted for this method, and they may be chosen from among the planets and the sun but not from the stars. The position coordinates of the vehicle thus obtained may be differentiated successively to get velocity and acceleration, but, as Fridlender points out, with relatively weak precision The method has been called navigation by resection (as opposed to intersection as used in triangulation).

In order to overcome this weakness Fridlender suggests a technique utilizing three platforms, one fixed in orientation in inertial space by high precision gyros and supplementary star trackers, a second having one pair of planet trackers, and a third having another pair of planet trackers. The method of determining position is no different than the resection method. The novelty of his scheme, Fridlender says, is that velocity and acceleration are obtained not by a differentiation process but rather by integration. The method would thus provide smoothing of the continuous velocity and acceleration outputs.

The justification for this conclusion should be in the mathematical development presented by Fridlender. Unfortunately the development is somewhat obscure and the conclusion doesn't clearly follow. For example, he defines V_x', V_y', V_z', V_z, V_y and V_x as the acceleration and velocity components due to the non-field-like forces. Thus, the integrands of Equations [2.1, 2.2 and 2.3] are identically zero for a body in free fall, and hence $k_1, k_2, \ldots, k_6$ in Equations [2.4, 2.5 and 2.6] cannot be arbitrary constants, but must be chosen for every flight to fit the geometry of the desired free fall orbit and the configuration of platforms.

In Section 4 Fridlender acknowledges this difficulty and suggests a set of "compensations" which, when examined, present the same problems since the terms having coefficients $a, b, c, \ldots, n$ are also identically zero for the same reasons. Perhaps the obscurity in the mathematics lies in the language translation though two independent translations have not reconciled the problem.

—Joel Carroll
Arma Division
American Bosch Arma Corp.

[2] Numbers in parentheses indicate References at end of paper.

1 Montani, A., "Proportionality Between Gravity and Inertia," *Missile Design and Development*, Dec. 1959, pp. 24ff.

2 Savet, P. H. and Carroll, J., "Space Navigation by Gravity Gradient," *Arma Engng.*, vol. 2, no. 5, June-July 1959, pp. 23–28.

3 Larmore, L., "Celestial Observations for Space Navigation," *Aero Space Engng.*, vol. 18, Jan. 1959, p. 37.

Dynamics of a Gyroscope With Two Degrees of Freedom

M. Z. LITVIN-SEDOY

Gyroscopes with two degrees of freedom are used to measure the absolute angular velocity of various bodies (aircraft, etc.) (1, 2).[1] The static theory of a two-degree gyroscope starts with the assumption that at each instant of time the deviation of the gimbal from its reference position in the body is determined by its relative equilibrium under the action of the gyroscopic moment and the moment of the restoring force. This assumption is admissible to a certain extent if the instrument is used only to stabilize the angular position of the object in space or when the disturbing forces on the object are relatively weak. However, when controlling unsteady angular motions of an object or in the case of large disturbances, an estimate of the angular velocity of the object based on static theory may lead to noticeable errors and to the occurrence of false signals. In addition, deviations of the geometric and mass parameters of the instrument from their ideal (rated) values, as occur in actual constructions, impose supplementary errors on the results of the measurement of the angular velocity of the object. It is therefore advisable to investigate the conditions under which false signals arise in the instrument under arbitrary linear and angular displacements of the object, with allowance for the most substantial deviations of the actual construction of the instrument from the design data.

1 WE CONSIDER a real gyroscope with two degrees of freedom under the following assumptions: The gimbal mounting of the gyroscope is rigid and its axis of rotation is neither a central axis nor the principal axis of the controlled object. The axes of the gyroscope and of the gimbal are not perpendicular. Since the gyroscope's own angular velocity Ω is much greater than the absolute and relative angular velocities of the gimbal, we assume that the possible static or dynamic unbalance of the gyroscope proper manifests itself only in bending of the gyroscope shaft and in high frequency oscillations of the gimbal relative to the object. These phenomena, and also elastic vibrations in the bearings, are disregarded in our consideration and the gyroscope axis is assumed to be the straight line joining the centers of its bearings in the gimbal (Fig. 1).

We note that this representation of the instrument covers also the case when the gyroscope and gimbal axes do not intersect (Fig. 1): In fact, the latter circumstance is reflected only in the values of the moments of inertia (axial and centrifugal) of the gyroscope plus gimbal frame about the axes fixed in the frame, and also in the position of the center of mass of this system in a plane perpendicular to the gimbal axis. Nonetheless, since we wish to facilitate the calculation of the characteristic constants of the system from the basic primary parameters that determine the assembly of the instrument, we shall treat separately, in the geometric description of the instrument, the case when the gyroscope and gimbal axes cross.

We introduce the following right-handed rectangular coordinate systems: *oxyz*, stationary; *Cabc*, bound to the body and serving as a reference for the determination of the relative rotation of the gimbal (the axis *Ca* is aligned with the gimbal axis); $C\xi\eta\zeta$, connected with the frame (the axis $C\xi$ coincides with the axis *Ca*). The system $C\xi\eta\zeta$ is defined in the following manner (Fig. 1): We represent the positive direction of the axis of the gyroscope's own rotation by the unit vector $\mathbf{g}^\circ$; this axis, by assumption, can make an arbitrary angle with the gimbal axis. We project the vector $\mathbf{g}^\circ$ on the plane Π_1, which is perpendicular to the gimbal axis. We define a plane Π_2 with the aid of the following two intersecting lines: The projection of the vector $\mathbf{g}^\circ$ on the plane Π_1, and some other line which is parallel to the gimbal axis and intersects the gyroscope axis. By the nature of the construction, Π_2 is perpendicular to Π_1.

We draw a line perpendicular to the plane Π_2 such that the line intersects the gimbal axis, and we translate this perpendicular line parallel to itself along the gimbal axis. The point H, at which this perpendicular intersects the gimbal axis at the same time that it also intersects the gyroscope axis, is taken to be as the origin C of the two aforementioned moving coordinate systems. The axis $C\zeta$ is drawn parallel to the plane Π_2 so that the angle ν between the vector $\mathbf{g}^\circ$ and the positive direction of the line $C\zeta$ is acute: $\nu = L(\mathbf{g}^\circ, C\zeta)$, $|\nu| < 90$ deg; the case $|\nu| = 90$ deg has no practical sig-

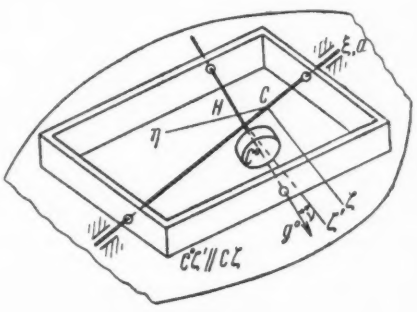

Fig. 1

Translated from *Izvestiia Akademii Nauk SSSR, Otdelenie Tekhnicheskikh Nauk, Mekhanika i Mashinostroenie* (Bull. USSR Acad. Sci., Div. Tech. Sci., Mechanics and Machine Building), no. 5, 1959, pp. 72–78.

[1] Numbers in parentheses indicate References at end of paper.

nificance. This choice of a reference system $C\xi\eta\zeta$, fixed to the gimbal, allows us to determine the angular position of the gyroscope axis (the vector $\mathbf{g}^\circ$) relative to the gimbal by means of a single parameter, namely the angle ν.

Let $\mathbf{\Omega}^\circ$ be a unit vector of the gyroscope's own angular velocity

$$\mathbf{\Omega} = \Omega\mathbf{\Omega}^\circ \ (\Omega > 0 \text{ for } \mathbf{\Omega}^\circ = \mathbf{g}^\circ \text{ and } \Omega < 0 \text{ for } \mathbf{\Omega}^\circ = -\mathbf{g}^\circ)$$

$\mathbf{a}^\circ$, $\mathbf{b}^\circ$, $\mathbf{c}^\circ$ and ξ°, η°, ζ° are unit vectors corresponding to the symmetry axes of the systems $Cabc$ and $C\xi\eta\zeta$.

We introduce the following notation:

I_1, I_2 and I_3	=	moments of inertia of gimbal about axes $C\xi$, $C\eta$ and $C\zeta$ respectively
I_{12}, I_{23} and I_{31}	=	corresponding inertia products
I	=	moment of inertia of gyroscope about its own shaft
$\mathcal{E}$	=	its equatorial (central) moment of inertia
m_1	=	mass of gyroscope
m_2	=	mass of gimbal
s	=	distance from point H to center of mass C° of gyroscope (by definition, center C° lies on gyroscope axis)
$h = (CH)$	=	distance between gimbal and gyroscope axes ($h > 0$ if point H lies above point C, as in Fig. 1)
β, γ	=	coordinates of center of mass of gimbal, measured along axes $C\eta$ and $C\zeta$ respectively

We denote by φ the angular coordinate of the gimbal relative to the body; the positive direction of the angle φ is indicated in Fig. 2. We shall call an instrument in which

$$I_{12} = I_{23} = I_{31} = 0 \qquad h = s = \beta = \gamma = 0 \qquad \nu = 0$$

an ideal gyroscope with two degrees of freedom.

Let the body on which the gyroscope is mounted carry out arbitrary three-dimensional motion in the system $oxyz$, and let the moving origin C have a linear velocity $\mathbf{v} = \mathbf{v}(t)$ and an instantaneous angular velocity $\boldsymbol{\omega} = \boldsymbol{\omega}(t)$.

We shall call the direction of the vector of angular velocity $\boldsymbol{\omega}$ of the object the axis of the absolute insensitivity of a gyroscope with two degrees of freedom, the gimbal axis of which is fixed in the body, if the gimbal of the instrument does not respond to the motion of the object under any variation of the angular velocity $\boldsymbol{\omega}(t)$ of the object, of the gyroscope's own angular velocity $\Omega(t)$, and of the components of the linear velocity $\mathbf{v}(t)$ of the origin C of the system of coordinates connected with the object.

We shall correspondingly call the direction of the vector $\boldsymbol{\omega}$ the axis of the translational intensitivity of the gyroscope, if the gimbal of the instrument does not respond to motion of the object under any variation of $\omega(t)$ and of the components of $\mathbf{v}(t)$ at a given angular velocity of the gyroscope itself.

We shall correspondingly call the direction of the vector $\boldsymbol{\omega}$ the axis of limited insensitivity of the gyroscope, if motions $\boldsymbol{\omega}(t)$, $\mathbf{\Omega}(t)$ and $\mathbf{v}(t)$, to which the instrument does not respond, exist simultaneously with such to which it does respond.

The problem reduces to determining the foregoing insensitivity axis of a gyroscope with two degrees of freedom, under the assumptions made above.

2 Let us write down the differential equation of the relative oscillations of the gimbal plus gyroscope system (we shall denote this system by Γ)

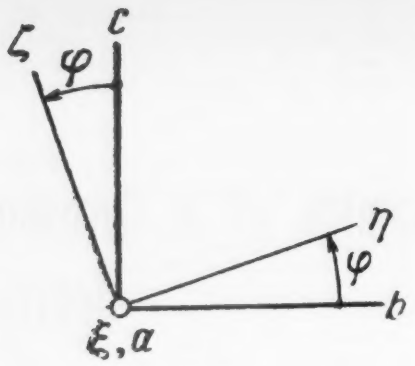

Fig. 2

$$(d\mathbf{K}/dt) + \mathbf{v} \times \mathbf{Q} = \mathbf{M} \qquad \mathbf{K} = \sum_{(\Gamma)} \mathbf{r}_i \times m_i\mathbf{v}_i$$

Here $\mathbf{K}$ is the kinetic moment of the absolute motion of the system (Γ) relative to the moving origin C, i.e., $\mathbf{v}_i$ is the absolute velocity of the elementary mass m_i, while $\mathbf{r}_i$ is its radius vector relative to the moving origin C.

Let $\mathbf{Q}$ be the absolute momentum and $\mathbf{M}$ the principal moment of the external forces applied to the system (Γ), both relative to the moving origin C. The external moments on the gimbal axis comprise the restoring moments (produced, for example, by the centering spring of the gimbal) and the viscous and dry friction moments. We write the expressions for the vectors $\mathbf{K}$, $\mathbf{Q}$, ω and $\mathbf{v}$ in terms of their components along the axes of the bound coordinate systems

$$\mathbf{K} = K_1\xi^\circ + K_2\eta^\circ + K_3\zeta^\circ \qquad \mathbf{Q} = Q_1\xi^\circ + Q_2\eta^\circ + Q_3\zeta^\circ$$
$$\boldsymbol{\omega} = \omega_a\mathbf{a}^\circ + \omega_b\mathbf{b}^\circ + \omega_c\mathbf{c}^\circ = \omega_1\xi^\circ + \omega_2\eta^\circ + \omega_3\zeta^\circ$$
$$\mathbf{v} = v_a\mathbf{a}^\circ + v_b\mathbf{b}^\circ + v_c\mathbf{c}^\circ = v_1\xi^\circ + v_2\eta^\circ + v_3\zeta^\circ$$

The equations of the kinetic moment about the gimbal axis is of the form

$$(dK_1/dt) + \omega_2K_3 - \omega_3K_2 + v_2Q_3 - v_3Q_2 = M_1$$

with

$$M_1 = \mathbf{M}\xi^\circ \qquad \omega_1 = \omega_a$$
$$\omega_2 = \omega_b\cos\varphi + \omega_c\sin\varphi \qquad \omega_3 = \omega_c\cos\varphi - \omega_b\sin\varphi$$

After calculating the projections of the vectors $\mathbf{K}$ and $\mathbf{Q}$ on the axes $C\xi$, $C\eta$ and $C\zeta$ we obtain a nonlinear second-order differential equation in the angular coordinate of the gimbal $\varphi(t)$

$$\begin{aligned}(I_1 + \mathcal{E}_0\cos^2\nu + I\sin^2\nu + m_1h^2)(\ddot{\varphi} + \omega_a^\cdot) + I\Omega\omega_2\cos\nu - I\dot{\Omega}\sin\nu + (m_1hs\sin\nu - I_{12})(\omega_b^\cdot\cos\varphi + \omega_c^\cdot\sin\varphi - \omega_a\omega_3) - \\ [(I - \mathcal{E}_0)(\sin 2\nu/2) + I_{13}](\omega_c^\cdot\cos\varphi - \omega_b^\cdot\sin\varphi + \omega_a\omega_2) + \\ [(I - \mathcal{E}_0)\cos^2\nu + I_3 - I_2 + m_1h^2]\omega_2\omega_3 + (I_{23} + m_1hs\cos\nu)(\omega_2^2 - \omega_3^2) + \\ (d_1\cos\varphi - d_2\sin\varphi)w_b + (d_2\cos\varphi - d_1\sin\varphi)w_c + \kappa\dot{\varphi} + k\varphi + T = 0 \quad [1]\end{aligned}$$

where

w_b, w_c	=	projections of acceleration w of moving origin C on axes Cb and Cc
w_b	=	$\mathbf{w} \times \mathbf{b}^\circ = v_b^\cdot + \omega_cv_a - \omega_av_c$
w_c	=	$\mathbf{w} \times \mathbf{c}^\circ = v_c^\cdot + \omega_av_b - \omega_bv_a$
κ	=	coefficient of viscous friction in relative motion of gimbal

k = angular stiffness of centering spin
T = moment of dry friction on gimbal axis
$\mathcal{E}_0 = \mathcal{E} + m_1 s^2$
$d_1 = m_1 s \cos \nu + m_2 \gamma$
$d_2 = m_1 h + m_2 \beta$

3 To determine the axes of absolute insensitivity of the gyroscope with two degrees of freedom, we find the direction cosines l, m and n of the axes of absolute insensitivity in the coordinate system *Cabc*, which is fixed in the object. In order not to exclude beforehand the possibility of the unknown axes vibrating in the object, these cosines will be assumed to be time dependent.

Let the angular velocity $\boldsymbol{\omega}$ of the object be directed around the insensitivity axis; then

$$\boldsymbol{\omega} = (l\mathbf{a}^\circ + m\mathbf{b}^\circ + n\mathbf{c}^\circ)\omega \qquad \omega \equiv \omega(t)$$
$$\omega_a = l\omega \qquad \omega_b = m\omega \qquad \omega_c = n\omega \qquad [2]$$

where

$$l = \cos(\boldsymbol{\varepsilon}^\circ, \mathbf{a}^\circ)$$
$$m = \cos(\boldsymbol{\varepsilon}^\circ, \mathbf{b}^\circ)$$
$$n = \cos(\boldsymbol{\varepsilon}^\circ, \mathbf{c}^\circ)$$

$\boldsymbol{\varepsilon}^\circ$ is the unit vector in one of the two directions on the unknown line

$$l^2 + m^2 + n^2 = 1$$

Since we wish to display this phenomenon in pure form, let us consider it without allowance for dry friction ($T = 0$).

From the definition of the absolute-insensitivity line, the instrument cannot sense the angular velocity of the object directed around this axis: The gimbal remains in a state of relative rest with the centering spring of the instrument unstressed, in spite of the rotation of the object about this axis. Let us agree to measure the angle φ as seen in Fig. 2, from the direction corresponding to the unstressed spring. Inserting the value $\varphi \equiv 0$ and the quantities [2] into [1], we obtain the condition under which the instrument becomes insensitive to the considered motion of the object

$$A\dot{\omega} + B\omega^2 + C\Omega\omega + D\dot{\Omega} + E\omega + d_1 w_b + d_2 w_c = 0 \qquad [3]$$

Here

$$A = Pl + Qm + Rn \qquad C = Im\cos\nu \qquad D = -I\sin\nu$$
$$B = -Qln + Rlm + [(I - \mathcal{E}_0)\cos^2\nu + I_2 - I_2 + m_1h^2]nm + (I_{23} + m_1hs\cos\nu)(n^2 - m^2)$$
$$E = P\dot{l} + Q\dot{m} + R\dot{n} \qquad P = I_1 + I\sin^2\nu + \mathcal{E}_0\cos^2\nu + m_1h^2$$
$$Q = m_1hs\sin\nu - I_{12} \qquad R = -[\tfrac{1}{2}(I - \mathcal{E}_0)\sin 2\nu + I_{13}] \qquad [4]$$

The direction (l, m, n) defines the axes of absolute insensitivity of the gyroscope only if the following conditions are satisfied

$$A = B = C = D = 0 \qquad E = 0 \qquad d_1 = d_2 = 0 \qquad [5]$$

In fact, if at least one of the coefficients of [3] differs from zero, [3] expresses a certain connection (differential or finite) between the variables ω, Ω, v_a, v_b, v_c, or in our particular case, a certain restraint imposed on any of these functions.

Then the gyroscope will fail to respond only to motion which is confined to [3], and the direction of the vector $\boldsymbol{\omega}$ becomes an axis in a limited, not absolute, insensitivity only.

The condition $C = 0$ reduces to the equality $m = 0$: The unknown axis is perpendicular to the axis *Cb* of the tied reference *Cabc*, i.e., to the sensitivity axis of the instrument as obtained by static theory.

The condition $D = 0$ stipulates $\sin\nu = 0$, i.e., the gyroscope axis must be perpendicular to the gimbal axis. The condition $F = 0$ is obtained by differentiating both halves of the equation $A = 0$ with respect to time, i.e., these two equations reduce to a single one. The conditions $d_1 = d_2 = 0$ denote that the center of mass of the system (Γ) lies on the axis of the gimbal, i.e., the system (Γ) should not have pendulum properties. Thus, the axis of absolute insensitivity exists if the system of three equations

$$(I_1 + \mathcal{E}_0 + m_1h^2)l - I_{13}n = 0$$
$$[I_{13}l + (I_{23} + m_1hs)n]n = 0$$
$$l^2 + n^2 = 1 \qquad [6]$$

with respect to the two unknowns l and n has a solution corresponding to physical reality. The second equation in [6] is satisfied if at least one of the following two equations is satisfied

$$n = 0 \qquad I_{12}l + (I_{23} + m_1hs)n = 0 \qquad [7]$$

It follows however, from the condition $n = 0$ by virtue of [6], that $l = 0$, and the equations $l = 0$ and $n = 0$ contradict the condition $m = 0$, which was derived in the foregoing. Consequently $n \neq 0$ and Equation [7] is satisfied. The first equations of [6 and 7] are compatible only when the system (Γ) has parameters that satisfy the relation

$$\begin{vmatrix} I_1 + \mathcal{E}_0 - m_1h^2 & -I_{13} \\ I_{12} & I_{23} + m_1hs \end{vmatrix} = 0 \qquad [8]$$

Relation [8] is physically realizable: Writing down the difference $\rho = I_1 - 2I_{23}$ and eliminating from it the moment of inertia I_1 with the aid of [8], we verify that the condition $\rho \geqslant 0$ is observed if any of the following two pairs of inequalities is satisfied

$$I_{23} + m_1hs \geqslant 0 \qquad I_{13}I_{31} \leqslant [\mathcal{E} + m_1(h^2 + s^2) + 2I_{23}](I_{23} + m_1hs)$$
$$I_{23} + m_1hs \leqslant 0 \qquad I_{13}I_{31} \geqslant [\mathcal{E} + m_1(h^2 + s^2) + 2I_{23}]|I_{23} + m_1hs|$$

These are physically realizable.

Let us consider a gyroscope for which relations [4 and 8] are satisfied. Then

$$l = \lambda n$$

where by virtue of Equation [8]

$$\lambda = \frac{I_{31}}{I_1 + \mathcal{E} + m_1(h^2 + s^2)} = -\frac{I_{23} + m_1hs}{I_{12}}$$

Consequently, the absolute-insensitivity line of the gyroscope is defined by the direction cosines

$$l = \pm\frac{\lambda}{\sqrt{1 + \lambda^2}} \qquad m = 0 \qquad n = \pm\frac{1}{\sqrt{1 + \lambda^2}}$$

Both solutions reduce to a single one, for the difference in signs determines merely the choice of the positive direction of $\boldsymbol{\varepsilon}^\circ$ on the absolute-insensitivity line. Since λ = const, the absolute-insensitivity line is oriented in the body in an invariant manner.

If the axes of the system $C\xi\eta\zeta$ are the principal axes of the gimbal, then $\lambda = 0$ and the axis of absolute insensitivity may be any line parallel to the gyroscope axis. If at least one of the conditions [4] is not satisfied, there is no absolute-insensitivity axis.

In that case we find for each direction in the object such a rotation $\omega = \omega(t)$ of the object about this direction, for which the gimbal goes into relative motion; this may occur also for rotation of the object about the gyroscope axis. This property of the gyroscope is one of the sources of false signals.

4 Let us determine the axes of translational insensitivity of a gyroscope with two degrees of freedom. In this case the function $\Omega = \Omega(t)$ is specified a priori.

Equation [3] assumes the form

$$A\dot{\omega} + B\omega^2 + C'\omega + D' + d_1 w_b + d_2 w_c = 0$$

where

$$C' = C\Omega + E \qquad D' = D\dot{\Omega}$$

and the conditions of translational insensitivity are

$$A = B = 0 \qquad C' = 0 \qquad D' = 0 \qquad d_1 = d_2 = 0$$

When $\Omega \neq 0$, the condition $D' = 0$ goes into the condition $\nu = 0$. Then the equations $A = 0$ and $C' = 0$ yield $m = 0$ and the axis of translational insensitivity coincides with the axis of absolute insensitivity.

5 Let us determine the axes of limited insensitivity of a gyroscope with two degrees of freedom. If one or several of the quantities A, B, C, D, E, d_1 and d_2 in Equation [3] are different from zero, then Equation [3] defines explicit variations of the variables ω, Ω, w_b and w_c, which are not sensed by the gyroscope under zero initial conditions: $\varphi(0) = 0$, $\dot{\varphi}(0) = 0$.

The number of constraints G, capable of giving rise to limited-insensitivity axis, is

$$G = \sum_{\sigma=1}^{7} \binom{7}{\sigma} = 2^7 - 1 = 127$$

For example, at $d_1 = d_2 = 0$, $A \neq 0$, $B \neq 0$, $C \neq 0$, $D \neq 0$ and $F = 0$ there exist limited insensitivity lines for the angular velocities $\omega \equiv \omega(t)$, which satisfy the differential equation

$$A\dot{\omega} + B\omega^2 + C\Omega\omega + D\dot{\Omega} = 0 \qquad [9]$$

If the gyro's own velocity $\Omega = \Omega(t)$ is specified, the last equation becomes a Riccati equation (3) in the velocity ω of the object, which in turn becomes a Bernoulli equation if $\nu = 0$ or $\Omega = \text{const}$. Since the quantities A, B and C in [9] depend on the cosines l, m and n, then any direction (l, m, n) in the body corresponds to a continuum of pairs of functions $\omega(t)$ and $\Omega(t)$, at which this direction determines the line of limited insensitivity.

At $A \neq 0$, $B = C = D = 0$, $F = 0$ and $d_1 = d_2 = 0$, the insensitivity is produced when $\omega = \text{const}$. Then $\nu = 0$ and there exist two lines of limited insensitivity

$$l = \pm 1 \qquad m = n = 0 \qquad (\text{axis } Ca)$$

$$l = \pm \frac{\mu}{\sqrt{1+\mu^2}} \qquad m = 0$$

$$n = \pm \frac{1}{\sqrt{1+\mu^2}} \qquad \mu = -\frac{I_{23} + m_1 hs}{I_{12}}$$

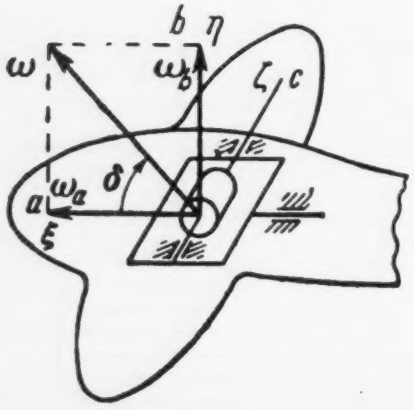

Fig. 3

If condition [8] is also satisfied, then the second line becomes the line of absolute insensitivity, and the parameters λ and μ have the same meaning.

6 Let us consider an ideal gyroscope with two degrees of freedom. In this case

$$A = (I_1 + \mathcal{E})l \qquad B = (I - \mathcal{E} + I_3 - I_2)mn$$
$$C = Im \qquad D = 0 \qquad E = \dot{A} \qquad d_1 = d_2 = 0$$

We put $\Omega = \text{const}$, $l = \text{const}$, $m = \text{const}$ ($n = \text{const}$). Then the limited sensitivity curves when the body velocity is defined by the equation

$$A\dot{\omega} + B\omega^2 + C\Omega\omega = 0$$

i.e., when

$$\omega(t) = \omega(0)\frac{\Omega}{[\Omega - (B/C)\omega(0)]\exp[(C/A)\Omega t] - (B/C)\omega(0)} \qquad [10]$$

Let us consider the measurement of the banking of an airplane with the aid of an ideal gyroscope. We choose the axes Ca, Cb and Cc in accordance with Fig. 3. In static theory it is assumed that if the vector $\boldsymbol{\omega}$ of the angular velocity of the airplane has a nonzero component along the sensitivity axis Cb of the instrument, perpendicular to the plane of the wings, then the gimbal should deflect from its initial position, at which $\varphi = 0$ and $\dot{\varphi} = 0$. Actually, this statement is not always true.

Assume that the airplane goes through a turn, defined by simultaneous change in azimuth and in banking angle: The vector of instantaneous angular velocity of the airplane lies in the symmetry plane of the airplane, forming with the Ca axis a constant angle δ, $0 < |\delta| 90$ deg. Then

$$A = (I_1 + \mathcal{E})\cos\delta \qquad B = 0 \qquad C = I\sin\delta$$

The angular velocity of the airplane varies then in accordance with [10], which for this particular turn has the form

$$\omega = \omega_0 \exp\left(-\frac{I\Omega\tan\delta}{I_1 + \mathcal{E}}\,t\right)$$

where $\omega_0 = \omega(0)$ is the total value of the angular velocities of the airplane and the gimbal relative to stationary space at $t = 0$. Furthermore, $\omega_0 = 0$ and $\Omega \neq 0$. Then the direction of the vector $\boldsymbol{\omega}$ will be the insensitivity axis: The gimbal of the instrument will stay at rest in the airplane, in spite of the fact that the latter rotates about the axis Cb (the sensitivity axis of the instrument according to static theory) with an angular velocity

$$\omega_b = \omega\sin\delta = \omega_0 \exp\left(-\frac{I\Omega\tan\delta}{I_1 + \mathcal{E}}\,t\right)\sin\delta \neq 0$$

Here

$$\omega_a = \omega\cos\delta \qquad \omega_a^{\cdot} = -\frac{I\Omega\tan\delta}{I_1 + \mathcal{E}}\,\omega_a$$

$$\operatorname{sign}\omega_a^{\cdot} = \begin{cases} -\operatorname{sign}\omega_a \text{ for } \Omega\tan\delta > 0 \\ \operatorname{sign}\omega_a \text{ for } \Omega\tan\delta < 0 \end{cases}$$

We have thus established the motion of an object, in which $\varphi(t) = 0 (t > 0)$ if $\varphi(0) = 0$ and $\dot{\varphi}(0) = 0$. We can find in a similar manner the motions under which the relative oscillations of the gimbal take place in accordance with a prescribed law $\varphi \equiv \varphi(t)$, $t \geq 0$. To find all three components ω_a, ω_b and ω_c of the angular velocity of the body it is necessary not only to mount three gyroscopes with two degrees of freedom, but also to introduce a computer to evaluate these components in accordance with a program defined by a system of three equations of type [1].

The author is indebted to A. Yu. Ishlinskii for reading this paper in manuscript and for comments.

References

1 Grammel, R., "The Gyroscope," vol. II (Russian translation), Foreign Literature Press, 1950.

2 Solov'ev, Ya. I., "Giroskopicheskie pribory i avtopiloty (Gyroscopic Instruments and Autopilots), Oborongiz, 1947.

3 Stepanov, V. V., "Kurs differentsial'nykh uravnenii" (A Course in Differential Equations), Gosfizmatgiz, 7th ed., 1958.

—Original received May 9, 1959

Reviewer's Comment

This paper discusses the factors which determine the axis of insensitivity of single degree of freedom gyroscopes. It represents a research contribution which is original in terms of published American literature. It is of significance from two points of view: First of interest, is the difference in nomenclature which exists between the Western and Russian literature with regard to gyroscopics. In general, in the West the degrees of freedom of a gyroscope is determined from the number of free gimbal axes, while apparently the Russians base the number of degrees of freedom upon the inputs, which can result in influencing the output. The second point of view that is indicative to the designer of gyroscopes is the influence of inaccuracies in manufacture and structural deformation upon the performance of rate gyroscopes.

—Charles J. Mundo Jr.
Raytheon Manufacturing Co.

Condensation Shocks in Supersonic Nozzles

A. A. STEPCHIKOV
Moscow Aviation Institute

THE PRINCIPAL working medium in most thermodynamic and gasdynamic processes is atmospheric air, which is usually considered as an ideal gas and its moisture content neglected. In most cases such a simplification is justified in practice. Cases are encountered, however, when the presence of moisture leads to effects that cannot be explained if atmospheric air is considered to be a perfectly dry gas mixture. One such process is the expansion of atmospheric air in a nozzle of a supersonic wind tunnel, accompanied by a shock soon past the critical cross section caused by the condensation of water vapor. In analogy with adiabatic shocks, the slowing down caused by the sudden condensation of water vapor has been called a condensation shock. The instantaneous condensation of water vapor is of great significance not only in the expansion of gas in Laval nozzles, but also in high velocity gasdynamics as a whole, and in many thermodynamic and chemical processes in which the working medium is moist gas.

The first question that arises in the analysis of the condensation shock problem is the determination of the conditions under which intense condensation of water vapor begins.

One might think that there would be no difficulties here whatever, if the moist air is considered as a mixture of dry air and superheated water vapor. Such mixtures usually come under the definition of an ideal gas, and by using certain known thermodynamic equations for gas mixtures it is, therefore, possible to determine the instant when saturation occurs under changing external conditions; this instant can be considered as the start of condensation.

The variation of the saturation pressure P_s under changing external conditions can be determined from the conditions of equilibrium of a two-phase system, using the Clapeyron-Clausius equation

$$\frac{dP_s}{dT} = \frac{l}{AT\Delta v}$$

This equation can be integrated if we know the dependence of the phase-transition heat l on the temperature and the variation of the volume Δv with temperature and pressure. The solution will yield the dependence of the saturation pressure on the temperature in the case of condensation near a plane water surface. In the absence of the latter, the vapor will condense on droplets, on extraneous particles (dust), i.e., on so-called condensation nuclei. A higher vapor pressure is necessary, however, for this to happen, owing to the action of surface-tension forces.

The saturation pressure of a vapor over a curved surface can be found from the equation

$$dP_r = \frac{2\sigma}{r^2}\,\frac{\rho_v}{\rho_l - \rho_v}\,dr$$

where

P_r = vapor pressure above curved surface
σ = coefficient of surface tension
r = radius of curvature of condensation nucleus
ρ_v, ρ_l = densities of vapor and of liquid

Translated from *Izvestiia Vysshykh Uchebnykh Zavedenii, Seriia Aviatsionnaya Tekhnika* (Bulletin of the Higher Institutions of Learning, Aviation Engineering Series), no. 3, 1959, pp. 119–129.

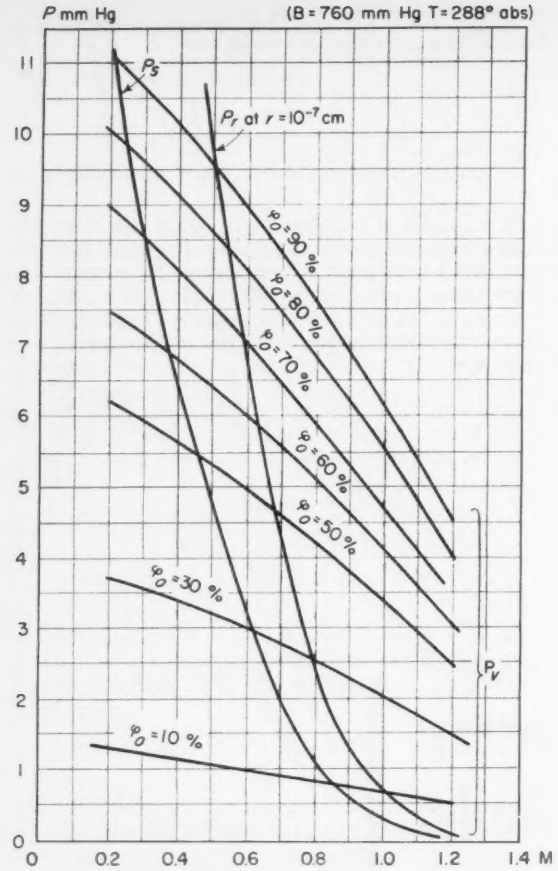

Fig. 1 Dependence of saturation pressure P_s and vapor pressure P_v on Mach number of gas stream

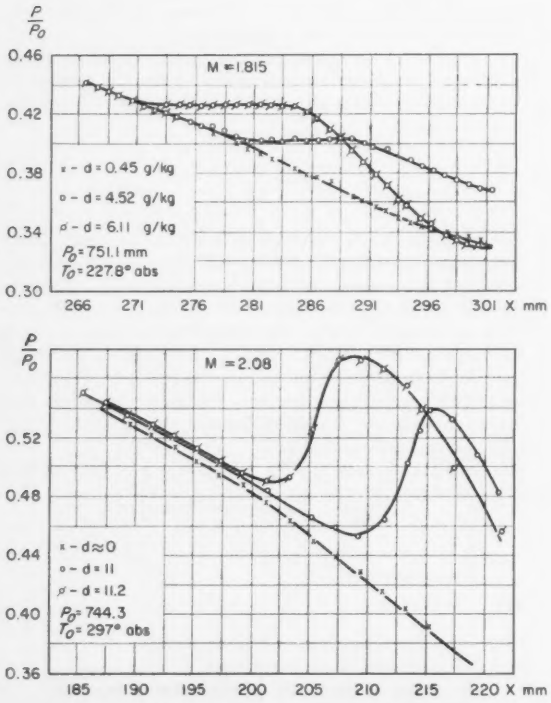

Fig. 2 Variation of relative pressure along nozzle

These equations can be solved in terms of the Mach number of the stream moving in the nozzle. Fig. 1 shows the dependence of the saturation pressure on the Mach number of the stream for a flat and curved surface. The same figure shows curves for the variation of the partial pressure of vapor corresponding to various initial moisture contents φ_0.

$$P_v = \frac{P_{s_0}}{\{1 + [(k-1)/2]M^2\}^{k/(k-1)}}$$

$$P_s = P_{s_0}\left(1 + \frac{k-1}{2}M^2\right)^{a/AR_v} \times \exp\left[\frac{l_0}{AR_v T_0}\left(-\frac{k-1}{2}M^2\right)\right]$$

We see that when moist air expands in a supersonic nozzle the condensation of water vapor should occur in the subsonic portion of the nozzle, regardless of how the saturation pressure is computed. This is not confirmed by experiment, however. Numerous experiments in wind tunnels in which atmospheric air has been expanded prove that the condensation begins in the supersonic portion of the nozzle. This is clearly seen from the curves of the distribution of pressure along the nozzle, obtained for the expansion of air with different moisture contents (Fig. 2), and from photographs of the condensation shock (Fig. 3).

This discrepancy between theory and experiment can be attributed to the fact that the rate of variation of the external conditions is considerably greater than the speed with which equilibrium is established. In the thermodynamic theory of phase transformations, which we have employed, one considers usually not the process of these transformations, but only the equilibrium between the initial and the newly created phases. The problem of what gives rise to the new phase remains unsolved, and even the kinetic theory, while describing in sufficient detail the ground process of the newly formed phase once it has been produced and has reached a certain development, does not describe fully the process of creation itself of the new phase.

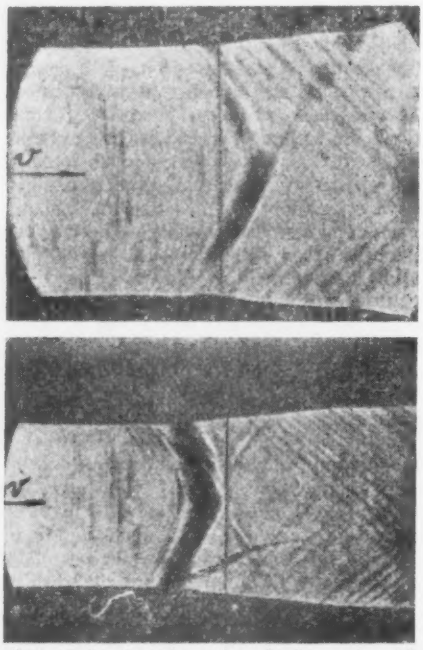

Fig. 3 Photograph of condensation shocks made with optical instrument IAB-451

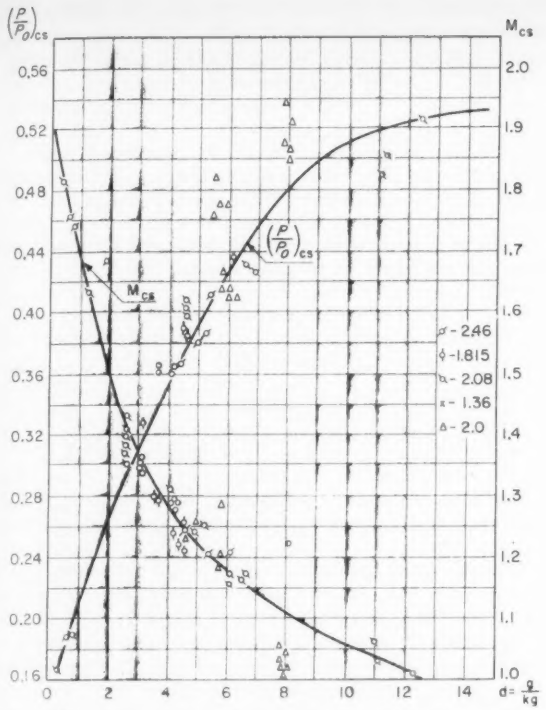

Fig. 4 Dependence of relative pressure and Mach number of start of condensation on humidity

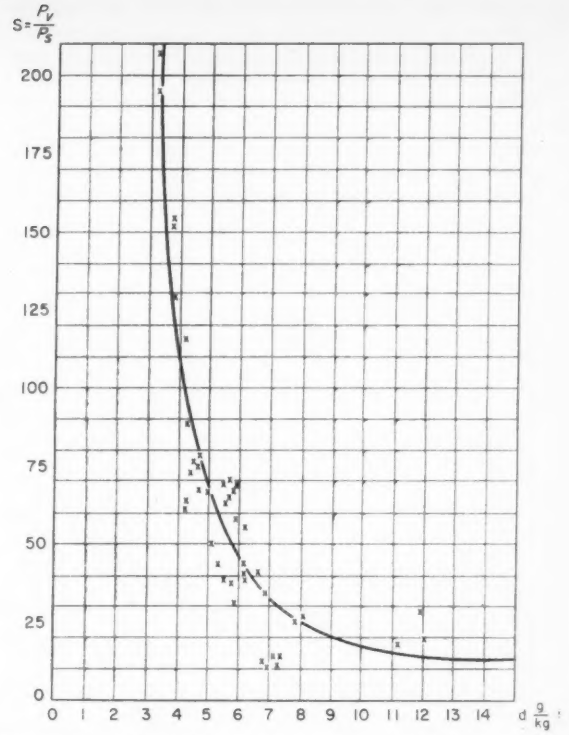

Fig. 5 Dependence of supersaturation S needed to start condensation on humidity

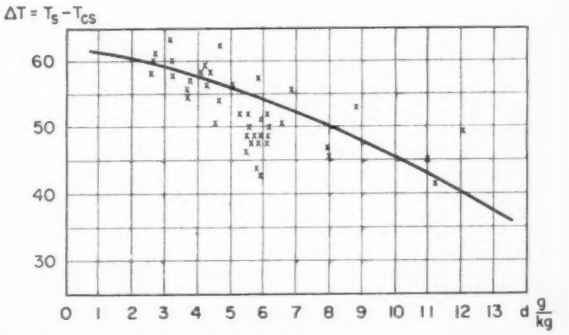

Fig. 6 Dependence of adiabatic supercooling ΔT on humidity

As can be seen from the distribution of the pressure along the nozzle (Fig. 2), the condensation process begins at a certain supercooling of the stream, and consequently at a certain degree of supersaturation.

To determine the instant when condensation takes place in the expansion of atmospheric air and the nozzle of a wind tunnel, special experiments have been set up. For this purpose the pressure distribution was measured on the wall and on the axis of the nozzle during expansion of dry and moist air. The instant of occurrence of condensation was determined by comparing the expansion adiabats of the moist and dry air. Up to a certain portion of the nozzle, as can be seen from the curves (Fig. 2), the "dry" and "moist" adiabats are the same; then they begin to move apart. The start of condensation is taken to be the instant of separation of the curves. Experiments were carried out in nozzles having different flow Mach numbers and different constructions. Flat, rigid and flexible nozzles, designed for Mach numbers from 1.3 to 2.5, were used for the purpose. The greatest number of experiments was carried out in expansion of atmospheric air with natural humidity, which ranged from 2 to 8 gm of moisture per kg of air. A humidity greater than 8 gm/kg was produced by drawing the atmospheric air at very low velocity through moist cloth. This made it possible to increase the humidity to 12–13 gm/kg. To obtain dry air, gel dessicants were used.

Fig. 4 shows the dependence of the relative pressure P/P_0 and of the Mach number of the start of condensation on the absolute humidity of the air d. As can be seen, the instant of start of condensation displays a definite dependence on the humidity and on the velocity. The greater the humidity, the smaller the velocity at which condensation occurs.

These data can be used to determine the supersaturation at which condensation takes place. The results of this calculation are given in Fig. 5. In order for condensation of the moist air moving through the nozzle to begin, a certain supersaturation is necessary; the smaller the air humidity, the greater this supersaturation. Whereas under atmospheric conditions condensation occurs at supersaturation values close to unity (1.001–1.12), in a wind tunnel one needs supersaturation values that are greater by factors of tens and hundreds. The data obtained make it possible to calculate this factor. Fig. 6 shows the dependence of the adiabatic supercooling on the absolute humidity d

$$\Delta T = T_s - T_{cs}$$

where

T_s = saturation temperature
T_{cs} = temperature of start of condensation shock

It is interesting to note that this dependence of ΔT on d refutes the statements made by German and British researchers (1, 2)[1] that the adiabatic supercooling is independent

[1] Numbers in parentheses indicate References at end of paper.

of air humidity. Their mistake was that they analyzed the dependence on the relative humidity, which cannot be used to characterize either the thermodynamic or the kinetic probability of occurrence of condensation.

After the conditions of the start of the condensation are determined, a very important question arises—that of how the condensation is produced, whether by further growth of the condensation nuclei already present when saturation is reached, or by production of new nuclei. To answer this question, let us calculate the rate of growth of a drop during condensation, using the diffusion equation

$$\frac{dm}{dt} = 4\pi r^2 D \frac{d\rho}{dr}$$

or the heat conduction equation

$$l \frac{dm}{dt} = 4\pi r^2 K \frac{dT}{dr}$$

In these equations the change in density and temperature along the radius is given approximately by the following equations

$$\frac{d\rho}{dr} \approx \frac{\rho_l - \rho_v}{r_0} \qquad \frac{dT}{dr} \approx \frac{T_l - T}{r_0}$$

Bearing this in mind, we can determine the size of the drop

$$r_0 = \sqrt{\frac{2k}{l} \frac{T_l - T}{\rho_l} \times t} \qquad r_0 = \sqrt{2D \frac{\rho_l - \rho_v}{\rho_l} \times t}$$

One of these equations was used to calculate the curves of increase in drop radius with time t for different values of supercooling (Fig. 7).

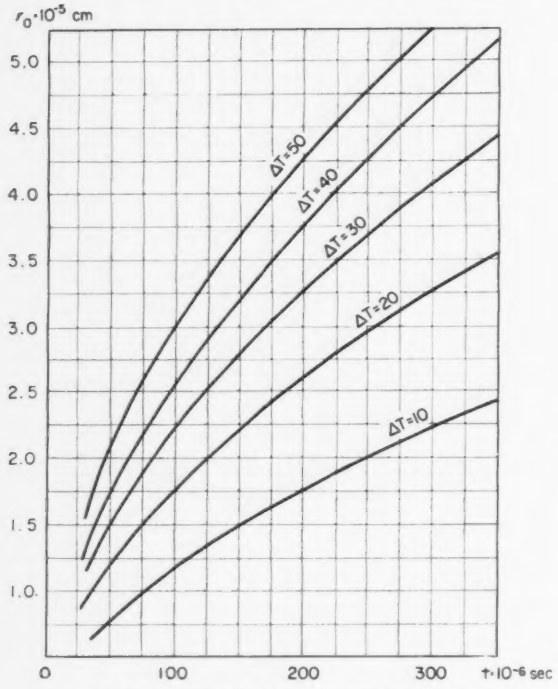

Fig. 7 Growth of drop in condensation

Using these equations one can show that the condensation in a Laval nozzle, due to the growth of the drops, is so insignificant that it can be disregarded:

Let $\Delta T = T_l - T = 50$ deg, then $r = 3.05 \times 10^{-3}\sqrt{t}$.

Let the volume of gas be 1 cm³ and let 5 cm be the distance covered by the gas in 137 μsec.

During this time the drop reaches a size $r = 3.6 \times 10^{-5}$ cm.

Assume that 1 cm³ contains 100,000 condensation nuclei (this is a very large number). Then in a 5-cm section in this volume there would condense the following quantity of moisture

$$G = (4/3)\pi r^3 \rho_l \times n = 1.95 \times 10^{-8} \quad \text{gm/cm}^3$$

This result shows that at a moderate humidity of atmospheric air, 8 gm/kg, less than 0.4 per cent of the condensation would be precipitated on the condensation nuclei. But if the condensation due to the growth of the already present nuclei is insignificant, then the condensation must be influenced by the rate of formation of new nucleating drops.

A similar process takes place in a cloud chamber, where vapor free of condensation centers is expanded adiabatically. An approximately fourfold supersaturation is necessary under similar conditions for condensation. Various authors (3–5) have obtained equations for the rate of formation of condensation centers in cloud chambers.

For a case where there are no extraneous particles, Volmer (5) derives the equation

$$\ln I = \ln 9.5 \times 10^{25} + \ln \left(\frac{P_s}{T}\right)^2 \sqrt{\frac{\mu\sigma}{\rho_l}} + 2 \ln S - 17.49 \times \left(\frac{\mu}{\rho_l}\right)^2 \left(\frac{\sigma}{T}\right)^3 \frac{1}{(\ln S)^2}$$

where

I = speed production of condensation centers per unit time and unit volume
μ = molecular weight
σ = coefficient of surface tension
S = supersaturation

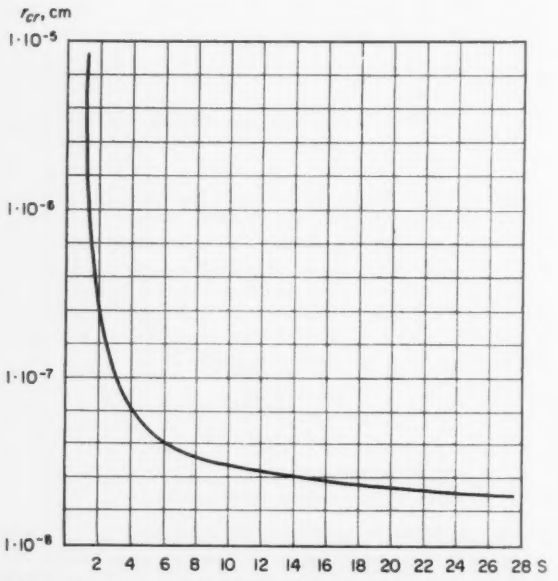

Fig. 8 Dependence of critical radius of condensation nucleus on supersaturation

This equation is obtained under the assumption of constant supersaturation, although usually condensation is accompanied by a reduction in the supersaturation. To be sure, in the nozzle of a wind tunnel the reduction in supersaturation due to the precipitation of the moisture is partially offset by the reduction in temperature due to the expansion. However, this compensation is far from sufficient to maintain the

supersaturation constant. To solve the last equation it is necessary to know the supersaturation at which condensation nuclei are produced, the saturation pressure, the temperature and the coefficient of surface tension. It is still impossible to make any recommendation whatever concerning these quantities.

A determination of the number of condensation nuclei does not solve the problem, for to calculate the amount of precipitated moisture it is also necessary to know the size of the condensation nuclei and their rate of growth.

It is obvious that the minimum size of a condensation nucleus will depend on the value of supersaturation that is capable of compensating for the surface-tension forces.

When its size is smaller than r_{cr}, the drop must evaporate. Fig. 8 shows a curve of the critical dimensions of nucleation drops as a function of the supersaturation needed for their existence.

We see that a supersaturation of approximately 235 is necessary to produce a drop measuring 2.0×10^{-8} cm.

Calculations based on the critical drop dimensions and on the rate of nucleus formation, as determined from the foregoing equation, have shown that the amount of precipitated moisture is of the same order as that due to the growth of the condensation nuclei already existing.

The heat liberated in the condensation of so negligible an amount of moisture is quite insufficient to make this process deviate from adiabatic, as shown by experiment (Fig. 2). In this connection, a need arises for developing a more exact theory as regards the determination of the rate of production of nucleation droplets and their actual dimensions. It is also necessary to determine the amount of moisture precipitated in the condensation shock, the change in the gas parameters and the length of the shock.

The movement of a gas in a channel of variable cross section, accompanied by condensation, can be represented as the result of different actions—geometric, thermal and hydraulic, and the last two factors depend on the amount of moisture precipitated as a result of the condensation. Neglecting the liquid phase, let us write the equation of motion

$$(M^2 - 1)\frac{dW}{W} = \frac{dF}{F} - \frac{dG}{G} - \frac{k-1}{A}\frac{g}{a^2}\,dQ$$

Bearing in mind that

$$dQ = r(dG/G)$$

we can find the change in gas flow resulting from condensation for a known channel shape and for the variation of pressure over its length

$$\frac{dG}{G} = \frac{[(M^2 - 1)/kM^2](dP/P) + (dF/F)}{1 + (r/C_pT)}$$

dG is the amount of liquid condensed over a channel element of length dx.

We introduce the concept of degree of condensation α

$$\alpha = G_l/G_v$$

where G_v is the total amount of vapor before the start of condensation, i.e.

$$\alpha = \frac{dG/G}{G_v/G} = \frac{dG}{G \times d}$$

where $d = G_v/G$ is the absolute humidity of the gas in gm/kg of dry gas. Then the degree of condensation will be given by

$$\alpha = \frac{[(M^2 - 1)/kM^2](dP/P) + (dF/F)}{[1 + (r/C_pT)] \times d \times 10^{-3}}$$

Numerous experiments on the distribution of pressure along the nozzle have demonstrated that condensation initiated at such high values of supersaturation leads to the precipitation of all the moisture contained in the gas. It has also been established that the length of the condensation shock depends on the absolute humidity of the gas expanding in the nozzle and is sufficiently large (Fig. 9). By comparing the dry and moist expansion adiabats, one can determine all the parameters of the gas stream over the condensation region. Fig. 10 shows the variation of the supersaturation in the condensation zone as a function of the fraction of precipitated condensate for different initial humidities of the expanding air.

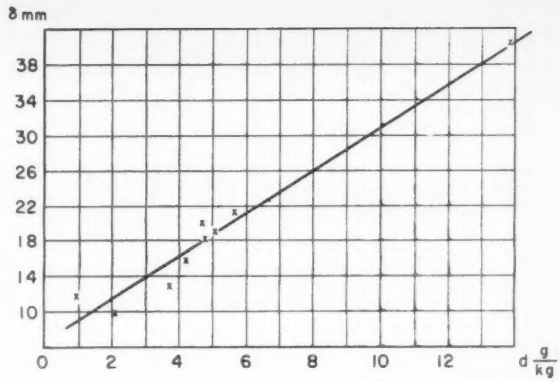

Fig. 9 Thickness of condensation shock

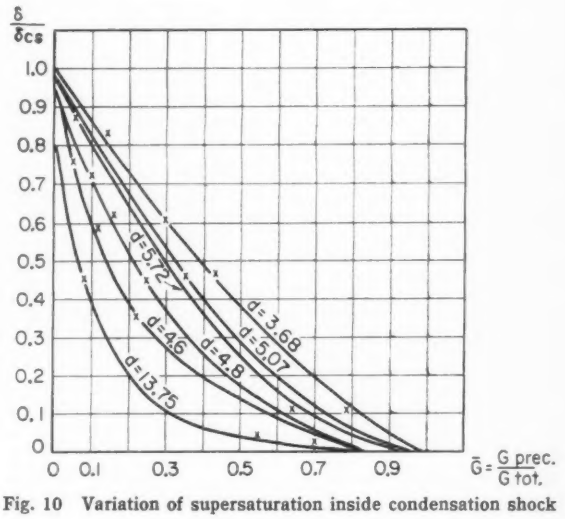

Fig. 10 Variation of supersaturation inside condensation shock

The data given here give a sufficiently complete description of the physical picture of the course of condensation in a gas expanding in a Laval nozzle and can be used to develop a condensation theory under analogous conditions.

References

1 Oswatitsch, Kl., "Kondensationsstösse in Lavaldüsen," VDI—Z—t Bd 86, Nr 47/48 s. 702, 1942.

2 Zukasiewics, J., "Effects of Air Humidity in Supersonic Wind Tunnel," in "Proceedings of the 2nd International Congress of Applied Mechanics," vol. 2, part II, 1948.

3 Tunitskii, N., "On the Condensation of Supersaturated Vapors," *Zhurnal fizicheskoi khimii* (J. of Physical Chemistry), vol. XV, no. 10, 1941.

4 Becker, R. and Döring, W., "Kinetishe Behandlung der Rainbildung in übersättigten Dampfen," *Annalen der Physik*, 5. Folge, Bd 24, 1935.

5 Volmer, M., "Kinetic der Phasenbildung," 1939.

—*Original received February 9, 1959*

Perturbations of Orbits of Artificial Satellites Due to Air Resistance

YU. V. BATRAKOV and
V. F. PROSKURIN

WHEN the orbit of an artificial satellite passes at a relatively low altitude above the Earth's surface, the satellite experiences a noticeable air drag over a certain portion of its orbit. The net result of the periodically repeated drag is a reduction in the total kinetic energy of the satellite and, as a consequence, a rapid increase in the secular variation of the form and dimensions of the orbit. These secular variations cause the satellite to drop lower and eventually to be destroyed in the denser layers of the atmosphere.

The peculiarities of the motion of artificial satellites in an atmosphere have not yet been sufficiently well studied. The papers devoted to this problem consider only certain of the most important properties of the motion—the secular perturbations (1)[1] and perturbations with periods considerably longer than the period of one revolution of the satellite.

In the present investigation we undertook to obtain the general form of first-order perturbations in the elements of an elliptic satellite orbit, caused only by the resistance of the atmosphere. It is assumed here that the Earth's atmosphere has a fully spherical density distribution and that the attraction of the Earth can be replaced by the attraction of a mass point, placed at its center of mass and having the same mass as the Earth. Under these assumptions, along with the secular perturbations, there are obtained also faster perturbations whose periods do not exceed the period of one revolution of the satellite. As far as we know, these short-period perturbations, caused by the resistance of the air, have not yet been investigated. We also give a numerical example, which shows the comparative magnitude of the first-order perturbations due to the air resistance.

1 Equations of Motion and General Form of First-Order Perturbation

The resistive force, acting on a body moving with a velocity v in a rarefied air medium of density ρ is determined by the formula

$$F = \tfrac{1}{2} C_D S \rho v^2 \qquad [1]$$

where

S = area of transverse (frontal) section of body
C_D = drag coefficient

The force F is always directed opposite to the direction of motion of the body. As regards the air density, it is assumed that it decreases with the distance from the Earth's surface, which will be denoted by h.

If the mass of the moving body is m, then the perturbing acceleration due to the force F is equal to $\alpha \rho v^2$, where

$$\alpha = \frac{1}{2} C_D \frac{S}{m}$$

The coefficient α depends only on the form, dimensions and weight of the satellite.

The Lagrange equations for the perturbations of the elliptic orbit have the following form (2)

$$\begin{aligned}
(da/dt) &= 2a^2 e \sin\theta \times S' + 2a^2 p r^{-1} T' \\
(de/dt) &= p \sin\theta \times S' + p(\cos\theta + \cos E) T' \\
\sin i (d\Omega/dt) &= r \sin(\theta + \Pi - \Omega) W' \\
(di/dt) &= r \cos(\theta + \Pi - \Omega) W' \\
e \frac{d\Pi}{dt} &= 2e \sin^2 \frac{i}{2} \frac{d\Omega}{dt} - p \cos\theta \times S' + (r + p) \sin\theta \times T' \\
\frac{d\epsilon}{dt} &= 2 \sin^2 \frac{i}{2} \frac{d\Omega}{dt} - 2r \sqrt{1 - e^2} \times S' + \\
&\quad \frac{e}{1 + \sqrt{1 - e^2}} [-p \cos\theta \times S' + (r + p) \sin\theta \times T']
\end{aligned} \qquad [2]$$

where

a = semimajor axis
e = eccentricity
i = inclination
Ω = longitude of node
Π = longitude of perigee
ϵ = average longitude of epoch
r = radius vector
θ = true anomaly
E = eccentric anomaly
p = $a(1 - e^2)$ = parameter of orbit

If we denote by S, T and W the components of the perturbing acceleration along the radius vector, along a direction perpendicular to the radius vector in the plane of the osculating orbit, and along the normal to the plane of the orbit, respectively, we obtain the following expressions

$$S' = \frac{1}{k_s \sqrt{mp}} S \qquad T' = \frac{1}{k_s \sqrt{mp}} T \qquad W' = \frac{1}{k_s \sqrt{mp}} W$$

where k_S is the Gaussian gravitational constant.

Since the perturbing force is directed opposite the velocity of the body, and the unperturbed motion is planar, the disturbed motion also remains planar, and the component W is equal to zero.

Noting that the projection of the velocity on the radius vector and on the direction perpendicular to the radius vector in the plane of the orbit are $\dot{r}$ and $r\dot{u}$, where $u = \theta + \omega$ is the angular distance of the satellite from the node of the orbit (the argument of latitude) and the dots designate differentiation with respect to time, and using the relations which are true for the unperturbed motion

$$\dot{r} = \frac{nae}{\sqrt{1 - e^2}} \sin\theta \qquad r\dot{u} = \frac{na^2 \sqrt{1 - e^2}}{r}$$

we obtain, accurate to quantities which are small to higher

Translated from "Iskusstvennye Sputniki Zemli" (Artificial Earth Satellites), no. 3, USSR Acad. Sci. Press, Moscow, 1959, pp. 39–46.

[1] Numbers in parentheses indicate References at end of paper.

order with respect to the perturbing forces, the following expressions

$$S' = -\alpha\rho \frac{ne}{(1-e^2)^{1/2}} \sqrt{1 + 2e\cos\theta + e^2} \times \sin\theta$$

$$T' = -\alpha\rho \frac{n}{(1-e^2)^{1/2}} \sqrt{1 + 2e\cos\theta + e^2}(1 + e\cos\theta)$$

.....[3]

Inserting [3] into [2] we obtain after several simplifications the following formulas

$$\frac{da}{dt} = -\frac{2\alpha\rho n a^2}{(1-e^2)^{1/2}} (1 + 2e\cos\theta + e^2)^{1/2}$$

$$\frac{de}{dt} = -\frac{2\alpha\rho n a}{(1-e^2)^{1/2}} (1 + 2e\cos\theta + e^2)^{1/2}(e + \cos\theta)$$

$$\frac{d\Omega}{dt} = \frac{di}{dt} = 0$$

$$e\frac{d\Pi}{dt} = -\frac{2\alpha\rho n a}{(1-e^2)^{1/2}} (1 + 2e\cos\theta + e^2)^{1/2} \times \sin\theta$$

$$\frac{d\epsilon}{dt} = \frac{2\alpha\rho n a e}{(1-e^2)^{1/2}} (1 + 2e\cos\theta + e^2)^{1/2} \times \left(\frac{\sqrt{1-e^2}}{1 + e\cos\theta} - \frac{1}{1 + \sqrt{1-e^2}}\right) \sin\theta$$

.....[4]

To obtain first-order perturbations in the elements of the satellite orbits, the right halves of [4] are best expanded in trigonometric series in the mean anomaly M or, what is the same, in the time. The air density ρ is by assumption a function only of the distance from the Earth's surface, which will be denoted by h. The quantity h is an even periodic function of the mean anomaly with period 2π, and consequently can be expanded in a Fourier series of only the cosines of the multiples of the mean anomalies. The functions $\cos\theta$ and $\sin\theta$ are also expanded in Fourier series in multiples of the mean anomaly, containing only the cosines or the sines, respectively.

It follows from this that after expansion of the right halves of Equations [4] in Fourier series in the mean anomaly, we have equations of the form

$$\frac{da}{dt} = a' + \sum_{j=1}^{\infty} a_j \cos jM$$

$$\frac{de}{dt} = e' + \sum_{j=1}^{\infty} e_j \cos jM$$

$$\frac{d\Omega}{dt} = \frac{di}{dt} = 0$$

$$\frac{d\Pi}{dt} = \sum_{j=1}^{\infty} \Pi_j \sin jM$$

$$\frac{d\epsilon}{dt} = \sum_{j=1}^{\infty} \epsilon_j \sin jM$$

.....[5]

where the coefficients of all of the sines and cosines are functions of the semimajor axis and the eccentricity, and also of the parameters of the law assumed for the distribution of the air density with altitude.

In the first approximation, the eccentricity and the semimajor axis are assumed to be constant; then integration of Equation [5] yields the following equations

$$a = a_0 + a'(t - t_0) + \sum \frac{a_j}{jn} \sin jM$$

$$\epsilon = \epsilon_0 + e'(t - t_0) + \sum \frac{e_j}{jn} \sin jM$$

$$\Omega = \Omega_0 \qquad i = i_0$$

$$\Pi = \Pi_0 - \sum \frac{\Pi_j}{jn} \cos jM$$

$$\epsilon = \epsilon_0 - \sum \frac{\epsilon_j}{jn} \cos jM$$

.....[6]

where

$a_0, e_0, \ldots$	=	constants of integration
t_0	=	instant of passage through perigee
M	=	$n(t - t_0)$
n	=	mean motion

Thus, the semimajor axis and the eccentricity contain secular terms in addition to the periodic perturbations, whereas the elements π and ϵ do not contain secular terms. The constancy of the elements i and Ω is evidence that the motion is planar. We note that the periodic disturbances in a and e are odd functions of M and vanish when $M = 0$, i.e., at the perigee of the orbit. The periodic disturbances of Π and ϵ are even functions and reach extremal value at the perigee and apogee.

The coefficients a' and e', as well as a_j, e_j, Π_j and ϵ_j can be calculated with the usual Fourier formulas

$$a' = \frac{1}{\pi}\int_0^{\pi} \frac{da}{dt}\, dM \qquad e' = \frac{1}{\pi}\int_0^{\pi} \frac{de}{dt}\, dM$$

$$a_j = \frac{2}{\pi}\int_0^{\pi} \frac{d\Pi}{dt} \cos jM dM \qquad e_j = \frac{2}{\pi}\int_0^{\pi} \frac{de}{dt} \cos jM dM$$

$$\Pi_j = \frac{2}{\pi}\int_0^{\pi} \frac{d\Pi}{dt} \sin jM dM \qquad \epsilon_j = \frac{2}{\pi}\int_0^{\pi} \frac{d\epsilon}{dt} \sin jM dM$$

.....[7]

either by numerical methods, or if possible in the form of explicit analytic dependences on a_0, on e_0 and on the parameters of the assumed distribution of density.

The signs of the coefficients a' and e', which determine the character of the evolution of the satellite orbit, can be determined without preliminary calculations. In fact, it follows from [4] that da/dt is always negative; consequently, a is also negative. As to the coefficient e', its negative sign follows from the fact that the derivative de/dt is negative in the interval $0 < \theta < \pi/2$ and exceeds in absolute magnitude all the values of de/dt when $\pi/2 < \theta < \pi$. It is assumed here that the density ρ is a decreasing function of the height of the satellite above the surface of the Earth and consequently a decreasing function of θ in the interval $(0, \pi)$. Since a' and e' have negative signs, both the semimajor axis and the eccentricity increase with time—the orbit decreases in size and approaches a circle more and more.

Equations [5] give a complete representation of the character of the first-order disturbances caused by air resistance. If second- and higher-order secular disturbances must be accounted for, the elements a and e must be represented by series

$$a = a_0 + a'(t - t_0) + a''(t - t_0) + \ldots$$
$$e = e_0 + e'(t - t_0) + e''(t - t_0) + \ldots$$

.....[8]

and the theoretical determination of the coefficients a'', e'', . . . is a more difficult problem than the determination of $a', e', \ldots$.

2 Example of the Calculation of Perturbations of Satellite Orbit Elements, Due to Air Resistance

In the calculation of the specific perturbations of the elements we need above all an explicit expression for the air density as a function of altitude. To obtain such an explicit expression, we use the model of the atmosphere used in (3), characterized by the data given in the first four columns of the table. The first column lists the altitude above the surface of the Earth, while the second, third and fourth list the concentrations of the N_2, O_2 and O molecules, which determine essentially the chemical composition and the property of the air at high altitudes. The values of the air density listed in the five columns have been calculated from the formula

$$\beta = m(N_2)n(N_2) + m(O_2)n(O_2) + m(O)n(O)$$

where $m(N_2) = 4.688 \times 10^{-23}$ g, $m(O_2) = 5.354 \times 10^{-23}$ g, $m(O) = 2.677 \times 10^{-23}$ g, are the masses of the particles, and $n(N_2)$, $n(O_2)$ and $n(O)$ are the numbers of molecules per unit volume. The sixth column lists the values of the densities in the practical system of units.

The dependence of the air density on the velocity, listed in the table, will be approximated by means of the formula

$$\beta = A[\log (h/10)]^B \qquad [9]$$

where A and B are certain parameters, and the logarithm to the base 10 is used. Taking logarithms of [9], we obtain

$$\log \beta = \log A + B \log \log (h/10) \qquad [10]$$

which relates the unknown $\log A$ and B linearly.

If we insert in Equation [10] the values of h (in km) and the corresponding values of the density from the sixth column, we obtain 15 tentative equations for $\log A$ and B. The use of the least-squares method yields

$$\log A = -6.98787 \qquad B = -26.8132 \qquad [11]$$

The values of the densities, calculated from Equation [9] with the parameters A and B from [11] are listed in the last column of the table.

Comparing the initial values of the density with the values obtained by formula [9] we see that in some cases the discrepancies between them reach 30 per cent of the value of the density. However, considering that the values known for the air density at high altitudes are subject to errors which exceed by several times the density values themselves, such discrepancies can be considered acceptable.

For the actual calculation of the disturbances let us simplify somewhat the Equations [4] and let us put for this purpose everywhere on the right halves of [4] (with the exception of the dependence on e) a value of zero for the eccentricity. In addition, we introduce

$$\rho^* = \left(\log \frac{h}{10}\right)^B \qquad [12]$$

Then the equations for elements a, e, Π and ϵ become

$$\frac{da}{dt} = -2\alpha A n a^2 \rho^* \qquad e\frac{d\Pi}{dt} = -2\alpha A n a \rho^* \sin M$$

$$\frac{de}{dt} = -2\alpha A n a \rho^* \cos M \qquad \frac{d\epsilon}{dt} = 0 \qquad [13]$$

The altitude h, which enters into the expression for ρ^*, is expressed in terms of M by means of the relations

$$h = r - R \qquad r = a(1 - e\cos E) \qquad E - e\sin E = M \qquad [14]$$

where R is the average radius of the Earth. For a numerical example let us take the following elements

$$\left.\begin{aligned} n_0 &= 5024°.40 \\ n' &= 1°.191 \\ e &= 0.099493 \end{aligned}\right\} \text{ daily} \qquad [15]$$

where n_0 and n' are related with a_0 and a' by

$$a_0^3 n_0^2 = k^2 m \qquad n' = -\frac{3}{4} \times \frac{n_0}{a_0} a' \qquad [16]$$

The value of k^2m is taken from (4), after first converting it into our system of units

$$k^2 m = 9.75787 \times 10^{18} \text{km}^3 \text{deg}^2/\text{day}^2$$

We then obtain from Equation [16]

$$a_0 = 7286.88 \text{ km} \qquad a' = -2.303 \text{ km/day} \qquad [17]$$

Using 7286.88 km for a_0 and 6367.55 km for R, as well as relations [14], we obtain by means of the usual harmonic-

	Number of particles per cm²				ρ, kg-sec²/m⁴	ρ, kg-sec²/m⁴
h	$n(N_2)$	$n(O_2)$	$n(O)$	ρ, g/cm³		
100	$2.82 \cdot 10^{13}$	$7.56 \cdot 10^{12}$	$1.09 \cdot 10^{12}$	$1.742 \cdot 10^{-9}$	$1.775 \cdot 10^{-7}$	$1.03 \cdot 10^{-7}$
110	$8.58 \cdot 10^{12}$	$8.25 \cdot 10^{10}$	$3.59 \cdot 10^{12}$	$4.989 \cdot 10^{-10}$	$5.084 \cdot 10^{-8}$	$3.47 \cdot 10^{-8}$
120	$2.54 \cdot 10^{12}$	$5.29 \cdot 10^{8}$	$1.06 \cdot 10^{12}$	$1.463 \cdot 10^{-10}$	$1.491 \cdot 10^{-8}$	$1.33 \cdot 10^{-8}$
130	$8.60 \cdot 10^{11}$	$1.72 \cdot 10^{7}$	$3.45 \cdot 10^{11}$	$4.917 \cdot 10^{-11}$	$5.010 \cdot 10^{-9}$	$5.70 \cdot 10^{-9}$
150	$1.47 \cdot 10^{11}$	...	$1.08 \cdot 10^{11}$	$9.707 \cdot 10^{-12}$	$9.891 \cdot 10^{-10}$	$1.33 \cdot 10^{-9}$
175	$2.73 \cdot 10^{10}$	...	$3.28 \cdot 10^{10}$	$2.164 \cdot 10^{-12}$	$2.205 \cdot 10^{-10}$	$3.01 \cdot 10^{-10}$
200	$4.31 \cdot 10^{9}$	...	$1.75 \cdot 10^{10}$	$6.653 \cdot 10^{-13}$	$6.779 \cdot 10^{-11}$	$8.87 \cdot 10^{-11}$
250	$3.28 \cdot 10^{8}$	...	$2.55 \cdot 10^{9}$	$8.299 \cdot 10^{-14}$	$8.457 \cdot 10^{-12}$	$1.29 \cdot 10^{-11}$
300	$4.71 \cdot 10^{7}$	...	$7.15 \cdot 10^{8}$	$2.118 \cdot 10^{-14}$	$2.158 \cdot 10^{-12}$	$2.95 \cdot 10^{-12}$
400	$1.93 \cdot 10^{6}$	...	$1.08 \cdot 10^{8}$	$2.958 \cdot 10^{-15}$	$3.014 \cdot 10^{-13}$	$3.33 \cdot 10^{-13}$
500	...	...	$2.63 \cdot 10^{7}$	$6.985 \cdot 10^{-16}$	$7.118 \cdot 10^{-14}$	$6.93 \cdot 10^{-14}$
600	...	...	$8.49 \cdot 10^{6}$	$2.255 \cdot 10^{-16}$	$2.298 \cdot 10^{-14}$	$3.04 \cdot 10^{-14}$
700	...	...	$3.41 \cdot 10^{6}$	$9.057 \cdot 10^{-17}$	$9.229 \cdot 10^{-15}$	$7.57 \cdot 10^{-15}$
800	...	...	$1.38 \cdot 10^{6}$	$3.665 \cdot 10^{-17}$	$3.735 \cdot 10^{-15}$	$3.30 \cdot 10^{-15}$
900	...	...	$7.33 \cdot 10^{5}$	$1.947 \cdot 10^{-17}$	$1.984 \cdot 10^{-15}$	$1.62 \cdot 10^{-15}$

analysis formulas (dividing the period into 24 parts) the following expansion

$$10^4\rho^* = 0.7433 + 1.4633\cos M + 1.3968\cos 2M + 1.2953\cos 3M + 1.1702\cos 4M + 1.0337\cos 5M + 0.8971\cos 6M + 0.7696\cos 7M + 0.6582\cos 8M + 0.5679\cos 9M + 0.5017\cos 10M + 0.4614\cos 11M + 0.2239\cos 12M \quad [18]$$

Equation [18] shows clearly how slowly the Fourier series for the function $\rho = \rho(M)$ converges.

Inserting [18] into [13] and integrating, we obtain both the secular and the periodic perturbations of the elements. All these perturbations will contain a factor αA, the accuracy of which is very low for various reasons. Firstly, the aerodynamic coefficient C_D is not too accurately known; in addition, the instantaneous cross-section area S may not be known with sufficient accuracy; finally, the coefficient A may be subject to large error. Therefore, instead of calculating the factor αA theoretically, it is much more convenient to determine it, starting with the quantity a given in Equation [17]. In fact, from the relation

$$a' = -2\alpha A n a^2 [\rho^*]$$

where the symbol $[\rho^*]$ denotes the free term in the Fourier series expansion, we obtain

$$2\alpha A n a^2 = -\frac{a'}{[\rho^*]} \quad [19]$$

Substituting [19] in [13] and integrating, we obtain

$$a = a_0 + \frac{a'}{[\rho^*]}\int \rho^* dt \qquad e\Pi = e\Pi_0 + \frac{a'}{a[\rho^*]}\int \rho^* \sin M\, dt$$

$$e = e_0 + \frac{a'}{[\rho^*]a}\int \rho^* \cos M\, dt \qquad \epsilon = \epsilon_0 \quad [20]$$

From [20], using [16, 17 and 18] we finally derive the following values of the perturbations for orbits having the elements [15].

$$\begin{aligned} a = d_0 - 2.303t &- 0.052\sin M - 0.004\sin 7M \\ &- 0.025\sin 2M - 0.003\sin 8M \\ &- 0.015\sin 3M - 0.003\sin 9M \\ &- 0.010\sin 4M - 0.002\sin 10M \\ &- 0.007\sin 5M - 0.002\sin 11M \\ &- 0.006\sin 6M - 0.001\sin 12M \end{aligned} \quad \ldots\ldots [21a]$$

$$\begin{aligned} e = e_0 - 0.0002584t &- 0.0000070\sin M - 0.0000005\sin 7M \\ &- 33\sin 2M - 4\sin 8M \\ &- 20\sin 3M - 4\sin 9M \\ &- 14\sin 4M - 2\sin 10M \\ &- 10\sin 5M - 2\sin 11M \\ &- 7\sin 6M - 1\sin 12M \end{aligned} \quad \ldots\ldots [21b]$$

$$\begin{aligned} \Pi = \Pi_0 + 0^\circ.00013\cos M &+ 0^\circ.00006\cos 6M \\ + 12\cos 2M &+ 5\cos 7M \\ + 11\cos 3M &+ 3\cos 8M \\ + 09\cos 4M &+ 2\cos 9M \\ - 08\cos 5M &+ 1\cos 10M \end{aligned} \quad \ldots\ldots [21c]$$

where the coefficients of the perturbations of the semimajor axis are given in kilometers. It is seen from Equations [21] that the amplitude [21c] of the largest periodic term of the semimajor axis is approximately 50 m, and the periodic perturbations in the longitude of the perigee reach half a second of arc. The perturbations of the element e are even smaller than the perturbations of the longitude of the perigee, since they contain the eccentricity of the orbit as a factor.

Thus, the periodic perturbations due to air resistance are sufficiently small and can be taken into account in processing visual and rough photographic observations of artificial Earth satellites.

References

1 Okhotsimskii, D. E., Eneev, T. M. and Taratynova, G. P., *Uspekhi Fiz. Nauk* (Advances in Physical Sciences), vol. 63, no. 1a, 1957. Translated by International Physical Index, New York.

2 Subbotin, M. F., "Kurs nebesnoi mekhaniki" (Course of Celestial Mechanics), vol. II, ONTI, 1937.

3 Mitra, S. K., "The Upper Atmosphere" (Russian translation), Foreign Literature Press, 1955.

4 Zhongolovich, I. D., *Byull. ITA* (Bulletin of the Institute of Theoretical Astronomy), vol. 6, 1957, p. 8.

Reviewer's Comment

This paper presents a general perturbations approach to the problem of a satellite encountering aerodynamic drag. Its principal value is in the author's attempt to retain periodic as well as secular terms in the variation of the orbital parameters. The fundamental effort of the author has been to expand Equations [2, 3 and 4], which presumbably have their ultimate origin in Moulton (1), into series in terms of the mean anomaly and then to integrate analytically these series.

The present paper seems to be reasonably correct; however, a few constructive criticisms are in order. First, the power of the author's generalized approach is somewhat weakened by his neglect of a rotating atmosphere. As has been pointed out by Rowell and Smith (2) and Vinti (3), if one considers a rotating atmosphere then there exist perturbative forces acting normal to the orbit plane, i.e., in the W direction. Thus there *does* exist a secular term in i and Ω. Second, the outdated densities found in Mitra's referenced book are utilized. Clearly, the more recent density tables given by Whitney (4) and others should be employed—other-

wise the numerical results would be in error by an order of magnitude. Third, in Equations [4, 13], etc., the perturbative variation in Π has an e in the denominator. For low eccentricity orbits, therefore, the perturbative variation of the perigee direction becomes infinite, a logical consequence of the fact that the perigee direction becomes undefined. Consequently, other variables such as those proposed by Herrick and Walters should be utilized (5). Fourth, the curve-fit error in the density variation amounting to 30 per cent has been rationalized by the author as being within the discrepancy in our knowledge of the atmosphere. Unfortunately, a systematic error given by his density approximation is not equivalent to the random error either in the uncertainty of atmospheric densities or in the solar generated variations identified by Jacchia. Hence, it might be preferable to seek a better method for approximating atmospheric densities. Perhaps the method proposed in Chapter 9 of (6) might prove to be more useful.

—Robert M. L. Baker, Jr.
Department of Astronomy
University of California, Los Angeles

1 Moulton, F. R., "Introduction to Celestial Mechanics," MacMillan Company, New York, 1914.

2 Rowell, L. N. and Smith, M. C., "Secular Variation in the Inclination of the Orbit of Earth Satellite (1957) and Air Drag," RAND Rep. no. P-1611, 1958.

3 Vinti, J. P., "Theory of the Effect of Drag on the Orbital Inclination of an Earth Satellite," *J. Research Nat. Bur. Standards*, vol. 62, 1959, pp. 79–88.

4 Whitney, C. A., "Atmospheric Conditions at High Altitudes from Satellite Observations," ARS Preprint no. 779-59, 1959.

5 Herrick, Samuel and Walters, L. G., "Project Mercury Task One Report," Aeronutronic Pub. no. U-468, 1959.

6 Baker, R. M. L., Jr., and Makemson, M., "Introduction to Astrodynamics," Academic Press, New York, 1960.

(Continued from page 656)

A straight line satisfactorily connects the points shown, but a linear extrapolation to extreme values obviously cannot be correct. The linearity of the portion of the curve shown is somewhat surprising, in view of the manner in which the results have been derived. For the gaseous discharge, if one considers the energy term corresponding to a Joule heating term j^2/σ and the resistance term corresponding to $1/\sigma$, then the resulting ratio is proportional to j^2. Here j and σ are current density and electrical conductivity, respectively, in the plasma. Since the magnetic field at the discharge in all cases is proportional to circuit current, the calculated ratio then may be considered to assume the significance of **j x B**, the magnetic pushing term of interest. The efficiency is calculated from the ratio of gas kinetic energy to capacitor energy; since the capacitor energy was held constant for these cases at 500 joules, the plotted curve may thus be interpreted as one of kinetic energy vs. a **j x B** body force. Second and third half cycle energies show the same linear effect, as might be expected.

In order to obtain a better idea of the effect of actual circuit parameters for these cases, it was considered advisable to compare the observed T-tube inductance and resistance values with total circuit values for the five cases. The reader is directed to (1) for the actual data. A ratio of T-tube inductance to resistance divided by the ratio of circuit inductance to resistance actually assumes the significance of a Q ratio (Q_d/Q_c). A plot of these values against the corresponding values of energy/resistance for the five cases in Fig. 1 is shown in Fig. 2, where again the assumed negative effect has been maintained. A bell-shaped connecting curve is indicated, with the highest magnetic effects occurring when Q of the T-tube circuit is small compared with its circuit Q value. This relationship has somewhat greater generality in that it suggests how one might vary inductance or resistance of the T-tube circuit, compared with the corresponding total circuit values, in order to attain higher energy conversion efficiencies.

These results involve considerable error and for this one set of parameters may be coincidental. However, this kind of experimental variation provides an interesting means of obtaining useful informaton concerning the nature of the discharge and acceleration process to which the T-tube lends itself especially well. It should be emphasized that these correlations have resulted from one input energy value only, and that other input energies, particularly low values, may show a different order in observed efficiencies. Qualitatively, one might expect for lower currents at the lower energies smaller magnetic pushing for any given geometry of the return leads. At any input energy, it is clear that the deliberate introduction of inductance to provide a magnetic field at the discharge can severely limit the efficiency of the acceleration process.

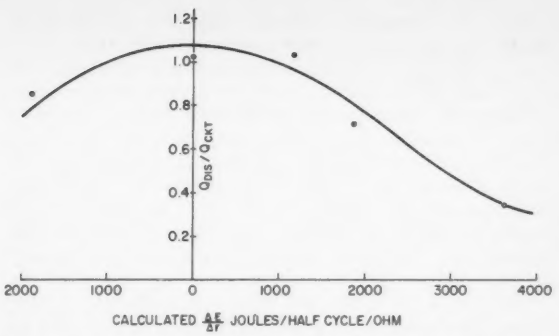

Fig. 2 Energy per unit resistance vs. Q ratio for various T-tube configurations

Acknowledgments

The author wishes to thank A. Sherman and G. Borman of this organization for interesting discussions concerning this correlation and B. Gorowitz of the General Electric Co. Missile and Space Vehicle Dept. for his part in making this communication possible.

References

1 Gorowitz, B. and Harned, B. W., "Electric Propulsion—Measurements With a Small Thrust Generator," paper 63T, SAE National Aeronautic Meeting, N. Y., April 3, 1959.
2 Kolb, A. C., "Magnetohydrodynamics," Stanford University Press, Calif., 1957, pp. 76–91.
3 Kash, S. W., Gauger, J., Starr, W. and Vali, V., "The Plasma in a Magnetic Field," Stanford University Press, Calif., 1958, pp. 99–109.
4 Cowling, T. G., "Magnetohydrodynamics," Interscience Pub., Inc., N. Y., 1957, chap. 6.

"Catastrophic" Changes in Burning Rate of Solid Propellants During Combustion Instability

J. E. CRUMP[1] and E. W. PRICE[2]

U. S. Naval Ordnance Test Station, China Lake, Calif.

Experimental results of a research program on combustion instability in solid propellants have revealed a "catastrophic" change in burning rate which is correlated with the occurrence of a harmonic relationship between a longitudinal acoustic mode and a tangential acoustic mode of the propellant chamber.

Received Feb. 29, 1960.
[1] Physicist, Research Department. Member ARS.
[2] Head, Aerothermochemistry Group. Member ARS.

THIS note is to report a new finding regarding the phenomenon of combustion instability in solid propellant rocket motors. The behavior observed is in sharp contrast to earlier results of the present research program (1–3)[3] and appears to be foreign to the mechanisms postulated in current theories of combustion instability.

In earlier notes (1,3) it was reported that burning rate excesses responsible for pressure increases during combustion instability were identified with the oscillation of combustion gases tangential to the solid propellant burning surface; i.e., the mechanism was somewhat like an erosive burning behavior. Fig. 1a indicates a typical "erosive" burning rate response.

During the current research while the authors were investigating selective damping of various longitudinal modes in an internal burning, circular cylindrical charge configuration

[3] Numbers in parentheses indicate References at end of paper.

(1–3), a new behavior occurred suggestive of the "catastrophic" pressure peaks noted in rocket motors. It was found that, if damping was designed to suppress selectively the lower longitudinal modes, extremely severe pressure peaks occurred (Fig. 1b). Analysis of the data showed that there were no frequencies present other than those which had been observed previously in tests not exhibiting "catastrophic" behavior, although there were both tangential and longitudinal modes present with appreciable severity. As more test data became available, it became increasingly evident that the "catastrophic" instability occurred at the same time or times during burning of any one configuration (one propellant, one conditioning temperature) and could be reproduced. A study of the high frequency response test records showed that the "catastrophic" pressure peaks occurred at times during burning when the frequency of one of the tangential modes was harmonically related to the frequency of one of the higher longitudinal modes. Although the frequencies were so high (10–53 kcps) that detection system response was very poor, it was often possible to actually see the harmonically related pressure oscillations (Fig. 2). In other tests, the presence of other modes made continuous observation of the "guilty" modes through the "catastrophic" peak impossible, but enough data where obtained to verify that the "guilty modes" were present and close to or at a condition of harmonically related frequencies. When the same modes were present but not close to harmonic relationship, pressures were near normal. The low longitudinal modes were conspicuously absent or of very low amplitude during the peaks. Measurements on partially burned charges interrupted during pressure peaks confirmed that the wave lengths of the "guilty" modes were harmonically related at that time during burning. Another conspicuous feature of the partially burned charges was a severe rippling and pitting of the burning surface (Fig. 3d). This rippling was somewhat similar to that observed under "normal" unstable burning (Figs. 3b,c), but the pattern was more severe and more complicated and looked somewhat like a composite of two perpendicular ripple patterns. (The increased burning surface due to the rippling would account for only 20–30 per cent of the pressure increase.)

To examine further the condition of modes with harmonically related frequencies, consider Fig. 4, in which the variation of frequency of the first two tangential modes is shown as a function of perforation diameter. The points shown by circles correspond to times during burning when the frequency of the tangential mode is harmonically related to the frequency of some longitudinal mode. The labels indicate the modes involved and the multiple relation of their frequencies. Thus a label $3f^{7L}$, on the f^{1T} curve means that, at that perforation diameter during burning, the frequency of the second

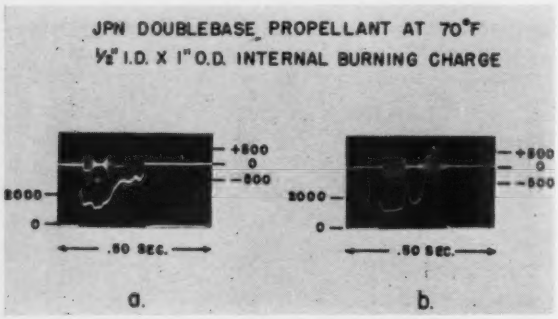

Fig. 1 Pressure-time curves with combustion instability showing: (a) Pressure increase due to oscillatory instability in longitudinal modes, primarily first and third (6-in. length charge); and (b) pressure increase (first peak after ignition) due to simultaneous oscillatory instability in the ninth longitudinal mode, 20,250 cps and the first tangential mode, 40,500 cps (10-in. length charge)

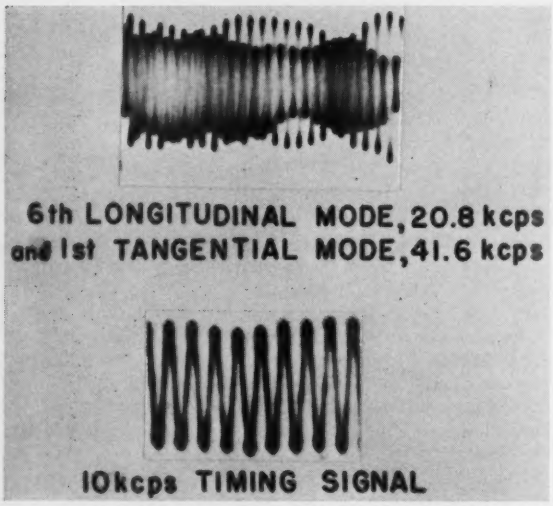

Fig. 2 Pressure oscillations during violent pressure peak showing presence of two harmonically related frequencies. JPN double-base propellant at 70 F, ½-in. ID × 1-in. OD × 6-in. length internal burning charge

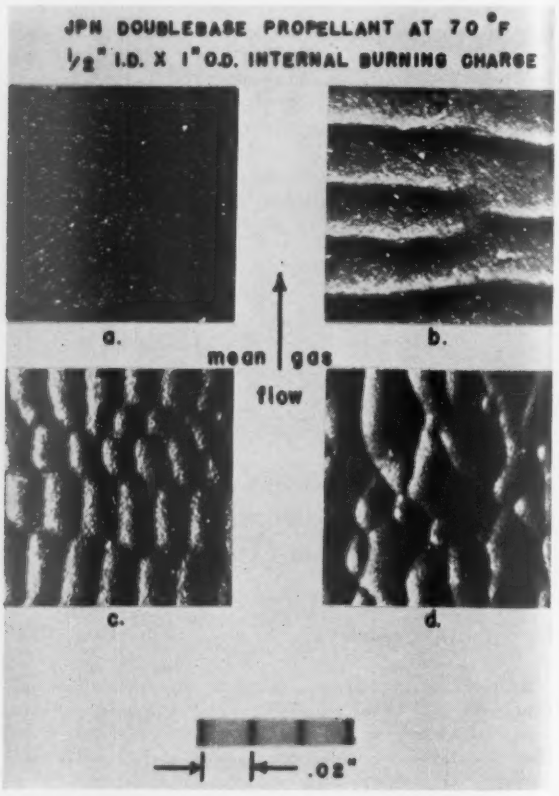

Fig. 3 Rippling of burning surface produced by severe oscillatory burning in various acoustic modes: (a) No oscillations; (b) longitudinal mode, 3600 cps; (c) tangential mode, 34,500 cps; (d) eighth longitudinal mode, 17,600 cps, and first tangential mode, 35,200 cps in harmonic relationship

tangential mode is three times the frequency of the seventh longitudinal mode. In Fig. 4, the combinations of frequencies actually evident during "catastrophic" pressure peaks on various tests with 10-in. long charges are indicated by the test numbers listed. No "catastrophic" peaks were observed that did not correlate closely with one or more of the critical points, and the modes involved were evident at those times with frequencies close to the indicated values. Similar results were obtained with other length charges. (Tests to date have been made only on JPN double-base propellant.)

No hypothesis is advanced at present regarding the mechanism of the singular behavior observed in these tests, but it seems clear that a coupling of longitudinal and tangential modes of gas oscillation is involved.

From a theoretical standpoint it is curious that any singular phenomenon should be related to a coupling of these modes, since they are orthogonal and theoretically cannot exchange energy. However, at large amplitude this is not true, since nonlinearities and viscosity come into play in a way not envisaged in the acoustic theory. Furthermore, the different modes are both being driven by the same finite energy source (i.e., the combustion front at the walls), and coupling must necessarily occur there. Under these conditions, the gas motion undoubtedly deviates materially from the acoustic model, and explanation of the behavior may not be possible in terms of the acoustic theory alone.

A crucial question arising from these observations of "catastrophic" changes in burning rate is whether the burning rate is increased as a result of an increase in amplitude of pressure oscillations of one or both of the "guilty" modes at the time their frequencies approach harmonic relationship, or whether the burning rate is merely more responsive to the conditions existing during the harmonic relationship. This question could not be resolved with the instrumentation used on the tests to date. It does seem clear that the singular increases in burning rate are not due to the occurrence of oscillatory behavior in any particular single acoustic mode or frequency, since the phenomenon has been observed to occur over an appreciable range of frequencies, does not occur at these frequencies until the tangential and longitudinal modes occur *together*, and then only if their frequencies approach a harmonic relationship.

At this point it cannot be determined to what extent the singular behavior described is related to rocket motor behavior, although there is no obvious reason why the same behavior should not occur in conventional rocket designs and sizes. The pressure-time curves (e.g., Fig. 1b) bear a striking resemblance to those familiar from rocket motor testing [e.g., (4)].

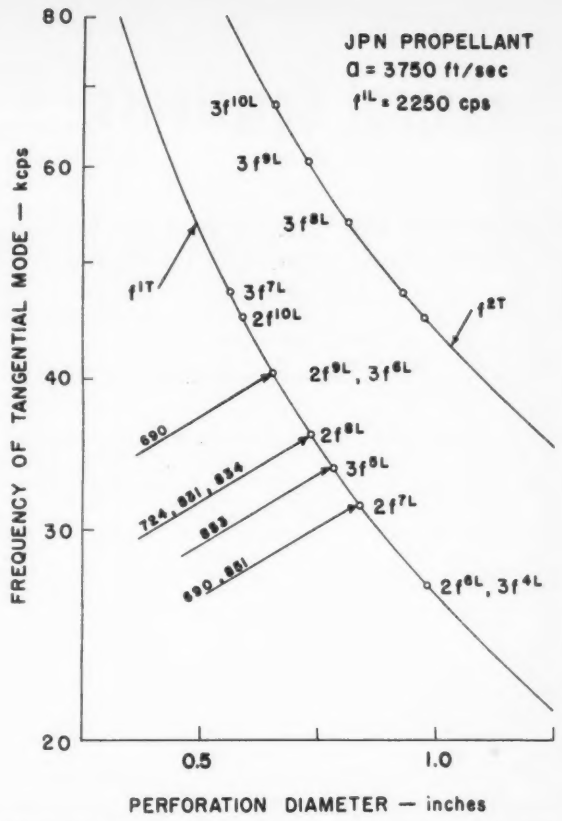

Fig. 4 Variation of frequency of modes during burning for JPN double-base propellant, ½-in. ID × 1-in. OD × 10-in. length internal burning charge

References

1 Price, E. W. and Sofferis, J. W., "Combustion Instability in Solid Propellant Rocket Motors," JET PROPULSION, vol. 28, no. 3, March 1958, pp. 190–193.

2 Price, E. W., "Experimental Research in Combustion Instability of Solid Propellants," presented at the meeting of the Western States Section of the Combustion Institute, March 24, 1959, San Diego, Calif.

3 Price, E. W., "Combustion Instability in Solid Propellant Rocket Motors," U. S. Naval Ordnance Test Station, China Lake, Calif., NavOrd 7023 (NOTS 2389), Dec. 21, 1959.

4 Green, L., Jr., "Observations on the Irregular Reaction of Solid Propellant Charges," JET PROPULSION, vol. 26, no. 8, Aug. 1956, p. 657.

Technical Comments

Corrections for "Interplanetary Trajectories Under Low Thrust Radial Acceleration"

GUENTHER AU[1]

University of Heidelberg, Heidelberg, Germany

IN COPELAND'S article in the April issue of this Journal (1),[2] several errors have been discovered in the computation of the transfer to Venus ($\alpha = -\frac{3}{5}$). Other corrections have already been noted by Karrenberg (2).

On page 269 of (1), we get from the transformation

$$r = (a \sin^2 \theta + b)/(c \sin^2 \theta + d)$$

$\theta = \pi/2$ for $r = 1$, and $\theta = 0$ for r = $\frac{3}{4}$. The interval for integration is [after Groebner and Hofreiter (3)]

$$r_1 \geq r \geq r_2$$

or

$$0 \leq \theta \leq \pi/2$$

Equations [17 and 18] are therefore

$$\phi(r) = 8\left[\frac{1}{16} F\left(\theta, \frac{1}{4}\right) - \left(\frac{5}{16}\right)\Pi\left(\theta, \frac{1}{4}, \frac{1}{4}\right)\right]$$

$$\tau(r) = \frac{3}{2}\left[3F\left(\theta, \frac{1}{4}\right) - 4E\left(\theta, \frac{1}{4}\right) - \frac{\sin 2\theta}{8\sqrt{1 - (1/16)\sin^2\theta}}\right]$$

The trajectory ϕ (r), shown in Fig. 1 of (1) therefore should be different, and the transfer time to Venus much longer, about 3 months.

Received March 11, 1960.

[1] Candidate, Physics; also Chairman, Nordbaden Pfalz-Saar Section, German Society for Rocketry and Space Travel. Member ARS.

[2] Numbers in parentheses indicate References at end of paper.

References

1 Copeland, J., "Interplanetary Trajectories Under Low Thrust Radial Acceleration," ARS JOURNAL, vol. 29, no. 4, April 1959, pp. 267–271.

2 Karrenberg, H. K., "Note on 'Interplanetary Trajectories Under Low Thrust Radial Acceleration'," ARS JOURNAL, vol. 30, no. 1, Jan. 1960, pp. 130–131.

3 Groebner and Hofreiter, Integraltafel 1. Teil, Springer-Verlag, Wien und Innsbruck, 1949.

Hypersonic Axisymmetric Nozzles

ROBERT J. CRESCI[1]

Polytechnic Institute of Brooklyn, Freeport, N. Y.

In view of a recent publication of (1)[2] which presents an evaluation of the various design parameters involved in the utilization of axisymmetric nozzles, it may be of interest to call attention to another (2). Presented in (2) is a series of hypersonic axisymmetric nozzle coordinates obtained by applying the method of characteristics to transform a spherical source flow into a uniform, parallel flow. The design Mach number was varied between 6 and 20, and the half-cone angles were taken in 2-deg increments between 6 and 20 deg. All the contours presented correspond to a constant value of the ratio of specific heats (γ) equal to $\frac{7}{5}$. Additional coordinates are being computed using a value of $\gamma = \frac{5}{3}$.

The method of analysis consists of assuming a source flow downstream of the sonic line and expanding the flow to a Mach number slightly below the design value. At this point, the characteristic line is determined from the equations for a supersonic compressible source; this forms one boundary of the transition region, in which the flow is obtained by the method of characteristics. The boundary along the centerline is prescribed in order to insure a smooth transition between the source flow and the uniform flow. This is particularly important if the nozzle is to be used in a hypersonic wind tunnel where a constant Mach number distribution is required in the test section. At the beginning of the transition region the velocity and acceleration are equal to the values at the end of the source flow. At the termination of the transition region the Mach number is specified and the acceleration and first derivative of the acceleration are set equal to zero. The flow conditions in the transition region are then readily computed by the method of characteristics, since the boundaries are completely determined. Both the flow field and the nozzle streamlines were computed by the Digital Computation Branch of the Aeronautical Research Laboratory at Wright Air Development Division.

Several hypersonic wind tunnels have been constructed utilizing the coordinates of (2). A Mach 8 tunnel with a 50-in. test section diameter is presently in use at AEDC (3). A 24-in. diameter Mach 8 tunnel has also been in operation at the Polytechnic Institute of Brooklyn since early 1959, and at present, a Mach 12 tunnel is nearing completion (4). Both of these installations report a "nearly uniform flow over a large region with negligible gradients in Mach number."

It is of interest to note that an analysis essentially the same as that of (2) has been performed independently by Yu (5). In this report, coordinates are presented for a range of Mach numbers between 5 and 20 and for maximum wall deflection angles of 6 and 10 deg. Three values of γ were used in the computations: $\frac{6}{5}$, $\frac{7}{5}$ and $\frac{5}{3}$.

Received April 20, 1960.

[1] Research Associate, Department of Aeronautical Engineering and Applied Mechanics.

[2] Numbers in parentheses indicate References at end of paper.

References

1 Landsbaum, E. M., "Contour Nozzles," ARS JOURNAL, vol. 30, no. 3, March 1960, pp. 244–250.

2 Cresci, R. J., "Tabulation of Coordinates for Hypersonic Axisymmetric Nozzles," WADC TN 58-300, AD 204 213, Oct. 1958, Polytechnic Institute of Brooklyn Rep. no. 463.

3 Sivells, J., "Operational Experience with a 50 Inch Diameter Mach 8 Tunnel," presented at joint meeting of STA-AGARD Wind Tunnel and Model Testing Panel, Marseille, France, Sept. 1959.

4 Zakkay, V., "Status Report of the Hypersonic Facility of the Polytechnic Institute of Brooklyn," presented at the 13th Semi-Annual Supersonic Tunnel Association Meeting, Dallas, April 1960.

5 Yu, Y.-N., "A Summary of Design Techniques for Axisymmetric Hypersonic Wind Tunnels," AGARDograph 35, Nov. 1958.

New Patents

George F. McLaughlin, *Contributor*

Folding stabilizing fins (2,923,241). W. C. House, Claremont, Calif., assignor to Aerojet-General Corp.

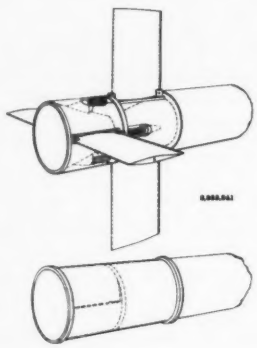

Fin assembly made of sheets of thin, tough, resilient material bonded at forward and rear edges. Sheets flatten to enable them to be wrapped around the missile.

Jet deflecting apparatus (2,916,873). N. K. Walker, Kensington, Md., assignor to Advanced Research Associates, Inc.

Vaporized liquid injected at low velocity into the nozzle downstream from the throat and side walls, forming a jet of high temperature gas. The liquid causes jet breakaway from the walls, deflecting the jet.

Rocket launcher (2,916,969). N. W. Pion, Covena, Calif., assignor to North American Aviation, Inc.

Jettisonable pad composed of parallel plastic disks extending from demountable means for attachment to an airframe. Holes in disks retain rockets in firing position.

Propellant powder (2,916,996). R. E. Coffee, Berkeley, Mo., assignor to Olin Mathieson Chemical Corp.

Progressively burning smokeless powder grain. Powder base containing solid high explosive in the core is enclosed by a smooth envelope having no high explosive particles. A coating of deterrent is applied to the envelope.

Operation of solid propellant rockets (2,917,894). H. M. Fox (ARS member), Bartlesville, Okla., assignor to Phillips Petroleum Co.

Means for igniting propellant charges in a main combustion chamber, and a communicating auxiliary chamber within the main chamber.

Jet propelled propeller or rotor blade (2,917,895). Brig. Gen. H. A. Boushey (ARS member), Washington, D. C.

Rotary blade with a propulsion unit at its outer end. The axes of the compressor and turbine are perpendicular to the plane of blade rotation.

Electrically heated jet propulsion unit (2,918,004). A. E. C. Denovan, D. J. Hodgson and H. Kremer, Highgate, London, England.

Casing of nonconductive plastic in which an electrical conductor is imbedded to preheat the contained explosive material to an efficient temperature, irrespective of the ambient temperature.

Sheet propellant (2,918,005). G. Schecter and W. J. Kroeger (ARS member), Philadelphia, Pa., assignors to the U. S. Army.

Lightweight charge comprising layers of sheet propellant mounted on a tubular support filled with an explosive for ignition of the charge. Ignition proceeds radially outward from the support.

Destruction engines carrying a hollow charge (2,918,006). H. P. von Zborowski, Paris, France.

Flying missile consisting of an annular wing forming a tunnel-shaped passage. A mass of explosive is housed in the wing outside the passage. Movable means extends in front of the wing for engagement with a target to detonate the explosive upon contact.

Heat resisting wall structure (2,919,549). L. Haworth and R. J. Shire, Belper, England, assignors to Rolls-Royce, Ltd.

Gas turbine engine combustion equipment comprising an outer air casing structure containing a flame tube made up of H-section strips. Pressure cooling air is fed to the spaces between the walls of the tube.

Combustion chamber screech eliminator (2,919,550). W. E. Kaskan and A. E. Noreen (ARS member), Cincinnati, Ohio.

Flameholder having a trailing edge mounted in the flow path of combustible fluid, the edge forming screech-causing vortices. An annular member of long and narrow cross section offering minimum resistance to flow, has its longitudinal axis parallel to the fluid flow direction, eliminating screech.

Flameholder (2,920,445). F. W. Bailey, Wayne Township, N. J., assignor to Curtiss-Wright Corp.

Deflector within an auxiliary chamber and forming a fire zone. A fuel supply line extends through the zone, and fuel is ignited in the chamber.

Shock positioning means (2,920,446). E. D. Renard, W. Hartford, Conn., assignor to United Aircraft Corp.

Supersonic inlet for a power plant. Means for sensing whether the shock is upstream or downstream, and for controlling the flow by bleeding air from inside to outside the inlet.

Helicopter with body attaching means (2,920,841). A. Junker, Vesenaz-Geneva, Switzerland.

Chassis having the form of an open-ended cylinder surrounded by a fuel tank with driving blades mounted radially on opposite sides, and driven by jet engines at blade tips. The chassis is fastened around the waist of a pilot.

Patents have been issued to A. M. Lippisch, Cedar Rapids, Iowa, for five different wingless aircraft, assigned to Collins Radio Co. These patents are: **Ducted aircraft with fore elevators (2,918,229); Fluid sustained and fluid-propelled aircraft (2,918,230 and 2,918,231); Twin-shroud aerodyne (2,918,232);** and **Aerodyne with external flow (2,918,233).**

Differential area piston pumping system (2,918,791). L. Greiner, Richmond, Va., assignor to Experiment, Inc.

Movable partition between the primary propellant agent chamber and the pressure generating chamber. Pressure in the generating chamber moves the partition to effect injection of propellant into the combustion chamber.

Balloon having reinforced structure (2,919,082). O. C. Winzen (ARS member) and V. H. Winzen, Mendota Township, Minn., assignors to Winzen Research, Inc.

Elongated reinforcing tapes secured to the envelope for part of their extension, and unsecured at their other ends. An excess of envelope material is supplied between unsecured portions when the envelope is inflated.

Balloon and method of launching (2,919,083). V. E. Suomi and O. C. Winzen (ARS member), Mendota Township, Minn., assignors to Winzen Research, Inc.

Balloon train comprising a launch balloon and a main balloon connected by a restricted gas conducting member. Means for inflating the launch balloon apart from the main balloon.

Differential transformer accelerometer (2,923,904). G. M. Hieber, Berkeley Heights, N. J., assignor to Gulton Industries, Inc.

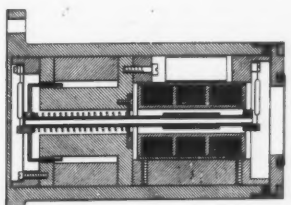

Instrument for recording changes in velocity of guided missiles. Measures vibration, shock, acceleration and changes in direction. Radios data on stresses encountered on its return trip, aiding the study of re-entry conditions.

Aircraft design (186,963). N. Price, Westwood, Calif.

Wingless body with conical nose air intake. The propulsive exhaust and control surfaces are located at the rear of the body.

Method of propelling rockets (2,919,541). Dr. J. E. Mahan (ARS member), Bartles-

---

EDITOR'S NOTE: Patents listed above were selected from the Official Gazette of the U. S. Patent Office. Printed copies of patents may be obtained from the Commissioner of Patents, Washington 25, D. C., at a cost of 25 cents each; design patents, 10 cents.

ville, Okla., assignor to Phillips Petroleum Co.

An oxidant and fuel for simultaneous injection into the combustion chamber. Fuel consists of 90 to 10 per cent of mercaptan, and 10 to 90 per cent of hydrocarbon polyamine containing not more than 30 carbon atoms.

Pulse-jet units or thermo-propulsive pulsatory discharge nozzles (2,919,542). P. Servanty, P. Le Rouzo, G. Bouchet, J. Legrand and A. Bozec, Paris, France, assignors to SNECMA Co.

Exhaust pipe and a reversed air admission device, the ends of which face toward the rear of the unit. A cowling surrounds part of the unit, and allows direct suction of ambient air.

Fluid flow control (2,919,543). A. Sherman, De L. Ferris and S. Lehrer (ARS members), Pompton Lakes, N. J., assignors to the U. S. Air Force.

Control of liquid from two pressurized containers, each having a valve piston for movement between closed and open positions. Means for biasing the valves by means of fluid conducted through a conduit between a control piston and the two valve pistons.

Thrust reverser nozzle (2,919,545). D. B. Tschudy, Canton, Ohio, assignor to Goodyear Aircraft Corp.

Nacelle surrounding the exhaust nozzle, and providing a passage for flow of cooling air between. A pivoted door forms part of the nozzle wall. Movement of the door deflects the exhaust gas and cooling air.

Servo-powered jet deflecting nozzle (2,919,546). C. V. David, San Diego, Calif., assignor to Ryan Aeronautical Co.

Servo vanes mounted so as to be moved to selected positions relative to the direction of flow of the jet stream. The stream biases the vanes and causes a movable nozzle to shift according to the controlled shifting of the vanes.

Igniter (2,920,450). C. E. Seglum, Wallingford, Pa., assignor to the U. S. Navy.

Device for combustion of reactants. The air-fuel mixture is vaporized in a U-shaped preheater tube where it is ignited and produces a flame directed into the combustion chamber.

Aircraft configuration (2,920,842). J. L. Decker and C. J. Koch (ARS member), Baltimore, Md., assignors to The Martin Co.

Reaction motor propelled aircraft capable of supersonic speeds and having good low-speed stability and control characteristics. Wings have 50 to 70 deg sweepback.

Turbojet boost augmenter (2,920,843). A. Ferri (ARS member), Rockville Centre, N. Y., assignor to Curtiss-Wright Corp.

Two-spool gas turbine with a thrust augmenter having a third-stage turbine driven by gases from the second stage. A portion of the gases exhaust directly into the surrounding atmosphere.

Universal world time and star map (2,921,386). A. J. Stafano, San Diego, Calif.

Base plate with a semi-circular mask having a time ring area, a large star disk, and a small world map. The upper portion of the base defines the momentary night areas of the star disk which has radial lines to align them with the time ring.

Afterburner control (2,921,433). B. N. Torell, Wethersfield, Conn., assignor to United Aircraft Corp.

Two-spool gas turbine power plant with one spool ungoverned. Means for varying the area of the exhaust nozzle as a function of the speed of the ungoverned spool.

Variable thrust gas turbine engine (2,921,434). P. R. Spadaro (ARS member) and P. C. Holden, Mission, Kans., assignors to the USAF.

Bipass duct divided into separate portions. Flameholders adjacent the duct outlet to stabilize the ignited mixture flowing from the outlet. Means for varying the distance between flameholders and the duct, to vary the thrust.

Directional control for aircraft (2,921,435). F. Landgraf, San Diego, Calif., assignor to Ryan Aeronautical Co.

Tiltable baffle universally pivoted on a deflector cone at the longitudinal axis of a gas generator exhaust nozzle. Actuating means connected to tilt the baffle.

Moisture separator (2,921,646). D. M. Poole, Huntington, N. Y., assignor to Fairchild Engine and Airplane Co.

Filter at the inlet of a housing for moving gaseous fluid to form droplets of moisture. Droplets are moved by centrifugal force into an accumulating chamber.

Production of low temperature liquids (2,922,285). R. S. Rae, Santa Monica, Calif., assignor to The Garrett Corp.

Method of simultaneously producing liquid hydrogen and liquid oxygen.

Production of liquid oxygen (2,922,286). R. S. Rae, Santa Monica, Calif., assignor to The Garrett Corp.

Device for producing liquid oxygen from atmosphere for use as an oxident for an engine.

Book Reviews

Ali Bulent Cambel, Northwestern University, *Associate Editor*

Foundations of Aerodynamics, by A. M. Kuethe and J. D. Schetzer, second edition, John Wiley and Sons, Inc., New York; Chapman and Hall, Ltd., London, 1959, 446 + xiv pp. $9.75

Reviewed by Arthur A. Kovitz
Northwestern University

The appearance of a second edition of any textbook is a measure of the success of the first edition and indicative of changes in the needs of students using the book. It could also mean that the students' needs were not met by the first edition, but in view of the first edition's longevity (1950 publication date), this would seem to be an erroneous conclusion. Both the student and the teacher (this reviewer used the book in both capacities) have found the first edition extremely useful. However, we could ask if the second is of such a nature that those possessing a first edition should immediately trade it in for the second? Furthermore, should those seeking to obtain their first copy of "Kuethe and Schetzer" buy the first edition at a possible bargain price, or should they demand the second edition even at list price? I hope that the following few paragraphs will contribute toward answering these questions.

The general layout and organization of the first and second editions are quite similar. Inviscid flow is covered in the first eleven chapters of both, whereas viscous flow is given the last seven chapters in the first and the last five chapters in the second edition. The first edition contains two appendixes, one on dimensional analysis and another on the derivation of the Navier-Stokes and energy equations. The second edition also contains these two appendixes plus an appendix on real fluid effects in high speed flight and one on the aerodynamic characteristics of wings (which used to be the last chapter of the first edition). All tables and charts are grouped at the end of the book in the second edition. There is an excellent oblique shock chart included with the newest edition. Both the first and second editions do not contain anything on conformal mapping applied to two-dimensional incompressible flow.

If one were to look for topics covered in the second edition, but *not* the first, one would list: (a) One-dimensional flow with heat addition, (b) wings in compressible flow, and (c) boundary layers in compressible flow. These topics were merely mentioned in the first edition, but are now given serious treatment.

Even though the list of new topics is not impressive, several chapters and sections have been rewritten to advantage. These include the chapters on energy relations, one-dimensional compressible flow and incompressible wing theory. Sections on three-dimensional boundary layers, the turbulent boundary layer equations and turbulent boundary layer analyses, to mention only a few, have been greatly expanded. The authors should be congratulated for injecting a more leisurely and expansive feeling into their second effort in contrast to what this reviewer perceives to be a recent trend toward the all too comprehensive and "concise" products of textbook writers.

If one returns now to the questions posed earlier, they might be answered as follows:

Those owning a copy of the first edition should not hasten to buy the second. The

amount of new material is not overwhelming. What new material there is could be found in other books of a more specialized nature germane to the particular subject of interest to the reader. Those familiar with the contents of the first edition should be well equipped to pursue their interests in other, perhaps more advanced, sources.

On the other hand, those readers who do not own the first edition would be foolish to play the "smart shopper." This reviewer would urge them to get the second edition by all means. All the virtues of the first are retained, and several important topics have been added and the quality of exposition of the remaining subjects improved.

This reviewer has used the first edition in an introductory aerodynamics course and would not hesitate to use the second edition in the same or a slightly more advanced course.

Engineering Education in Russia, by Stephen P. Timoshenko, McGraw-Hill Book Co., Inc., New York, 1959, 47 pp. $2.75.

Reviewed by F. C. LINDVALL
California Institute of Technology

Engineering Education in the Soviet Union has been reported in considerable detail in publications by Korol, DeWitt and the ASEE Exchange mission. Much of the same factual information is given by Professor Timoshenko, but it assumes new significance in the historical and personal framework in which he is able to present it.

Professor Timoshenko sketches with some pride the engineering advances made by Russia in the days before the Revolution and describes the system of engineering education within which he studied and taught. Now, 40 years later, he revisits the old schools with which he was familiar, some new ones and Institutes of the Academy of Sciences. He describes the present patterns of engineering education and research, noting great similarity between present curricula and pre-Revolution study plans. The author recounts the unsuccessful Communist "reforms" of the early twenties as they affected engineering school admission and administration, and the gradual transition to the present admission by ability, and restoration of a substantial degree of autonomy in the administration of the internal affairs of the better schools.

Professor Timoshenko directs attention to a significant difference in present engineering education in the USSR and that of old Russia. The Soviet Union, through a series of "five year plans," has established technical educational requirements in all segments of the economy. As a result, many schools have come into being, some under various ministries other than the Ministry of Higher Education, to train engineering specialists of many types. The output of these schools can be matched to the planned needs in each specialty. Nevertheless a few of the better schools are on the older polytechnic scheme, in which the specialties or options are of broad coverage similar to those of pre-Revolutionary times.

Typical study programs are presented in the book, as well as an outline of typical preparation in the 10-year school plan, upon which admission to an engineering school is based. Research in engineering and graduate work is also discussed. However, in this small volume completeness of coverage of a complex program of education is not to be expected. Rather, the virtue of the book lies in the personal reactions of the author to things as they are now and as they were 40 years ago. The section on the Kiev Polytechnicum is particularly interesting as Professor Timoshenko takes us through familiar halls and into familiar lecture rooms. Throughout the book the author runs an instructive and interesting historical thread. The various illustrations, some quite personal, add much charm to this significant contribution to our knowledge of Soviet engineering education.

Turbulence—An Introduction to Its Mechanism and Theory, by J. O. Hinze, McGraw-Hill Book Co., Inc., New York, 1959, ix + 586 pp. $15.

Reviewed by W. H. REID
Brown University

The turbulent motion of fluids, though a common enough phenomenon, presents us with something of an enigma, for even after 75 years—if reckoned from the time of Reynolds—it still presents a challenging problem to the mathematician, physicist and engineer. This is not to say that there have not been important advances made in our understanding of the subject, particularly during the past few decades, but simply that the problem of turbulence has not been "solved." Nor would it appear that a full understanding of the problem can be expected in the near future.

It is important therefore that the existing results obtained by so very many workers, and still largely hidden in the specialist literature, should be brought together and made more readily accessible. This is the task that Professor Hinze has undertaken in the present book. It is a difficult task, and the author deserves our thanks for having carried it through so successfully.

In the first chapter we are introduced to the various statistical quantities, such as correlation functions and spectra, which provide the necessary tools for all of the later discussions. The following chapter on experimental techniques is largely devoted to the use of the hot-wire anemometer, for it is to this instrument more than to any other that we owe our present knowledge of the detailed structure of turbulent flows. The special case of isotropic turbulence—the one aspect of the subject for which there has been some theoretical success—is then described in some detail. This includes not only an account of the Kolmogoroff theory, the physical transfer theories of the Heisenberg type, and the so-called normal distribution theory, but also, where possible, a comparison with the relevant experimental data. The discussion of nonisotropic turbulence which then follows in Chapter 4, though not restricted to homogeneous turbulence, is necessarily shorter and less complete.

The final three chapters deal with transport processes, nonisotropic free turbulence and nonisotropic wall turbulence. Recent work in these fields has achieved considerable success through precise experimental work from which, guided by sound physical insight, a number of important ideas have emerged concerning the detailed structure of the turbulence under various flow conditions. Many of these results—too many to mention here—are presented in considerable detail.

This is the first to attempt so comprehensive an account of the subject. That it succeeds so well is perhaps chiefly due to its emphasis on the mutual dependence of experimental results and theoretical ideas.

Recent Research in Molecular Beams, A Collection of Papers Dedicated to Otto Stern on the Occasion of His Seventieth Birthday, edited by Immanual Estermann, Academic Press, Inc., New York, 1959, 190 pp.

Reviewed by A. E. FUHS
Space Technology Laboratories, Inc.

Every student of physics learns of the Stern-Gerlach experiment. In addition to this classic experiment, Otto Stern and his students and colleagues conducted a series of experiments to determine directly the distribution of velocities, to measure magnetic moments, to measure electric moments, to verify the existence of de-Broglie waves and other similar experiments suitable for molecular beams. During February 1958, Otto Stern celebrated his seventieth birthday. This volume is a collection of papers expressing the appreciation of the authors for the inspiration found in his work.

There are 10 papers, some of which are survey papers, others deal with a specific aspect of molecular beam research. The first paper, "Molecular Beam Research in Hamburg, 1922–1933," by I. Estermann, reviews the 30 papers which were published by Stern's group.

At the Institute for Basic Research in Science, University of California, Berkeley, molecular beam methods have been used to determine the spins and moments of radioactive nuclei having short half lives. The results of these investigations are summarized in W. A. Nierenberg's paper, "Molecular and Atomic Beams at Berkeley."

Of interest to the engineering scientist working in the field of astronautics is the experimental work reported by Marcus and McFee, "Velocity Distributions in Potassium Molecular Beams." Refined experimental techniques permit measurement of velocity with an uncertainty of less than 1 per cent. Experimental data are presented for a wide range of oven pressures. In the appendix, corrections are derived for finite angular spread of beam, higher order spectra and similar experimental factors.

Vernon Hughes's paper, "Electron Magnetic Moment and Atomic Magnetism," is a survey outlining the reasons for interest in the electron magnetic moment. Results of quantum electrodynamical

theory for the value of electron magnetic moment are given. Equations appropriate for describing atomic magnetism of polyelectronic atoms are discussed. The third section briefly outlines experimental procedure for several measurements of magnetism of free electrons, hydrogen and other atoms. The experimental results agree well with theory of relativistic corrections and virtual radiative processes which tends to confirm the theory.

Two unusual atomic beam experiments are described in "Hyperfine Structure Measurements in the Metastable 2S State of Hydrogenic Atoms" by P. Kusch. Background information is given in the first section of the paper, followed by a description of the atomic hydrogen and the ionized helium three experiment.

In "Shapes of Molecular Beam Resonances," by N. F. Ramsey procedures are described for rapid calculation of molecular beam resonances using a digital computer. Irregularities causing a deviation of the center of the resonance from the Bohr frequency are enumerated.

In "Comparison of Methods for the Determination of Nuclear Spin as Applied to Radioactive Nuclei" V. W. Cohen discusses the techniques using optical or microwave spectroscopy, nuclear or paramagnetic resonance or atomic beams. The advantages and disadvantages of each method are clearly given. Results obtained by each method are tabulated, including measurements reported as recently as October 1958. Special problems peculiar to radioactive nuclei and separation of isotopes to obtain a test sample are discussed.

Of particular interest to the astronautical engineer is F. C. Hurlbut's paper, "Molecular Scattering at the Solid Surface." To calculate the forces on a body in a rarefied gas flow it is necessary to know the details of the interaction at the surface. The experimental apparatus used to determine the energy and momentum interchange when a molecular beam is directed at a surface is described. The results of the measurements and the relation of the results to drag are discussed.

In "Some Applications of Molecular Beam Techniques to Chemistry" by S. Datz and E. H. Taylor, molecular collisions are studied extensively. This paper is an outstanding critical survey; 118 references are considered. The discussion of ionization at a surface is of interest to propulsion engineers, and the approach to kinetics is of interest for combustion.

The final chapter is an article by J. E. Sherwood, T. E. Stephenson and S. Bernstein titled "A Stern-Gerlach Experiment on Polarized Neutrons." A magnetized iron mirror was used to polarize the neutron beam which was analyzed in slot-wedge type deflecting field. Results and analysis were in agreement.

An excellent selection of papers, such as are assembled in this book, permit the reader to obtain a feeling for the ranges and limitations of molecular beam techniques.

Technical Literature Digest

M. H. Smith, *Associate Editor*
The James Forrestal Research Center, Princeton University

Propulsion and Power (Combustion System)

The Effect of Rapid Liquid-phase Reaction on Injector Design and Combustion in Rocket Motors, by Gerard W. Elverum Jr. and Peter Staudhammer, *Calif. Inst. Tech., Jet Prop. Lab., Progr. Rep.* 30–4, Aug. 1959, 42 pp.

The Application of Solid Propellant Rocket Motors to Boost Space Vehicles, by Giulio Panelli, *Inst. Aeron. Sci., Paper* 60–53, Jan. 1960, 6 pp.

Considerations in the Design of Chemical Rocket Powerplants for Space Applications, by Stanley Lehrer, *Inst. Aeron. Sci., Paper* 60–24, Jan. 1960, 32 pp.

The Marquardt Research Field Laboratory—Small Scale Facility Development for Hypersonic Ramjet Research, by J. W. Braithwaite, *The Marquardt Corp.*, Van Nuys, Calif., *Rep.* MR 20,042, June 1959, 7 pp.

Energy Requirements of Rockets, by G. Leitmann and G. Zebel, *Raketentechnik und Raumfahrtforschung*, vol. 3, no. 4, Oct.–Dec. 1959, pp. 116–117. (In German.)

Rocket Nozzles and Exhaust Jets, by E. T. B. Smith, *Spaceflight*, vol. 2, no. 5, Jan. 1960, pp. 151–154.

On Rao's Method for the Computation of Exhaust Nozzles, by G. Guderly, *Zeitschrift für Flugwissenschaften*, vol. 7, no. 12, Dec. 1959, pp. 345–350.

EDITOR'S NOTE: Contributions from Professors E. R. G. Eckert, J. P. Hartnett, T. F. Irvine Jr. and P. J. Schneider of the Heat Transfer Laboratory, University of Minnesota, are gratefully acknowledged.

Replaceable Solid Propellant Cartridges for Emergency Power in Space, by Norman J. Bowman, *J. Brit. Interplanet. Soc.*, vol. 17, Nov.-Dec. 1959, pp. 169–172.

Dual Burning Propulsion Systems for Satellite Stages, by B. P. Martin, *J. Astronaut. Sci.*, vol. 7, no. 1, 1960, pp. 21–22.

Free-jet Investigation of 20-inch Ramjet Combustor Utilizing High-heat-release Pilot Burner, by James G. Henzel Jr. and Carl B. Wentworth, *NACA Res. Mem.* E53H14, Oct. 1953, 35 pp.

Altitude Investigation of 20-inch-diameter Ram-jet Engine with Annular-piloted Combustor, by James G. Henzel Jr. and Arthur M. Trout, *NACA Res. Mem.* E54G12, Aug. 1954, 26 pp.

Preliminary Report of Experimental Investigation of Ram-jet Controls and Engine Dynamics, by G. Vasu, F. A. Wilcox and S. C. Himmel, *NACA Res. Mem.* E54H10, Oct. 1954, 70 pp.

Performance of Five Low-temperature-ratio Ram-jet Combustors Over Range of Simulated Altitudes, by Carl B. Wentworth, *NACA Res. Mem.* E54H13, Nov. 1954, 29 pp.

The Axial-flow Compressor in the Free-molecule Range, by Charles H. Kruger, *Mass. Inst. Tech., Dept. Mech. Engng.* DSR 7-8120, Jan. 1960, 90 pp.

Experimental Investigation of a Flat-plate Paddle Jet Vane Operating on a Rocket Jet, by Aleck C. Bond, *NACA Res. Mem.* L50I20, Nov. 1950, 47 pp.

Theory of Liquid Propellant Rocket Combustion Instability and Its Experimental Verification, by Luigi Crocco, Jerry Grey and David T. Harrje, ARS JOURNAL, vol. 30, no. 2, Feb. 1960, pp. 159–168.

Propulsion and Power (Non-Combustion)

Analysis of One-dimensional Ion Rocket with Grid Neutralization, by Harold Mirels and Burt M. Rosenbaum, *NASA TN* D-266, March 1960, 43 pp.

Magnetohydrodynamic Energy Conversion Techniques, by Richard J. Rosa and Arthur R. Kantrowitz, *Avco-Everett Res. Lab., Res. Rep.* 86, April 1959, 18 pp.

Optimum Power Generation from a Moving Plasma, by Joseph L. Neuringer, *J. Fluid Mech.*, vol. 7, Feb. 1960, pp. 287–301.

Electric Energy Sources and Conversion Techniques for Space Vehicles, by Volney C. Wilson, *Inst. Aeron. Sci., Paper* 60–31, Jan. 1960, 11 pp.

Research on High Intensity Ionic Jets, by Gordon L. Cann and Adriano C. Ducati, *Plasmadyne Corp., Santa Ana, Calif., AFOSR TN* 59-167, Nov. 1959, 36 pp.

Pebble Bed Nuclear Reactors for Space Vehicle Propulsion, by M. M. Levoy and J. J. Newgard, *Inst. Aeron. Sci., Paper* 60–39, Jan. 1960, 12 pp.

Plasma Propulsion by a Rapidly Varying Magnetic Field, by M. M. Klein and K. A. Brueckner, *Gen. Electric Co., Missile & Space Vehicle Dept.*, TIS R59SD453, Dec. 1959, 36 pp.

A Novel System for Space Flight Using a Propulsive Fluid Accumulator, by Sterge T. Demetriades, *J. Brit. Interplanet. Soc.*,

vol. 17, Sept.-Oct. 1959, pp. 114–119.

Directing of Intense Photon Beams by Means of an Electron Gas Mirror, by E. Sänger, *Astron. Acta*, vol. 5, no. 5, 1959, pp. 566–586. (In German.)

An Experimental Magnetohydrodynamic Power Generator, by Richard J. Rosa, *Avco-Everett Rep.* AMP 42, Jan. 1960, 7 pp.

Electrical Space Propulsion, by R. H. Boden, *Inst. Aeron. Sci., Paper* 60–55, Jan. 1960, 62 pp.

Propulsion Requirements of a Manned Lunar Mission, by D. E. Serrill and H. J. McClellan, *Inst. Aeron. Sci., Paper* 60–30, Jan. 1960, 12 pp.

Rapid Approximate Method for Analyzing Nuclear Rocket Performance, by Alan H. Stenning, ARS JOURNAL, vol. 30, no. 2, Feb. 1960, pp. 169–172.

Fuel Cells for Space Vehicles, by M. G. Del Duca, J. M. Fuscoe and T. A. Johnston, ASTRONAUTICS, vol. 5, March 1960, p. 36.

The Value of Transport Mean Free Path for D_2O, by D. W. Hone, *J. Nuclear Energy: Part A*, vol. 11, Nov. 1959, pp. 34–38.

On the Mechanism of the Pinch Effect, by T. Goto, M. Sato and T. Uchida, *Nuovo Cimento*, vol. 14, no. 5, Dec. 1959, pp. 1065–1075.

Characteristics of a Light Element Applied as Working Gas in an Unconventional Heated Rocket, by I. Sänger-Bredt, *Raketentechnik und Raumfahrtforschung*, vol. 4, no. 1, Jan.–March 1960, pp. 7–16. (In German.)

Experiment to Obtain Reaction Thrust in a Laboratory Model of an Ion Engine, by Yu. Ya. Stavisskii, I. I. Bondarenko, V. I. Krotov, S. Ya. Lebedev, V. Ya. Pupko and E. A. Stumbur, *Soviet Phys., Tech. Phys.* (*trans. of Zhurnal Tekhicheskoi Fiziki*), vol. 4, Feb. 1960, pp. 875–878.

Propellants and Combustion

High Performance Solid Rocket Propellants: Thermodynamic Data for Combustion Products, by John S. Gordon, *Thiokol Chem. Corp., Reaction Motors Div.*, Denville, N. J., *Rep.* RM 210–E3, Jan. 1960, 171 pp.

The Effect of Sound Oscillations on Combustion and Heat Transfer, by Walter W. Wharton, J. W. Connaughton, B. D. Allan and W. D. Williams, *Army Rocket & Guided Missile Agency, Ordn. Missile Labs., Div. ARGMA TR* 1c36R, Dec. 1959, 35 pp.

Cryogenic Propellant Storage for Round Trips to Mars and Venus, by G. R. Smolak and R. H. Knoll, *Inst. Aeron. Sci., Paper* 60–23, Jan. 1960, 30 pp.

Rapid Determination of Acetone in Penetaerythritol Trinitrate by Gas Chromatography, by Everett M. Bens and Donald H. Stewart, *Naval Ordn. Test Station, NavOrd Rep.* 7014, Nov. 1959, 15 pp.

Volumetric Determination of Hydroxyl in Polypropylene Glycols, by Eugene A. Burns and Ralph F. Muraca, *Calif. Inst. Tech., Jet Prop. Lab., Progr. Rep.* 30–11, May 1959, 16 pp.

Diisocyanate Linked Polymers, I: Dilute-solution Properties of Toluene Diisocyanate Extended Polypropylene Glycol, by J. Moacanin, *Calif. Inst. Tech., Jet Prop. Lab., Progr. Rep.* 30–6, May 1959, 11 pp.

Some Remarks on Free Radicals and Their Possible Use in Rocket Propulsion, by Olgierd Woeczek, *J. Brit. Interplanet. Soc.*, vol. 17, Sept.-Oct. 1959, pp. 133–136.

Considerations Pertaining to Spherical-vessel Combustion, by J. Grumer, E. B. Cook and T. A. Kubala, *Combustion & Flame*, vol. 3, Dec. 1959, pp. 437–446.

On the Existence of Steady State Flames, by A. L. Berlad and C. H. Yang, *Combustion & Flame*, vol. 3, Dec. 1959, pp. 447–452.

Quenching Diameters of Some Fast Flames at Low Pressures, by Evelyn Anagnostou and A. E. Potter Jr., *Combustion & Flame*, vol. 3, Dec. 1959, pp. 453–458.

Further Measurements of Turbulence Intensity in Flame Zones, by A. A. Westenberg and J. L. Rice, *Combustion & Flame*, vol. 3, Dec. 1959, pp. 459–466.

The Cooperative Mechanism in the Ignition of Dust Dispersions, by H. M. Cassel and I. Liebman, *Combustion & Flame*, vol. 3, Dec. 1959, pp. 467–476.

Flame Quenching in Converging Rectangular Channels, by A. L. Berlad, R. D. Rowe and C. H. Yang, *Combustion & Flame*, vol. 3, Dec. 1959, pp. 477–480.

The Effect of External Factors on the Formation of Detonation in Saturated Knallgas-steam Mixtures, by L. B. Adler, E. C. Hobaica and J. A. Luker, *Combustion & Flame*, vol. 3, Dec. 1959, pp. 481–494.

The Burning Velocity of Hydrogen-air Mixtures and Mixtures of Some Hydrocarbons with Air, by T. G. Scholte and P. B. Vaags, *Combustion & Flame*, vol. 3, Dec. 1959, pp. 495–502.

The Influence of Small Quantities of Hydrogen and Hydrogen Compounds on the Burning Velocity of Carbon Monoxide-air Flames, by T. G. Scholte and P. B. Vaags, *Combustion & Flame*, vol. 3, Dec. 1959, pp. 503–510.

Burning Velocities of Mixtures of Hydrogen, Carbon Monoxide and Methane with Air, by T. G. Scholte and P. B. Vaags, *Combustion & Flame*, vol. 3, Dec. 1959, pp. 511–521.

Notes on Gaseous Nitric Acid-Hydrocarbon Flames, by J. Mertens and R. L. Potter, *Combustion & Flame*, vol. 3, Dec. 1959, pp. 522–528.

Theory of the Burning of Monopropellant Droplets, by F. A. Williams, *Combustion & Flame*, vol. 3, Dec. 1959, pp. 529–534.

Thermal Initiation of Explosives, by John Zinn and Charles L. Mader, *J. Appl. Phys.*, vol. 31, Feb. 1960, pp. 323–327.

Diffusion Coefficients in Flames and Detonations with Constant Enthalpy, by Joseph O. Hirschfelder, *Phys. Fluids*, vol. 3, Jan.-Feb. 1960, pp. 109–112.

Statistical Study of Accelerating Flames, by R. A. Stern, A. J. Laderman and A. K. Oppenheim, *Phys. Fluids*, vol. 3, Jan.-Feb. 1960, pp. 113–120.

Work on Atomic Spectroscopy in the USSR, by S. E. Frish, *Soviet Phys.-Uspekhi*, vol. 2 (68), May-June 1959, pp. 343–351.

Recent Developments in Molecular Spectroscopy in the USSR, by B. S. Neporent, *Soviet Phys.-Uspekhi*, vol. 2 (68), May-June 1959, pp. 352–364.

Methods and Apparatus for Low-temperature Optical and Spectral Investigations, by V. P. Babenko, V. L. Broude, V. S. Medvedev and A. F. Prikhot'ko, *Instruments & Experimental Tech.* (*trans. of Pribory i Tekhnika Eksperimenta*), no. 1, Jan.-Feb. 1959, pp. 119–124.

A Research Study to Advance the State-of-the-art of Solid Propellants Grain Design, by *Thiokol Chem. Corp., Elkton Div., Quarterly Prog. Rep.* 2, Aug. 1-Nov. 1, 1959, 43 pp., 53 refs.

Free Fall and Evaporation of JP-1 Jet Fuel Droplets in a Quiet Atmosphere, by Herman H. Lowell, *NASA TN* D-199, March 1960, 47 pp.

An Experimental Investigation of the Chemistry and Interconversion of Boron Hydrides, by Riley Schaeffer, *Wright Air Dev. Center, TN* 59–258, July 1959, 44 pp.

Solutions for Complex Systems of Chemical Reaction Kinetics, Part I: An Irreversible Unimolecular Reaction Followed by a Second Irreversible Unimolecular Reaction, by Daniel D. Konowalow, James E. Blair, Joseph Hirschfelder and Farrington Daniels, *Wright Air Dev. Center, TN* 59–243, Part I, Aug. 1959, 36 pp.

Frozen Free Radicals, by G. K. Minkoff, **Progress in Cryogenics,** vol. 1, ed. by K. Mendelssohn, Heywood & Co., London, 1959, pp. 137–178.

Viscosity and Thermal Conductivity of Liquid Boron Trifluoride, by A. N. Spencer and Mc. J. Todd, *Brit. J. Appl. Phys.*, vol. 11, Feb. 1960, pp. 60–63.

The Physicochemical Properties of Pure Nitric Acid, by S. Alexander Stern, J. T. Mullhaupt and Webster B. Kay, *Chem. Revs.*, vol. 60, April 1960, pp. 185–208.

Combustion Calorimetry with Fluorine: Constant Pressure Flame Calorimetry, by G. T. Armstrong and R. S. Jessup, *J. Res., Nat. Bur. Standards, A. Phys. & Chem.*, vol. 64A, Jan.-Feb. 1960, pp. 49–60.

Experimental Study of Zero-flow Ejectors Using Gaseous Nitrogen, by William L. Jones, Harold G. Price Jr. and Carl F. Lorenzo, *NASA TN* D-203, March 1960, 23 pp.

Trails of Axi-symmetric Hypersonic Blunt Bodies Flying Through the Atmosphere, by Saul Feldman, *Avco-Everett Res. Lab., Res. Rep.* 82, Dec. 1959, 92 pp.

Research on Combination Phenomena at High Pressures, by Rudolph Edse, William A. Strauss and Michael C. Fong, *Wright Air Dev. Center, TN* 59–328, Jan. 1959, 23 pp.

Combustion Instability in Solid Rockets Using Propellants with Suspended Metallic Powders, by Sin-I Cheng, *Princeton Univ., Dept. Aeron. Engng., Rep.* 482, Sept. 1959, 31 pp.

Transportation of Liquid Fluorine, by Paul M. Ordin, *NACA Res. Mem.* E55I23, Nov. 1955, 17 pp.

Investigation of the Liquid Fluorine-Liquid Diborane Propellant Combination in a 100-pound-thrust Rocket Engine, by Paul M. Ordin, Howard W. Douglass and William H. Rowe, *NACA Res. Mem.* E51I04, Nov. 1951, 40 pp.

Recent Advances in Condensed Media Detonations, by S. J. Jacobs, ARS JOURNAL, vol. 30, no. 2, Feb. 1960, p. 151–158, 102 refs.

Experimental Investigation of Propellant Erosion, by Tage Marklund and Arne Lake, ARS JOURNAL, vol. 30, no. 2, Feb. 1960, pp. 173–178.

Estimate of Chemical Space Heating Rates in Gas-phase Combustion with Application to Rocket Propellants, by David A. Bittker and Richard S. Brokaw, ARS JOURNAL, vol. 30, no. 2, Feb.1960, pp. 179–185.

Mixture Ratio Distribution in the Drops of Spray Produced by Impinging Liquid Streams, by Dezso Somogyi and Charles E. Feiler, ARS JOURNAL, vol. 30, no. 2, Feb. 1960, pp. 185–187.

Chemical Nonequilibrium Effects on Hydrogen Rocket Impulse at Low Pressure, by J. Gordon Hall, A. Q. Eschenroeder and J. J. Klein, ARS JOURNAL, vol. 30, no. 2, Feb. 1960, pp. 188–190.

Pure Shock Environmental Testing of Condensed-phase Unstable Materials, by T. A. Erikson, ARS JOURNAL, vol. 30, no. 2, Feb. 1960, pp. 190–191.

Expansion of Liquid-Oxygen RP-1 Combustion Products in a Rocket Nozzle, by Frederick S. Simmons, ARS JOURNAL, vol. 30, no. 2, Feb. 1960, pp. 193–194.

Hydrogen for the Space Age, by Richard J. Coar and Charles H. King Jr., ASTRONAUTICS, vol. 5, March 1960, p. 26.

A Thermoanalytical Study of the Ignition and Combustion Reactions of Black Powder, by C. Campbell and G. Weingarten, *Trans. Faraday Soc.*, vol. 55, Dec. 1959, p. 2221.

Burning Selenium and Barium Peroxide Powders, by L. B. Johnson Jr., *Ind. Engng. Chem.*, vol. 52, March 1960, pp. 241–244.

How to Predict Flammability in Ozonization Reactions, by W. E. Cromwell, *Ind. Engng. Chem.*, vol. 52, March 1960, pp. 245–252.

Trapped Free Radical Concentrations, by Charles E. Hecht, *J. Chem. Phys.*, vol. 32, Feb. 1960, pp. 365–373.

Short-range Interaction Between a Hydrogen Molecule and a Hydrogen Atom, II, by William J. Jameson Jr. and Henry Aroeste, *J. Chem. Phys.*, vol. 32, Feb. 1960, pp. 374–402.

Molecular Diffusion Studies in Gases at High Temperature, IV, Results and Interpretation of the CO_2-O_2, CH_4-O_2, H_2-O_2, CO-O_2, and H_2O-O_2 Systems, by R. E. Walker and A. A. Westenberg, *J. Chem. Phys.*, vol. 32, Feb. 1960, pp. 436–441.

Infrared Emission Spectra of Gaseous B_2O_3 and B_2O_2, by David White, David E. Mann, Patrick N. Walsh and Armin Sommer, *J. Chem. Phys.*, vol. 32, Feb. 1960, pp. 481–487.

Infrared Emission Spectrum of Gaseous HBO_2, by David White, David E. Mann, Patrick N. Walsh and Armin Sommer, *J. Chem. Phys.*, vol. 32, Feb. 1960, pp. 488–514.

Interactions Between Ground State Oxygen Atoms and Molecules: O–O and O_2-O_2, by Joseph T. Vanderslice, Edward A. Mason and William G. Maisch, *J. Chem. Phys.*, vol. 32, Feb. 1960, pp. 515–537.

Velocity of Compressional Waves in Liquid Hydrogen Fluoride and Some Thermodynamic Properties Derived Therefrom, by Robert T. Lagemann and C. Harry Knowles, *J. Chem. Phys.*, vol. 32, Feb. 1960, pp. 561–603.

Expansion Engines for Hydrogen Liquefiers, by Edmund H. Brown, *J. Res., Nat. Bur. Standards, C: Engng. & Instr.*, vol. 64c, Jan.-March 1960, pp. 25–48.

Square-wave Generator for the Study of Exploding Wires, by T. J. Tucker, *Rev. Sci. Instr.*, vol. 31, Feb. 1960, pp. 165–168.

Continuous Oscillographic Method for Measuring the Velocity and Conductivity of Stable and Transient Shock in Solid Cast Explosives, by Adolph B. Amster, Paul A. Kendall, Leo J. Veillette and Burton Harrell, *Rev. Sci. Instr.*, vol. 31, Feb. 1960, pp. 188–192.

Method for the Study of Deflagration to Detonation Transition, by Adolph B. Amster, *Rev. Sci. Instr.*, vol. 31, Feb. 1960, p. 219.

The Combustion of Gaseous Aldehydes, Studies by Flash Photolysis and Kinetic Spectroscopy, by J. F. McKellar and R. G. W. Norrish, *Proc. Roy. Soc., London*, vol. 254, Feb. 1960, pp. 147–162.

How to Use Fuel as a Heat Sink, by G. L. Roth and O. L. Williamson, *Space/Aeron.*, vol. 33, March 1960, p. 56.

Materials and Structures

Initial Investigation of Arc Melting and Extrusion of Tungsten, by Fred A. Foyle, Glen E. McDonald and Neal T. Saunders, *NASA TN* D-269, March 1960, 35 pp.

The Effect of Axial Constraint on the Instability of Thin Circular Cylindrical Shells under External Pressure, by Josef Singer, *Tech. Res. & Dev. Foundation, Ltd., Haifa, Israel, TN* 1, Sept. 1959, 17 pp.

Thermo-elastic Equations Applicable to Thick-wall, Pointed Shells of Revolution, by R. D. Sutherland and R. G. Shook, *Convair/Pomona, Calif., TM*-349-14, Jan. 1960, 29 pp.

The Investigation of the Mechanism of Substructural Formation in Refractory Metals and the Relation to the Observed Mechanical Properties, by A. Iannucci, J. Intrater, G. Murray and S. Weinig, *Wright Air Dev. Center, TR* 59-441, Pt. 1, July 1959, 26 pp.

Cratering and Shock Wave Phenomena in Steel Plates at High Impact Speeds, by Earle B. Mayfield and James W. Rogers, *J. Appl. Phys.*, vol. 31, March 1960, pp. 472–473.

Exploratory Investigation of Several Coated and Uncoated Metal, Refractory, and Graphite Models in a 3,800° F. Stagnation Temperature Air Jet, by Otto F. Trout, *NASA TN* D-190, Feb. 1960, 73 pp.

Vaporization of a Refractory Oxide During Hypersonic Flight, by S. M. Scala, *Heat Transf. & Fluid Mech. Inst., Univ. Calif.*, June 1959, pp. 181–192.

Thermal Stresses in Missile Nose Cones, by A. J. A. Morgan and Carlos H. Christensen, *Inst. Aeron. Sci., SMF Fund, Paper* FF-24, Jan. 1960, 81 pp.

The Performance of Ablation Materials as Heat Protection for Re-entering Satellites, by W. R. Warren and N. S. Diaconis, *Inst. Aeron. Sci., Paper* 60–49, Jan. 1960, 34 pp.

Graphite as a Structural Material in Conditions of High Thermal Flux, by A. J. Kennedy, *Cranfield, Coll. Aeron., CoA Rep.* 121, Nov. 1959, 32 pp.

Preparation of High Purity W, Mo, Ta, Cb, and Zr, by George A. Moore and L. L. Wyman, *Wright Air Dev. Center, Tech. Rep.* 59–314, Oct. 1959, 9 pp.

Uranium Dioxide Compatibility with Refractory Metals, Carbides, Borides, Nitrides, and Oxides between 3500° and 5000°F, by James J. Gangler, William A. Sanders and Isadore L. Drell, *NASA TN* D-262, Feb. 1960, 28 pp.

The Metallurgical Challenge of Missilery, by W. Stuart Lyman, *Battelle Tech. Rev.*, vol. 9, Jan. 1960, pp. 3–7.

Basic Design Criteria for Moon Building, by John S. Rinehart, *J. Brit. Interplanet. Soc.*, vol. 17, Sept.-Oct. 1959, pp. 126–129.

Qualitative Measurements of the Effective Heats of Ablation of Several Materials in Supersonic Air Jets as Stagnation Temperatures up to 11,000°F, by Bernard Rashis, William G. Witte and Russell N. Hopko, *NACA Res. Mem.* L58E22, June 1958, 25 pp.

Investigation of Tantalum in a 3,800°F Supersonic Airstream, by Otto F. Trout Jr. and Jerry L. Modisette, *NACA Res. Mem.* L57J07a, Jan. 1958, 13 pp.

Preliminary Investigation of Graphite, Silicon Carbide, and Several Polymer-glass-cloth Laminates in a Mach Number 2 Air Jet at Stagnation Temperatures of 3,000°F and 4,000°F, by Francis W. Casey Jr. and Russell N. Hopko, *NACA Res. Mem.* L57K15, Jan. 1958, 18 pp.

Limited Tests of Molybdenum Coated with Molybdenum Disilicide in a Supersonic Heated-air Jet and Brief Description of the Coating Facility, by E. M. Fields and N. T. Wakelyn, *NACA Res. Mem.* L57I12, Jan. 1958, 21 pp.

The Behavior of Beryllium and Beryllium Copper in a 4,000°F Supersonic Air Jet at a Mach Number of 2, by William H. Kinard, *NACA Res. Mem.* L57G31, Oct. 1957.

Behavior of Some Materials and Shapes in Supersonic Free Jets at Stagnation Temperatures up to 4,210°F, and Descriptions of the Jets, by E. M. Fields, Russell N. Hopko, Robert L. Swain and Otto F. Trout Jr., *NACA Res Mem.* L57K26, Feb. 1958, 59 pp.

Fluid Dynamics, Heat Transfer and MHD

Mass Transfer Cooling Near the Stagnation Point, by Leonard Roberts, *NASA Tech. Rep.* R-8, 1959, 16 pp.

Radiation by Plasma Oscillations in a Bounded Plasma in a Magnetic Field, by H. W. Wyld Jr., *Space Tech. Labs., Inc., Phys. Res. Lab.*, PRL-9-23, Oct. 1959, 26 pp.

Magnetohydrodynamics and Aerodynamic Heating, by Rudolf X. Meyer, *Space Tech. Labs., Inc., Phys. Res. Lab.*, June 1958, 16 pp.

On the Interpenetration of a Plasma and Its Confining Electromagnetic Wave Field, by Eirch S. Weibel, *Space Tech. Labs., Inc., Aeron. Res. Lab.*, ARL-57-1012, May 1957, 27 pp.

A Study of Plasma Stability in Microwave Cavities by a Frequency-shift Analog, by Robert A. Swanson, *Space Tech. Labs., Inc., Phys. Res. Lab.*, TR-59-0000-00813, 1959, 12 pp.

Transport Phenomena of a Rarefied and Fully Ionized Gas in the Presence of a Strong Magnetic Field, by Toyoki Koga, *Univ. Southern Calif., Los Angeles, Engng. Center, USCEC Rep.* 56-210, Feb. 1960, 18 pp.

Measurement of the Diffusion of Electrons Out of Strong Shock Waves, by H. Groenig, *Aachen, Tech. Hochschule, Inst. f. Mech., Final Report,* June 1959, 34 pp.

Vector Polar Method for Shock Interactions with Area Disturbances, by A. K. Oppenheim and R. A. Urtiew, *Univ. Calif., Berkeley, TN* DR 4, July 1959, 144 pp. (*AFOSR TN* 59-701.)

Studies in Hypervelocity Impact, by G. D. Anderson, *Stanford Res. Inst., Poulter Labs., Tech. Rep.* 018–59, Dec. 1959, 43 pp.

Evaluation of Thermal Problems of Relatively Low Orbital Altitudes, by Lawrence D. Wing, *Aero/Space Engng.*, vol. 19, March 1960, pp. 58–60.

On the Problems of Re-entry into the Earth's Atmosphere, by Alfred C. Robinson and Algimantas J. Besonis, *J. Astron. Sci.*, vol. 7, no. 1, 1960, pp. 7–20.

The Boundary Layer Near the Stagnation Point in Hypersonic Flow Past a Sphere, by T. K. Herring, *J. Fluid Mech.*, vol. 7, Feb. 1960, pp. 257–272.

Some Solutions for Electromagnetic Problems Involving Spheroidal, Spherical,

and Cylindrical Bodies, by James R. Wait, *J. Res., Nat. Bur. Standards, B: Math. & Math. Phys.*, vol. 64B, Jan.-March 1960, pp. 15–32.

General Theory of Electrically Conducting Perfect Gas Flow Past a Three-dimensional Thin Body, by Shigenori Ando, *J. Phys. Soc. Japan*, vol. 15, Jan. 1960, pp. 157–166.

A Linearized Theory of Magnetohydrodynamic Flow Past a Fixed Body in a Parallel Magnetic Field, by Hirowo Yosinobu, *J. Phys. Soc. Japan*, vol. 15, Jan. 1960, pp. 175–188.

Magnetohydrodynamic Flow Past a Sphere, by Kanefusa Gotoh, *J. Phys. Soc. Japan*, vol. 15, Jan. 1960, pp. 189–196.

Some General Considerations of the Heating of Satellites, by Alfred J. Eggers, Thomas J. Wong and Robert E. Slye, *J. Heat Transfer*, vol. 81, no. 3, Nov. 1959, pp. 308–314.

Radiator Areas of Thermopile Generators in Space, by Douglas L. Kerr, *Aero/Space Engng.*, vol. 18, Sept. 1959, pp. 57–62, 66.

Heat Transport by Convection in Presence of an Impressed Magnetic Field, by Yoshinari Nakagawa, *Phys. Fluids*, vol. 3, no. 1, Jan.-Feb. 1960, pp. 87–93.

Aerodynamic-heating Data Obtained from Free-flight Tests Between Mach Numbers of 1 and 5, by Charles Rumsey, Robert Piland and Russell Hopko, *NASA TN* D-216, Jan. 1960, 21 pp.

Note on the Calculation of Equilibrium Skin Temperatures, by Hans C. Vetter, *J. Aero/Space Sci.*, vol. 26, no. 11, Nov. 1959, pp. 757–758.

Mass Transfer Cooling Experiments on a Hemisphere at M = 5, by G. E. Anderson, C. J. Scott and D. R. Elgin, *Univ. Minnesota, Inst. Tech., Rosemount Aeron. Lab., Res. Rep.* 166, Aug. 1959, 17 pp.

Local Heat Transfer and Recovery Temperatures on a Yawed Cylinder at a Mach Number of 4.15 and High Reynolds Numbers, by Ivan E. Beckwith and James J. Gallagher, *NASA Mem.* 2-27, April 1959, 59 pp.

Compressible Flat-plate Boundary-layer Flow with an Applied Magnetic Field, by William B. Bush, *J. Aero/Space Sci.*, vol. 27, no. 1, Jan. 1960, pp. 49–58.

Similitude of Hypersonic Real-gas Flows over Slender Bodies with Blunted Noses, by Hsien K. Cheng, *J. Aero/Space Sci.*, vol. 26, Sept. 1959, pp. 575–585.

A Simplified Study on the Nonequilibrium Couette and Boundary-layer Flows with Air Injections, by Paul M. Chung, *NASA TN* D-306, Feb. 1960, 69 pp.

Heat Transfer Measurements at a Mach Number of 2 in the Turbulent Boundary Layer on a Flat Plate Having a Step-wise Temperature Distribution, by Raul J. Conti, *NASA TN* D-159, Nov. 1959, 27 pp.

Heat and Mass Transfer in a Turbulent Boundary Layer, by D. R. Davies and D. E. Bourne, *Int. Cong. Appl. Mech.*, 9th, Brussels, 1958, *Proc.*, vol. 4, 1959, pp. 50–59. (In English.)

Analysis of Turbulent Flow and Heat Transfer on a Flat Plate at High Mach Numbers with Variable Fluid Properties, by Robert G. Deissler and Albert L. Loeffler, *NASA Tech. Rep.* R-17, 1959, 33 pp.

Laminar, Transitional, and Turbulent Mass Transfer Cooling Experiments at Mach Numbers from 3 to 5, by C. J. Scott, G. E. Anderson and D. R. Elgin, *Univ. Minn., Rosemount Aeron. Lab., Res. Rep.* 162, Aug. 1959, 29 pp.

Exploratory Investigation of Transpiration Cooling of a 40° Double Wedge Using Nitrogen and Helium as Coolants at Stagnation Temperatures of 1,295°F to 2,910° F, by Bernard Rashis, *NACA Res. Mem.* L57F11, Aug. 1957, 18 pp.

Feasibility of Nose-cone cooling by the Upstream Ejection of Solid Coolants at the Stagnation Point, by William H. Kinard, *NACA Res. Mem.* L57K22, March 1958, 17 pp.

Preliminary Survey of Possible Cooling Methods for Hypersonic Aircraft, by Jack B. Esgar, Robert O. Hickel and Francis S. Stepka, *NACA Res. Mem.* E57L19, May 1958, 37 pp.

Experimental Ablation Cooling, by Aleck C. Bond, Bernard Rashis and L. Ross Levin, *NACA Res. Mem.* L58E15a, July 1958, 17 pp.

Some Effects of Fin Leading-edge Shape on Aerodynamic Heating at Mach Number 2.0 at a Stagnation Temperature of about 2,600°, by R. William M. Bland Jr., *NACA Res. Mem.* L57K12, Jan. 1958, 15 pp.

Experimental Investigation of the Effect of Yaw on Rates of Heat Transfer to Transverse Circular Cylinders in a 6500-foot-per-second Hypersonic Air Stream, by Bernard E. Cunningham and Samuel Kraus, *NACA Res. Mem.* A58E19, Aug. 1958, 45 pp.

Heat Transfer on an Afterbody Immersed in the Separated Wake of a Hemisphere, by Helmer V. Nielsen, *NACA Res. Mem.* A57K07a, Jan. 1958, 13 pp.

Preliminary Indications of the Cooling Achieved by Ejecting Water Upstream from the Stagnation Point of Hemispherical, 80° Conical, and Flat-faced Nose Shapes at a Stagnation temperature of 4,000° F, by Bernard Rashis, *NACA Res. Mem.* L57I03, Oct. 1957, 11 pp.

Magneto-fluid-mechanics of a Viscous, Electrically Conducting Fluid Contained Within Two Finite, Concentric, Rotating Cylinders in the Presence of a Magnetic Field, by Gerald W. Pneuman and Paul S. Lykoudis, *Purdue Univ., School Engng., Rep.* A-59-13, Aug. 1959, 83 pp.

Approximate Method for Determining Laminar Heat Transfer Rates, by Harold S. Pergament and Melvin Epstein, ARS JOURNAL, vol. 30, no. 2, Feb. 1960, pp. 206.

Maximum Turbulent Boundary Layer Heating Rates on a Hemispherical Nose, by Paul D. Arthur and James C. Williams III, ARS JOURNAL, vol. 30, no. 2, Feb. 1960, pp. 207–208.

Recombination of Atoms at Surfaces, Part 7: Hydrogen Atoms at Silica and Other Similar Surfaces, by M. Green, K. R. Jennings, J. W. Linnett and D. Schofield, *Trans. Faraday Soc.*, vol. 55, Dec. 1959, p. 2152.

Flow of Fluids—Unit Operations Review, by Murray Weintraub, *Ind. Engng. Chem.*, vol. 52, March 1960, pp. 257–258.

Thermal Conductivity of Binary Mixtures of Diatomic and Monatomic Gases, by B. N. Srivastava and A. K. Barua, *J. Chem. Phys.*, vol. 32, Feb. 1960, pp. 427–435.

The Stability and Transition of a Two-dimensional Jet, by Hiroshi Sato, *J. Fluid Mech.*, vol. 7, Jan. 1960, pp. 53–80.

A Shallow-liquid Theory in Magneto-hydrodynamics, by L. E. Fraenkel, *J. Fluid Mech.*, vol. 7, Jan. 1960, pp. 81–107.

Inviscid Flow of a Reacting Mixture of Gases Around a Blunt Body, by Wilbert Lick, *J. Fluid Mech.*, vol. 7, Jan. 1960, pp. 128–144.

Measurement of the Thermal Conductivities of Gases at High Temperatures, by R. G. Vines, *J. Heat Transfer (ASME Trans.)*, Series C, vol. 82, Feb. 1960, pp. 48–52.

Heat Conduction in a Melting Slab, by Stephen J. Citron, *J. Aero/Space Sci.*, vol. 27, March 1960, pp. 219–228.

Electrogasdynamic Motion of a Charged Body in a Plasma, by L. Kraus and H. Yoshihara, *J. Aero/Space Sci.*, vol. 27, March 1960, pp. 229–233.

General Theory of Plasma, by V. Ferraro, *Nuovo Cimento*, Suppl. to vol. 13, Series 10, no. 1, 1959, pp. 9–58.

Plasma Physics on Cosmical and Laboratory Scale, by B. Lehnert, *Nuovo Cimento*, Suppl. to vol. 13, Series 10, no. 1, 1959, pp. 59–110.

High Temperature Plasmas, by P. C. Thonemann, *Nuovo Cimento*, Suppl. to vol. 13, Series 10, no. 1, 1959, pp. 111–131.

Microwaves in Ionized Gas, by A. Gilardini, *Nuovo Cimento*, Suppl. to vol. 13, Series 10, no. 1, 1959, pp. 132–165.

Propagation and Production of Electromagnetic Waves in a Plasma, by R. Gallet, *Nuovo Cimento*, Suppl. to vol. 13, Series 10, no. 1, 1959, pp. 234–256.

Plasma Confinement by External Magnetic Fields, by J. G. Linhart, *Nuovo Cimento*, Suppl. to vol. 13, Series 10, no. 1, 1959, pp. 257–283.

Some Theoretical Aspects of Magnetohydrodynamics and Thermonuclear Fusion, by R. Lüst, *Nuovo Cimento*, Suppl. to vol. 13, Series 10, no. 1, 1959, p. 329.

Flow of Highly Rarefied Gases Around Oscillating Surfaces, by N. T. Pashchenko, *PMM: J. Appl. Math. & Mech.*, vol. 23, no. 4, 1959, pp. 1081-1089.

On the Propagation of Weak Waves in a Continuous Medium in the Presence of Radiant Energy Transfer, by Iu. S. Riazantsev, *PMM: J. Appl. Math. & Mech.*, vol. 23, no. 4, 1959, pp. 1126–1128.

Stable Confinement of a High-temperature Plasma, by R. F. Post, R. E. Ellis, F. C. Ford and M. N. Rosenbluth, *Phys. Rev. Letters*, vol. 4, Feb. 1960, pp. 166–169.

Thermal Waves in Irradiated Graphite, by D. C. Cooper and N. E. Hoskin, *Quart. J. Mech. & Appl. Math,*. vol. 12, Nov. 1959, pp. 393–406.

Linearized Theory of Plasma Oscillations, by L. Oster, *Revs. Modern Phys.*, vol. 32, Jan. 1960, p. 141.

The Imperial College Hypersonic Gun Tunnel, by J. L. Stollery, D. J. Maull and B. J. Belcher, *J. Roy. Aeron. Soc.*, vol. 64, Jan. 1960, pp. 24–32.

On Similar Solutions of the Boundary Layer Equations for Air in Dissociation Equilibrium, by R. L. Dommett, *J. Roy. Aeron. Soc.*, vol. 64, Jan. 1960, pp. 36–37.

Excitation of Waves in a Plasma, by A. G. Sitenko and Yu. A. Kirochkin, *Soviet Phys., Tech. Phys. (trans. of Zhurnal Tekhnicheskoi Fiziki)*, vol. 4, Jan. 1960, pp. 723–729.

Simple Waves in Magnetohydrodynamics, by A. I. Akhiezer, G. Ya. Lyubarskii and R. V. Polovin, *Soviet Phys., Tech. Phys. (trans. of Zhurnal Tekhnicheskoi Fiziki)*, vol. 4, Feb. 1960, pp. 849–854.

Doppler Effect in an Electron Plasma in a Magnetic Field, by K. A. Barsukov and A. A. Kolomenskii, *Soviet Phys., Tech. Phys. (trans. of Zhurnal Tekhnicheskoi Fiziki)*, vol. 4, Feb. 1960, pp. 868–870.

Equations of State of High Temperature Plasma, by Tobru Morita, *Progr. of Theor. Phys.*; vol. 22, no. 6, Dec. 1959, pp. 747–774.

Some Problems in Hydromagnetics, by K. P. Chopra, *Univ. Southern Calif., Engng. Center, USCEC Rep.* 56–205, Jan. 1959, 210 pp.

Correlation Formulas and Tables of Density and Some Transport Properties of Equilibrium Dissociating Air for Use in Solutions of the Boundary-layer Equations, by Nathaniel B. Cohen, *NASA TN* D-194, Feb. 1960, 37 pp.

Boundary-layer Stability Diagrams for Electrically Conducting Fluids in the Presence of a Magnetic Field, by Vernon J. Rossow, *NASA Tech. Rep.* R-37, 1959, 16 pp.

Stagnation-point Shielding by Melting and Vaporization, by Leonard Roberts, *NASA Tech. Rep.* R-10, 1959, 24 pp.

A Theoretical Investigation on the Use of Combustion Products for the Simulation of Hypersonic Flow, by Vito D. Agosta, *Wright Air Dev. Center, WADC TN* 59-81, March 1959, 23 pp.

A Theoretical Study of Stagnation-point Ablation, by Leonard Roberts, *NASA Tech. Rep.* R-9, 1959, 11 pp.

Heat Protection by Ablation, by R. M. Wood and R. J. Tagliani, *Inst. Aeron. Sci., Paper* 60–8, Jan. 1960, 14 pp.

Research at the National Physical Laboratory on the Properties of Gases at High Temperatures; Preliminary Spectrographic Measurements, by K. C. Lapworth, *Gt. Brit., Nat. Phys. Lab., NPL/-Aero 380*, June 1959, 37 pp.

A High-velocity Gun Employing a Shock-compressed Light Gas, by Carlton Bioletti and Bernard E. Cunningham, *NASA TN* D-307, Feb. 1960, 19 pp.

Axisymmetric Nozzles for Hypersonic Flows, by John D. Lee, *Ohio State Univ. Res. Foundations Aerodynam. Lab., TN* (ALOSU)-459-1, Sept. 1959, 24 pp.

Efficiency of Flush Oblique Nozzles Exhausting into Supersonic Streams Having Mach Numbers up to 4, by J. W. Cnossen, *United Aircr. Corp., Res. Dept.*, R-1285-10, Sept. 1959, 79 pp.

Inlet and Exhaust Nozzle Techniques Developed by United Aircraft Corporation Research Department, by Irving Twomey, *United Aircr. Corp.*, R-2000-98, June 1959, 33 pp.

The High Temperature Heater and Evaporative Film Cooling of Nozzle Throat Sections of the Rosemount Aeronautical Laboratories' Hypersonic Facility, by Rudolf Herman, Hans Leitinger and Walter L. Melnik, *Wright Air Dev. Center, Tech. Rep.* 58–376, July 1958, 50 pp.

A Relativistic Treatment of Strong Shock Waves in a Classical Gas, by A. W. Guess, *Air Force Cambridge Res. Center, GRD Res. Notes* 27, *AFCRC-TN-59-642*, Dec. 1959, 35 pp.

Shock-wave Structure Based on Ikenberry-Truesdell Approach to Kinetic Theory of Gases, by Robert E. Street, *NASA TN* D-365, Feb. 1960, 60 pp.

A Review of Magneto-hydrodynamics, by Y. A. Yoler, *Boeing Airplane Co.*, D1-82-0027, Oct. 1959, 69 pp.

Magnetohydrodynamic Shock Wave in a Collision-free Plasma, by F. J. Fishman, A. R. Kantrowitz and H. E. Petschek, *Avco-Everett Res. Lab., Res. Rep.* 85, Jan. 1960, 26 pp.

Magnetohydrodynamic Waves, by J. D. Cole, *Calif. Inst. Tech., Guggenheim Aeron. Lab.*, Jan. 1959, 28 pp.

Analysis of Two-stage Hot Water Ejectors, by O. Lutz and E. Riester, *Zeitschrift für Flugwissenschaften*, vol. 7, no. 12, Dec. 1959, pp. 350–355. (In German.)

Compressible Flow Tables $\gamma = 1.22$ Isentropic Process, by C. Hoebich, *Army Rocket & Guided Missile Agency, Ordn.*

Missile Labs. Div., ARGMA TN 1H1N-7, Dec. 1959, 87 pp.

Some Aspects of Non-equilibrium Flows, by Raynold Sedney, *Inst. Aeron. Sci., Paper* 60–4, Jan. 1960, 26 pp.

Heat Transfer, Recovery Factor and Pressure Distributions Around a Circular Cylinder Normal to a Supersonic Rarefied-air Stream, by O. K. Tewfik and W. H. Giedt, *Inst. Aeron. Sci., Paper* 60–46, Jan. 1960, 18 pp.

Hydraulic Analogue for One-dimensional Unsteady Gas Dynamics, by W. H. T. Loh, *J. Franklin Inst.*, vol. 269, Jan. 1960, pp. 43–55.

Experimental Investigation of a High-energy Density, High-pressure Arc Plasma, by Edward A. Martin, *J. Appl. Phys.*, vol. 31, Feb. 1960, pp. 255–267.

Absorption and Reflection Spectrum of a Plasma, by W. D. Hershberger, *J. Appl. Phys.*, vol. 31, Feb. 1960, pp. 417–422.

Microwave Determination of Plasma Density Profiles, by Charles B. Wharton and Donald M. Slager, *J. Appl. Phys.*, vol. 31, Feb. 1960, pp. 428–431.

Scattering Potential in Fully Ionized Gases, by O. Theimer and R. Gentry, *Phys. Rev.*, vol. 116, Nov. 15, 1959, pp. 787–792.

Transverse Compression Waves in a Stabilized Discharge, by Daryl Reagan, *Phys. Fluids*, vol. 3, Jan.-Feb. 1960, pp. 33–39.

Irreversible Processes in Ionized Gases, by R. Balescu, *Phys. Fluids*, vol. 3, Jan.-Feb. 1960, pp. 52–63.

Heat Transport by Convection, by Yoshinari Nakagawa, *Phys. Fluids*, vol. 3, Jan.-Feb. 1960, pp. 82–86.

Heat Transport by Convection in Presence of an Impressed Magnetic Field, by Yoshinari Nakagawa, *Phys. Fluids*, vol. 3, Jan.-Feb. 1960, pp. 87–93.

Performance of Hydromagnetic Plasma Gun, by John Marshall, *Phys. Fluids*, vol. 3, Jan.-Feb. 1960, pp. 134–135.

Flow of a Partially Ionized Gas in an Axial Magnetic Field, by P. J. Dickerman and C. F. Price, *Phys. Fluids*, vol. 3, Jan.-Feb. 1960, p. 137.

Absorption Coefficients for High-temperature Nitrogen, Oxygen, and Air, by B. H. Armstrong and R. E. Meyerott, *Phys. Fluids*, vol. 3, Jan.-Feb. 1960, pp. 138–139.

Ablation Cooling of High Velocity Ballistic Bodies at Re-entry into the Earth's Atmosphere, by E. Adams, *Raketentechnik und Raumfahrtforschung*, vol. 3, no. 4, Oct.-Dec. 1959, pp. 97–104. (In German.)

Confinement of a Plasma by a Magnetic Field, by A. Koller, *Raketentechnik und Raumfahrtforschung*, vol. 3, no. 4, Oct.-Dec. 1959, pp. 109–115. (In German.)

Stability of a Hollow Gas Conductor in a Magnetic Field, by L. M. Kovrizhnykh, *Soviet Phys.-JETP*, vol. 37, no. 6, Jan. 1960, pp. 65–66.

Radiative Processes Ahead of a Shock-wave Front, by L. M. Biberman and B. A. Veklenko, *Soviet Phys.-JETP*, vol. 37, no. 6, Jan. 1960, pp. 117–120.

On Convective Motion of a Conducting Fluid Between Parallel Vertical Plates in a Magnetic Field, by S. A. Regirer, *Soviet Phys.-JETP*, vol. 37, no. 6, Jan. 1960, pp. 149–152.

Passage of Particles Through a Plasma, by A. I. Larkin, *Soviet Phys.-JETP*, vol. 37, no. 6, Jan. 1960, pp. 186–191.

Summary of Instrumentation Development and Aerodynamic Research in a Hypersonic Shock Tunnel, Part II: Nozzle Flow Study and Flow Angularity Measurements, by Charles E. Wittliff and Merle R. Wilson, *Wright Air Dev. Center, Tech. Rep.* 58–401, Dec. 1958, 21 pp.

Aerodynamics of the Upper Atmosphere, by David J. Masson, ed. (Symposium, Santa Monica, Calif., June 8–10, 1959), *Rand Corp.* R-331, 1959, 1 vol.

Aerodynamics of Satellites, by S. A. Schaaf, *Paper* 1, 14 pp.

Meteoric Interaction with the Atmosphere: Theory of Drag and Heating and Comparison with Observations, by Carl Gazley Jr., *Paper* 6, 58 pp.

Rarefied-gas Dynamical Considerations in the Rocket-sounding Measurements, by V. C. Liu, *Paper* 7, 8 pp.

Progress in Studies of Sputtering by Beam Techniques, by F. C. Hurlbut and R. P. Stein, *Paper* 8, 13 pp.

Studies of the Interaction of High-velocity Atoms with Solid Surfaces by Means of Gas-discharge Devices, by Gottfried Wehner, *Paper* 9, 13 pp.

Problems in Gaseous Effusion, by H. W. Liepmann and J. D. Cole, *Paper* 10, 19 pp.

Equations of Flow in a Rarefied Atmosphere, by Harold Grad, *Paper* 11, 37 pp.

Analytic Representation of Surface Interaction for Free-molecule Flow with Application to Drag of Various Bodies, by R. Schamberg, *Paper* 12, 41 pp.

A Study of Near Free Molecule Flow, by D. Roger Willis, *Paper* 13, 32 pp.

Induction Drag on Satellites, by David B. Beard, *Paper* 17, 10 pp.

Notes on Surface Interation and Satellite Drag, by F. C. Hurlbut, *Paper* 21, 25 pp.

Flight Mechanics

Utilization of the Pilot in the Launch and Injection of a Multi-stage Orbital Vehicle, by E. C. Holleman, N. A. Armstrong and W. H. Andrews, *Inst. Aeron. Sci., Paper* 60-16, Jan. 1960, 31 pp.

The Calculation of Minimal Orbits, by G. C. Smith, *Astron. Acta*, vol. 5, no. 5, 1959, pp. 253–254.

The Three-body Problem Earth-moon-spaceship, by W. Gröbner and F. Cap, *Astron. Acta*, vol. 5, no. 5, 1959, pp. 287–312.

Graphic Solution of Some Earth Satellite Problems by Use of the Stereographic Net, by Robert E. Wallace, *J. Brit. Interplanet. Soc.*, vol. 17, Sept.-Oct. 1959, pp. 120–123.

A Generalization of the Minimum Impulse Theorem to the Restricted Three-body Problem, by Louis G. Vargo, *J. Brit. Interplanet. Soc.*, vol. 17, Sept.-Oct. 1959, pp. 124–126.

Orbital Elements, Trajectory Simulation, and Prediction for Earth Satellites, by A. D. Wasel, *J. Brit. Interplanet. Soc.*, vol. 17, Sept.-Oct. 1959, pp. 130–133.

Some Exact Solutions of the Equations of Motion of a Solar Sail with Constant Sail Setting, by Howard S. London, ARS JOURNAL, vol. 30, no. 2, Feb. 1960, pp. 198–200.

Hypervelocity Glider at Large Angles of Inclination, by W. H. T. Loh, ARS JOURNAL, vol. 30, no. 2, Feb. 1960, pp. 201–202.

Gravitational Torque on a Satellite of Arbitrary Shape, by Russell A. Nidey, ARS JOURNAL, vol. 30, no. 2, Feb. 1960, pp. 203–204.

Necessary Conditions for Optimal Rocket Trajectories, by D. F. Lawden, *Quart. J. Mech. & Appl. Math.*, vol. 12, Nov. 1959, pp. 476–487.

Choice of Flight Path for a Manned Space Vehicle to Mars and Venus, by K. A. Ehricke, *Raketentechnik und Raumfahrtforschung*, vol. 4, no. 1, Jan.-March 1960, pp. 16–22. (In German.)

Effects of Nose Corner Radii, Afterbody Section Deflections, and a Drogue Chute on Subsonic Motions of Manned-satellite Models in Reentry Configuration, by Willard S. Blanchard Jr. and Sherwood Hoffman, *NASA TN* D-223, March 1960, 16 pp.

The Combined Non-linear Effects of Earth Oblateness and Atmospheric Drag on a Near-Earth Satellite, by Trinidad Jaramillo, *Wright Air Dev. Center, Tech. Rep.* 59–513, Oct. 1959, 103 pp.

On the Motion of a Particle About an Oblate Spheroid, by D. G. Ewart, *J. Brit. Interplanet. Soc.*, vol. 17, Nov.-Dec. 1959, pp. 162–168.

Anisotrophy of Escape Velocity from the Moon, the Lunar Atmosphere, and the Origin of Craters, by Louis Gold, *J. Astron. Sci.*, vol. 7, no. 1, 1960, pp. 23–24.

Vehicle Design, Testing and Performance

Special Wind Tunnel Applications in Ballistic Missile Development, by Ellery B. May and James W. Clark, *Army Ballistic Missile Agency, U. S. Army Ordn. Missile Command*, Sept. 1959, 19 pp.

Economics and Technology of Large Step Rocket Recovery, by H. H. Koelle, *Raketentechnik und Raumfahrtforschung*, vol. 3, no. 4, Oct-Dec. 1959, pp. 105–108.

The Use of Rotors for the Landing and Re-entry Braking of Manned Spacecraft, by Chester R. Haig Jr., *Inst. Aeron. Sci., Paper* 60–17, Jan. 1960, 18 pp.

Some Observations on Supersonic Stabilization and Deceleration Devices, by James F. Connors and J. Calvin Lovell, *Inst. Aeron. Sci., Paper* 60–19, Jan. 1960, 16 pp.

Aerodynamics of the Upper Atmosphere, David J. Masson, ed. (Symposium, Santa Monica, Calif., June 8–10, 1959), *Rand Corp.*, R-331, 1959, 1 vol.

Orbit Dynamics and the Interpretation of Orbital Data, by C. A. Whitney, *Paper* 2, 24 pp.

Influence of Aerodynamic Drag on Satellite Orbits, by H. Potter Kerfoot, *Paper* 5, 19 pp.

Lift and Pitching Moment in Near-free-molecule Flow, by A. F. Charwat, *Paper* 15, 43 pp.

A Technique for Firing Dynamically Scaled Missile Models in Wind Tunnels and for Measuring Rocket-motor Sound and Pressure Fluctuations, by William J. Alford Jr. and Kenneth W. Goodson, *NASA TN* D-224, March 1960, 43 pp.

Space—A Special Report, *Missile Res. & Dev.*, vol. 7, no. 1, Jan. 1960, pp. 24–37.

Mercury Capsule and Its Flight Systems, by M. A. Faget and R. O. Piland, *Inst. Aeron. Sci., Paper* 60–34, Jan. 1960, 18 pp.

Review, Scope and Recent Results of Project Mercury Research and Development Program, *Inst. Aeron. Sci., Paper* 60–35, Jan. 1960, 18 pp.

Review of the Operational Plans for

Mercury Orbital Mission, by Charles W. Mathews, *Inst. Aeron. Sci., Paper* 60–36, Jan. 1960.

On the Methods and Economics of Recovering Boosters for Orbital Vehicles, by Paul R. Shipps, *Inst. Aeron. Sci., Paper* 60–29, Jan. 1960, 19 pp.

Operational Problems of Manned Orbital Vehicles, by Hubert M. Drake, Donald R. Bellman and Joseph A. Walker, *NACA Res. Mem.* H58D21, July 1958, 16 pp.

Rocket Test Stand Challenge, by B. F. Rose Jr., ASTRONAUTICS, vol. 5, March 1960, p. 28.

The Third USSR Cosmic Rocket (Lunik III), *Raketentechnik und Raumfahrtforschung,* vol. 4, no. 1, Jan.-March 1960, pp. 23–25. (In German.)

Measuring Satellite Explorer VI, *Raketentechnik und Raumfahrtforschung,* vol. 4, no. 1, Jan.-March 1960, pp. 26–27. (In German.)

Some Weight Considerations for Manned Lunar Missions, by Hans B. Schechter, ARS JOURNAL, vol. 30, no. 2, Feb. 1960, pp. 195–197.

Guidance and Control

On the Philosophy of Adaptive Control for Process Adaptive Systems, by M. Margolis and C. T. Leondes, *Univ. Calif. Los Angeles, Dept. Engng.,* Oct. 1959, 13 pp. (*AFOSR TN* 59-1199.)

On the Theory of Adaptive Control Systems, the Learning Model Approach, by M. Margolis and C. T. Leondes, *Univ. Calif. Los Angeles, Dept. Engng.,* Oct. 1959, 25 pp. (*AFOSR TN* 59-1200.)

Extended Synthesis Techniques for Multipole Sampled-data Control Systems, by E. B. Stear and C. T. Leondes, *Univ. Calif. Los Angeles, Dept. Engng.,* Oct. 1959, 12 pp. (*AFOSR TN* 59-1223.)

Optimum Re-entry into the Earth's Atmosphere by Use of a Variable Control Force, by Francis J. Marshall, *Wright Air Dev. Center, Tech. Rep.* 59–515, Oct. 1959, 127 pp., 83 refs.

Programming of Digital Computers for Determination of Stability and Control Characteristics, by D. E. Drake, E. R. Keown and J. K. Matlock, *Wright Air Dev. Center, Tech. Rep.* 59–290, vols. 1 & 2, July 1959, 586 pp.

Some Extensions of Liapunov's Second Method, by J. P. LaSalle, *RIAS, Baltimore, Md., Tech. Rep.* 60–5, 1960, 25 pp.

On Guidance and Control Requirements in Astronautics, by Robert E. Roberson, *J. Franklin Inst.,* vol. 269, March 1960, pp. 196–234.

Synthesis of Elements of Automatic Control Linear Systems, by I. A. Orurk, *Avtomatika i Telemekhanika,* no. 12, 1959, pp. 1595–1602. (In Russian.)

Analysis of Control Systems Tracking Failure Due to Fluctuating Noise Influence, by I. A. Bolshakov, *Avtomatika i Telemekhanika,* no. 12, 1959, pp. 1611–1622. (In Russian.)

Instruments to Determine Frequency Responses of Nonlinear Systems, by K. V. Zakharov and V. K. Svjatodykh, *Avtomatika i Telemekhanika,* no. 12, 1959, pp. 1679–1686. (In Russian.)

A Combined Aerodynamic and Guidance Approach for a Simple Homing System, by Robert A. Gardiner, *NACA Res. Mem.* L53I10a, Nov. 1953, 9 pp.

Controls: An Application of the Direct Method of Liapunov, by Solumon Lefschetz, *RIAS, Baltimore, Md., Tech. Rep.* 59–8, Dec. 1959, 11 pp.

Liapunov's Function and Boundedness of Solutions, by T. Yoshizawa, *RIAS, Baltimore, Md., Tech. Rep.* 59–7, Dec. 1959, 10 pp.

Perturbation Approach to the Effect of the Geomagnetic Field on a Charged Satellite, by H. R. Westerman, ARS JOURNAL, vol. 30, no. 2, Feb. 1960, pp. 204–205.

Effect of Certain Typical Nonlinearities on the Adjustment of a Mechanical Pilot, by M. E. Salukavadze, *Automation & Remote Control* (*trans. of Avtomatika i Telemekhanika*), vol. 20, no. 5, May 1959, pp. 529–540.

Study of Periodic Motions Arising in a Servomechanism Oscillatory Circuit at Constant Excitation, by I. N. Krutova, *Automation & Remote Control* (*trans. of Avtomatika i Telemekhanika*), vol. 20, no. 5, May 1959, pp. 541–551.

Application of Simulation in Analyzing Linear Pulse Systems with Variable Parameters, by G. P. Tartakovskii, *Automation & Remote Control* (*trans. of Avtomatika i Telemekhanika*), vol. 20, no. 5, May 1959, pp. 559–566.

Stability Criterion for Nonlinear Control Systems, by Chang Ssu-ying, *Automation & Remote Control* (*trans. of Avtomatika i Telemekhanika*), vol. 20, no. 5, May 1959, p. 647.

Some Simplified Stability Criteria for Nonlinear Controlled Systems, by A. K. Bedel'baev, *Automation & Remote Control* (*trans. of Avtomatika i Telemekhanika*),

vol. 20, no. 6, June 1959, pp. 664–678.

Stability of Nonlinear Controlled Systems, by E. N. Rozenvasser, *Automation & Remote Control* (*trans. of Avtomatika i Telemekhanika*), vol. 20, no. 6, June 1959, pp. 679–684.

Synthesis of Servosystem Correcting Devices in the Presence of Noise, by P. S. Matveev, *Automation & Remote Control* (*trans. of Avtomatika i Telemekhanika*), vol. 20, no. 6, June 1959, pp. 698–705.

On the Synthesis of Pulsed Correcting Devices for Servosystems, by A. A. Krasovskii, *Automation & Remote Control* (*trans. of Avtomatika i Telemekhanika*), vol. 20, no. 6, June 1959, pp. 706–717.

The Pure-analytic Approach to Intertial Guidance Design, by Bernard Kovit, *Space/Aeron.*, vol. 33, March 1960, p. 157.

Instrumentation and Communications

Radio Communication with a Space Probe, by W. T. Blackhand, *J. Brit. Interplanet. Soc.*, vol. 17, Nov.-Dec. 1959, pp. 159–161.

Long-range Detection by Star Occultation, by Harvey Dubner, *J. Astron. Sci.*, vol. 7, no. 1, 1960, pp. 1–6.

A New Type of Thermal Conductivity Gas Detector, I, by Shinzan Soma and Yu Takeuchi, *J. Phys. Soc. Japan*, vol. 15, Feb. 1960, pp. 333–335.

Aerodynamics of the Upper Atmosphere, by David J. Masson, ed. (Symposium, Santa Monica, Calif., June 8–10, 1959), *Rand Corp.* R-331, 1959, 1 vol.

Formation of a Radio Frequency at an Antenna During Falling Sphere Measurements, by G. A. Burns, W. J. Linder, J. F. Schorsch, H. L. Steel and H. F. Schulte, *Paper* 18, 25 pp.

On the Question of Diffraction of Radio Waves Over an Inhomogeneous Spherical Earth Surface, by Iu. K. Kalinin, *Radio Engng. & Electronics* (*trans. of Radiotekhnika i Elektronika*), vol. 3, no. 10, 1958, pp. 77–85.

Satellite Systems for Commercial Communications, by J. R. Pierce, *Inst. Aeron. Sci., Paper* 60–40, Jan. 1960, 12 pp.

Radioactive Tracers Find Jet Fuel Flow Rates, by J. D. Keys and G. E. Alexander, *Electronics*, vol. 33, Feb. 19, 1960, pp. 58–59.

High Temperature Measurement, by Vincent G. Shaw, *Instr. & Control Systems*, vol. 33, Jan. 1960, pp. 58–63.

The Ratio Pyrometer, by David L. Burk, *Instr. & Control Systems*, vol. 33, Jan. 1960, pp. 64–66.

Surface Temperature Measurement, by Walter K. Moen, *Instr. & Control Systems*, vol. 33, Jan. 1960, pp. 70–75.

Thermocouple Temperature Measurement Without Special Instruments, by Dale Kelly, *Instr. & Control Systems*, vol. 33, Jan. 1960, pp. 76–79.

Errors in Thermocouple Circuits, by Robert J. Almond, *Instr. & Control Systems*, vol. 33, Jan. 1960, pp. 80–82.

Temperature Measurement with Thermistors, by Robert M. Atkins, *Instr. & Control Systems*, vol. 33, Jan. 1960, pp. 86–89.

Using Thermocouples with Non-standard Reference Temperature, by Alvin B. Kaufman, *Instr. & Control Systems*, vol. 33, Jan. 1960, pp. 106–107.

Modulation Method of Identifying Weak Pulse Signals, by A. G. Gorelik and V. V. Kostarev, *Instruments & Experimental Tech.* (*trans. of Pribory i Tekhnika Eksperimenta*), no. 1, Jan.-Feb. 1959, pp. 80–84.

A Method of Measuring Pulse Amplitude Ratios, by A. A. Markov, *Instruments & Experimental Tech.* (*trans. of Pribory i Tekhnika Eksperimenta*), no. 1, Jan.-Feb. 1959, p. 142.

Installation for Obtaining Powerful Magnetic Fields of Short Duration, by V. R. Karasik, *Instruments & Experimental Tech.* (*trans of Pribory i Tekhnika Eksperimenta*), no. 1, Jan.-Feb. 1959, pp. 147–149.

On the Accuracy of Time Determination of a Sloping Signal, by V. I. Nikitenko, *Radio Engng. & Electronics* (*trans. of Radiotekhnika i Elektronika*), vol. 3, no. 10, 1958, pp. 86–97.

Non-stationary Random Processes in Linear Pulse Systems with Variable Parameters, by G. P. Tartakovskii, *Radio Engng. & Electronics* (*trans. of Radiotekhnika i Elektronika*), vol. 3, no. 10, 1958, pp. 98–114.

Satellites and Radio Astronomy, by W. L. Rae, *Spaceflight*, vol. 2, no. 5, Jan. 1960, pp. 137–142.

Techniques for Installation of High-temperature Foil Strain Gages, by Dr. R. L. Hauser, *Strain Gage Readings*, vol. II, Feb.-March 1960, pp. 41–44.

Contribution to the Calculation of Power Received by Scattering in Distant Tropospheric Propagation of Ultra-short Waves, by A. V. Prosin, *Telecommunications* (*trans. of Elektrosviasz*), no. 8, 1958, pp. 811–822.

Reducing Amplifier Distortion, by G. W. Holbrook, *Electronic Technology*, vol. 37, no. 1, Jan. 1960, pp. 13–19.

Transistor Matching Impedances, by A. G. Bogle, *Electronic Technology*, vol. 37, no. 1, Jan. 1960, pp. 28–30.

Space Technology and Image Sensing—Ten Papers, *J. Soc. Motion Picture & Television Engrs.*, vol. 69, no. 1, Jan. 1960.

The National Space Program, pp. 1–8.

Orbit Determination from Optical Tracking, by Douglas Duke, pp. 9–13.

Image Sensing as Applied to Meteorological Satellites, by David S. Johnson, pp. 14–17.

Image Sensors and Space Environment, by Milton Ritter and M. H. Mesner, pp. 18–24.

Infrared Imaging from Satellites, by R. A. Hanel and W. G. Stroud, pp. 25–26.

Pictorial Data Transmission from a Space Vehicle, by J. F. Baumunk and S. H. Roth, pp. 27–31.

Electrostatic Imaging and Recording, by E. C. Hutter, J. A. Inslee and T. H. Moore, pp. 32–34.

Satellite Astronomical Telescopes, by Nancy G. Roman, pp. 35–38.

Television and Lunar Exploration, by S. W. Spaulding, pp. 39–43.

Summary and Conclusions, by Sidney Sternberg, pp. 44–46.

Advancements in Microspectroscopy, by Robert F. Hummer, *U. S. Naval Ordn. Test Station, NOTS TP* 2372, Jan. 1960, 8 pp.

Instrumentation Studies for Plasma Jet and Hypersonic Wind Tunnel, by William W. Hill Jr. and Paul E. Stanley, *Purdue Univ., School Aeron. Engng., Rep.* A-59-12, Aug. 1959, 52 pp.

The Bang-bang Principle, by J. P. LaSalle, *RIAS, Baltimore, Md.*, TR 59–5, Nov. 1959, 16 pp. (*AFOSR TN* 59–1142.)

Calibration of Turbine Flowmeters for Cryogenic Operation, by Jerry Grey, ARS JOURNAL, vol. 30, no. 2, Feb. 1960, pp. 192–193.

Radio Interferometry, by Marcel J. E. Golay, ASTRONAUTICS, vol. 5, March 1960, p. 22.

Vibration Testing of Instruments, by William D. Huston, *Instr. & Control Systems*, vol. 33, Feb. 1960, pp. 234–238.

Acceleration Generators, by Alvin B. Kaufman, *Instr. & Control Systems*, vol. 33, Feb. 1960, pp. 240–248.

Measurement of Noise, Vibration, and Shock, by Charles E. White, *Instr. & Control Systems*, vol. 33, Feb. 1960, pp. 266–269.

Two Thermocouples Suitable for Measurement of Temperatures up to 2800°C, by D. A. Davies, *J. Sci. Instr.*, vol. 37, Jan. 1960, pp. 15–16.

Some Problems Relating to the Return-inclined Sounding of the Ionosphere, by B. I. Osetrov, *Radio Engng.* (*trans. of Radiotekhnika*), vol. 13, no. 12, 1958, pp. 1–13.

Radiowave Propagation in Surface Tropospheric Ducts, by V. A. Fok, L. A. Vainshtein and M. G. Belkina, *Radio Engng. & Electronics* (*trans. of Radiotekhnika i Electronika*), vol. 3, no. 12, 1958, pp. 1–27.

Investigation of Radiowave Scattering on Tropospheric Inhomogeneities in Refractive Index by a Method of Radio-astronomical Measurements, by M. A. Ievdokimov, *Radio Engng. & Electronics* (*trans. of Radiotekhnika i Electronika*), vol. 3, no. 12, 1958, pp. 28–42.

Optimum Detection in the Presence of Correlated Noise, by V. D. Zubakov, *Radio Engng. & Electronics* (*trans. of Radiotekhnika i Electronika*), vol. 3, no. 12, 1958, pp. 43–56.

On the Passage of a Pulse Train with Linearly Varying Carrier Frequency Through a Selective System, by I. S. Gonorovskii, *Radio Engng. & Electronics* (*trans. of Radiotekhnika i Electronika*), vol. 3, no. 12, 1958, pp. 104–117.

High-Speed Bolometer, by H. E. Stubbs and R. G. Phillips, *Rev. Sci. Instr.*, vol. 31, Feb. 1960, pp. 115–118.

Magnetically Driven Fast-acting Valve for Gas Injection into High Vacua, by B. Gorowitz, K. Moses and P. Gloersen, *Rev. Sci. Instr.*, vol. 31, Feb. 1960, pp. 146–148.

Thin-heater Thermal Conductivity Apparatus, by Nathaniel E. Hager Jr., *Rev. Sci. Instr.*, vol. 31, Feb. 1960, pp. 177–184.

Automatic Device for Recording Experimental Results Directly on Teleprinter Tape, by M. M. Winn and K. W. Ogilvie, *Rev. Sci. Instr.*, vol. 31, Feb. 1960, pp. 185–187.

Multistage Electrostatic Energy Analyzer with Two-dimensional Focusing, by M. M. Bredov, *Soviet Phys., Tech. Phys.* (*trans. of Zhurnal Tekhnicheskoi Fiziki*), vol. 4, Feb. 1960, pp. 940–948.

The Measurement of the Mutual Diffusion Coefficient of Gases by an Optical Method, by P. E. Suetin, G. T. Shchegolev and R. A. Klestov, *Soviet Phys., Tech. Phys.* (*trans of Zhurnal Tekhnicheskoi Fiziki*), vol. 4, Feb. 1960, p. 964.

Radio Link to Space Can Be Built with Today's Hardware, by Kurt H. Meissner, *Space/Aeron.*, vol. 33, March 1960, p. 141.

Atmospheric and Space Physics

Aerodynamics of the Upper Atmosphere, by David J. Masson, ed. (Symposium, Santa Monica, Calif., June 8–10, 1959), *Rand Corp.*, R-331, 1959, 1 vol.

A Preliminary Model Atmosphere Based on Rocket and Satellite Data, by H. K. Kallmann, *Paper* 3, 27 pp.

On the Problem of Obtaining Thermal Proton Background and Solar Wind Measurements in Space, by Michel Bader, *Paper* 20, 29 pp.

Geophysical Research Using Artificial Earth Satellites, by John F. Clark, *Inst. Aeron. Sci., Paper* 60–50, Jan. 1960, 14 pp.

The Meteorological Measurements and Field Program of Project Jet Stream from 1956 to 1958, by R. M. Endlich and R. M. Rados, *Air Force Cambridge Res. Center, Geophys. Res. Paper* 64, *AFCRC-TR-59-266*, Oct. 1959, 127 pp.

Space Probes and Persistence of Strong Tropopause Level Winds, by H. Salmela and N. Sissenwine, *Air Force Cambridge Res. Center, GRD Res. Notes* 26 *AFCRC-TN-59-652*, Dec. 1959, 9 pp.

Deduction of Vertical Thermal Structure of a Planetary Atmosphere from a Satellite, by J. I. F. King, *Gen. Electric Co., Missile & Space Vehicle Dept.*, TIS R59-SD477, 1959, 10 pp.

Astronomical Measurements with Rockets, Satellites, and Balloons, by A. P. Willmore, *J. Brit. Interplanet. Soc.*, vol. 17, Sept.-Oct. 1959, pp. 137–140.

The Current-jet Hypothesis of Whistler Generation, by W. C. Hoffman, *Planetary & Space Sci.*, vol. 2, no. 1, Oct. 1959, pp. 72–73.

Energies of Various Interactions Between Hydrogen and Helium Atoms and Ions, by Robert F. Fallon, Edward A. Mason and Joseph T. Vanderslice, *Astrophys. J.*, vol. 131, no. 1, Jan. 1960, pp. 12–14.

Interplanetary Gas, II: Expansion of a Model Solar Corona, by Joseph W. Chamberlain, *Astrophys. J.*, vol. 131, no. 1, Jan. 1960, pp. 47–56.

Geomagnetic and Current Control of E.-region Absorption, by J. E. Shaw, *Planetary & Space Sci.*, vol. 2, no. 1, Oct. 1959, pp. 1–9.

The Bound Free Continuum for C^{-*}, by R. G. Breene, *Planetary & Space Sci.*, vol. 2, no. 1, Oct. 1959, pp. 10–16.

Artificial Electron Clouds, IV: Thermal Ionization Study, Night Time Cesium Release at 101 km, by J. Pressman, F. F. Marmo and L. M. Aschenbrand, *Planetary & Space Sci.*, vol. 2, no. 1, Oct. 1959, pp. 17–32.

Arctic Atmospheric Structure to 250 km, by H. E. Lagow, R. Horowitz and J. Ainsworth, *Planetary & Space Sci.*, vol. 2, no. 1, Oct. 1959, pp. 33–38.

A Survey of Soviet Geophysical Literature, by J. J. Roark, *Geophysics*, vol. 24, no. 5, Dec. 1959, pp. 910–915.

Upper-air Densities and Temperatures from Eight IGY Rocket Flights by the Falling-sphere Method, *International Geophysical Year, IGY World Data Center, A: Rockets and Satellites, IGY Rocket Rep. Series* no. 5, Dec. 1959, 30 pp.

Magnetic Exploration of the Upper Atmosphere, International Geophysical Year, *IGY World Data Center, A: Rockets and Satellites, IGY Rocket Rep. Series* no. 4, Oct. 1959, 86 pp.

The Deceleration of Meteors During Their Passage Through the Earth's Atmosphere, by F. Verniani, *Nuovo Cimento*, vol. 14, no. 5, Dec. 1959, pp. 938–942.

The Stellar Plasma, by E. Schatzman, *Nuovo Cimento*, Suppl. to vol. 13, Series 10, no. 1, 1959, pp. 166–188. (In French.)

Stellar Atmospheres in Plasma, by L. Biermann, *Nuovo Cimento*, Suppl. to vol. 13, Series 10, no. 1, 1959, pp. 189–204.

The Interstellar Plasma, by H. C. van de Julst, *Nuovo Cimento*, Suppl. to vol. 13, Series 10, no. 1, 1959, pp. 205–233.

Optical and Radiophenomena Associated with a Solar Activity Centre, by C. De Jager, *Nuovo Cimento*, Suppl. to vol. 13, Series 10, no. 1, 1959, pp. 284–290.

The Observability of Hydromagnetic Phenomena on the Sun, by K. O. Kiepenheuer, *Nuovo Cimento*, Suppl. to vol. 13, Series 10, no. 1, 1959, pp. 305–310.

Magnetic Field in the Solar System, by T. Gold, *Nuovo Cimento*, Suppl. to vol. 13, Series 10, no. 1, 1959, pp. 318–323.

Human Factors and Bioastronautics

Psycho-social Problems of Manned Spaceflight, by George A. Peters, ASTRONAUTICS, vol. 5, March 1960, p. 30.

Human Factors—Newest Engineering Principles, by C. Celent, *Electronic Industries*, vol. 19, no. 2, Feb. 1960, pp. 85–100.

Life Support Systems for Space Vehicles, by Richard S. Johnston, Anton A. Tamas, William R. Turner, E. L. Hayes and Roland A. Bosee, *Inst. Aeron. Sci., SMF Fund Paper* FF-25, Jan. 1960, 40 pp.

Law, Sociology and Education

Legal Problems of Space, by A. Meyer, *Raketentechnik und Raumfahrtforschung*, vol. 4, no. 1, Jan.-March 1960, pp. 1–6. (In German.)

Index to Advertisers